The Topology of Hecke Correspondences

by

Paul E. Gunnells

B. S. in Mathematics, Stanford University 1989

Submitted to the Department of Mathematics
in partial fulfillment of the requirements for the degree of

Doctor of Philosophy

at the

MASSACHUSETTS INSTITUTE OF TECHNOLOGY

May 1994

Signature of Author ....
Department of Mathematics
May 1994

Certified by ....
Robert D. MacPherson
Professor of Mathematics
Thesis Supervisor

Accepted by ....
Science
David A. Vogan
Chairman, Departmental Committee on Graduate Studies

THE TOPOLOGY OF HECKE CORRESPONDENCES

by

Paul E. Gunnells

Submitted to the Department of Mathematics on
April 29, 1994, in partial fulfillment of the
requirements of for the Degree of Doctor of Philosophy in
Mathematics

ABSTRACT

Given two distinct primes p and ℓ, let $X(p)$ be a modular curve and let

$$(s,t)\colon C_\ell(p) \rightrightarrows X(p)$$

be a Hecke correspondence. We study the action of this correspondence on the cohomology of $X(p)$ by studying the topology of $C_\ell(p)$. Specifically, using s and t we lift a triangulation $\Delta(p)$ of $X(p)$ to two cell decompositions of $C_\ell(p)$. We then construct a space, the *universal Hecke correspondence* $\mathscr{C}_\ell$, such that every correspondence space $C_\ell(p)$ may be assembled from $\mathscr{C}_\ell$ using identifications that depend only on p.

We present two applications of our construction. First, using $\mathscr{C}_\ell$ we develop an algorithm to compute combinatorially the action of the Hecke correspondence on cohomology. Second, we present a combinatorial construction of certain classes in the *Eisenstein cohomology* of $X(p)$.

Thesis supervisor: Robert MacPherson
Title: Professor of Mathematics

ACKNOWLEDGMENTS

There are many people that had a part, large and small, in the development of this thesis. Let me simply provide a list of names in the style of Borges: Laura Anderson, Jonathan Beck, Jim Bryan, Paul Bryant, Lisa Court, Ken Fan, Mark Goresky, Bill Graham, Leonard Gravante, Mike Grossberg, Kathryn Gunnells, Farshid Hajir, Yi Hu, Dave McDonald, Pat McDonald, Janet Merritt, Larry Nolan, Phyllis Ruby, Mark Sepansky, Dennis Stewart, Elizabeth Sudderth, Ulrich Vollmer, Eric Weinstein, Chris Woodward, and David Yavin.

I am especially grateful to the following people, for their continued interest and support: Avner Ash, Eric Babson, Mark McConnell, Richard Scott, Glenn Stevens, David Vogan, and Siman Wong.

Above all, I owe a profound debt to Bob MacPherson, for his patience and mentorship.

Finally, a special thanks to my soulmate Carmela, for her compassion and understanding through this and many other trials.

Contents

CHAPTER I

Introduction

1. Statement of the Problem

The main objective of this thesis is to study the action of Hecke correspondences on the cohomology of spaces of lattices by studying the topology of the correspondences themselves. To explain what this means, we introduce the principal objects of our study.

We begin with configuration spaces of lattices. Let $L \subset \mathbb{R}^2$ be a lattice of rank two, and say that two lattices L and L' are equivalent if L can be carried into L' by a rotation and a homothety. Choose an odd prime p, and define a p-marking of L to be a surjective linear map $m\colon L \longrightarrow (\mathbb{Z}/p)^2$. Finally, define $\mathscr{Y}(p)$ to be the set of all pairs (L, m) modulo the relation that $(L, m) \sim (L', m')$ if there is a lattice equivalence $\Phi\colon L \longrightarrow L'$ such that $m = \Phi \circ m'$. We shall see that $\mathscr{Y}(p)$ is homeomorphic to a disjoint union of punctured Riemann surfaces, and that the genus of these surfaces is given by a cubic polynomial in p.

Now let $\ell \neq p$ be another prime, and let $\mathscr{C}_\ell^0(p) \subset \mathscr{Y}(p) \times \mathscr{Y}(p)$ be the space of pairs

$$\big\{((L, m), (L', m')) \bigm| [L : L'] = \ell \quad \text{and} \quad m' = m|_{L'}\big\}.$$

This space is also a disjoint union of punctured Riemann surfaces. Form two maps s and t from $\mathscr{C}_\ell^0(p)$ to $\mathscr{Y}(p)$ by projecting onto both factors. The diagram

$$(s, t)\colon \mathscr{C}_\ell^0(p) \rightrightarrows \mathscr{Y}(p)$$

is called a *Hecke correspondence*. Note that lifting by s and projecting by t takes a marked lattice into the collection of its index ℓ sublattices.

The vector space $H^1(\mathscr{Y}(p); \mathbb{C})$ is replete with important arithmetic information; in particular, it contains as a subspace all weight two modular forms of level p. We detect this information through the Hecke correspondences. Every Hecke correspondence induces an automorphism of $H^1(\mathscr{Y}(p); \mathbb{C})$ through

$$H^1(\mathscr{Y}(p)) \xrightarrow{s^*} H^1(\mathscr{C}_\ell^0(p)) \xrightarrow{t_!} H^1(\mathscr{Y}(p)).$$

This action is diagonalizable, and as ℓ ranges over all primes distinct from p, the actions of the various correspondences commute. Hence we may decompose

$H^1(\mathscr{Y}(p);\mathbb{C})$ into mutual eigenspaces for these correspondences. A central problem of classical and modern number theory is to understand this decomposition.

2. Historical Background

Many people have studied the action of Hecke correspondences; it would be futile to attempt a survey here. To give our work context, we review only those investigations that are our direct predecessors. We will discuss results in terms of homology rather than cohomology, but the reader may easily supply the appropriate duality.

We begin with *modular symbols*, introduced by Birch and developed extensively by Manin [Man72]. Here we briefly describe their construction. Each connected component $Y(p)$ of $\mathscr{Y}(p)$ is homeomorphic to $\Gamma(p)\backslash\mathbf{H}$, where $\Gamma(p) \subset SL_2(\mathbb{Z})$ is the principal congruence subgroup of level p and $\mathbf{H}$ is the upper half plane. Through a classical technique, $Y(p)$ is compactified by forming $\mathbf{H}^* := \mathbf{H} \cup \mathbb{Q} \cup \{\infty\}$ and topologizing so that $\Gamma(p)\backslash\mathbf{H}^*$ is closed compact surface. These new points $\mathbf{H}^* - \mathbf{H}$ are called *cusps*. Given a pair of cusps a, b, the modular symbol $[a,b] \in H_1(\Gamma(p)\backslash\mathbf{H}^*;\mathbb{R})$ is constructed as follows. We choose any reasonable path γ in $\mathbf{H}$ from a to b, and then integration along the image of γ in $\Gamma(p)\backslash\mathbf{H}^*$ gives a linear map from the holomorphic differential one-forms on $\Gamma(p)\backslash\mathbf{H}^*$ to $\mathbb{C}$. This linear map corresponds to an element of $H_1(\Gamma(p)\backslash\mathbf{H}^*;\mathbb{R})$. One can show that this is in fact a combinatorial construction, in other words only depends on the pair of cusps. Hecke correspondences act on modular symbols directly, and Manin showed that an application of the continued fraction algorithm can be used to compute this Hecke action.

Next we come to the work of Ash and Rudolph [AR79]. They studied the Hecke action on the homology of the higher-rank symmetric spaces

$$\Gamma(p)\backslash SL_n(\mathbb{R})/SO_n(\mathbb{R}).$$

Here $\Gamma(p)$ is now a subgroup of $SL_n(\mathbb{Z})$; in our geometric language this corresponds to studying the space of lattices in dimensions greater that 2. They were able to construct a generalization of the modular symbol with values in

$$H_{n-1}(\Gamma(p)\backslash SL_n(\mathbb{R})/SO_n(\mathbb{R});\mathbb{Z}),$$

and furthermore were able to appropriately generalize the continued fraction algorithm to compute the Hecke action on these classes.

Although the generalized modular symbol is a powerful tool, a shortcoming is that the Hecke action on many groups remain inaccessible. In contrast to $n = 2$, where $H^1(\mathscr{Y}(p))$ is the only interesting group, for $n \geq 3$ there are many others. Our research arose from a desire to study the Hecke action on these groups. Although we do not complete this program in this thesis, we believe our approach for $n = 2$ will generalize to higher dimensions.

3. Techniques

Now fix $n = 2$. Denote the compactification of $\mathscr{Y}(p)$ described in the previous section by $\mathscr{X}(p)$, and let $\{\text{cusps}\}$ denote $\mathscr{X}(p) - \mathscr{Y}(p)$. Elements of $\{\text{cusps}\}$ have a convenient interpretation as "lattices at infinity," and we may add a finite number of points to $\mathscr{C}^0_\ell(p)$ to form a diagram

$$(s,t)\colon \mathscr{C}_\ell(p) \rightrightarrows \mathscr{X}(p).$$

Although s and t are $(\ell+1)$-to-one over $\mathscr{Y}(p)$, they are two-to-one over $\{\text{cusps}\}$. This is independent of ℓ.

From the work of Voronoï [Vor08] there is a triangulation $\Delta(p)$ of $\mathscr{X}(p)$ that has $\{\text{cusps}\}$ as vertices. This triangulation is highly symmetric; for the cases $p=3$ and $p=5$, the connected components of $\mathscr{X}(p)$ are tetrahedra respectively icosahedra:

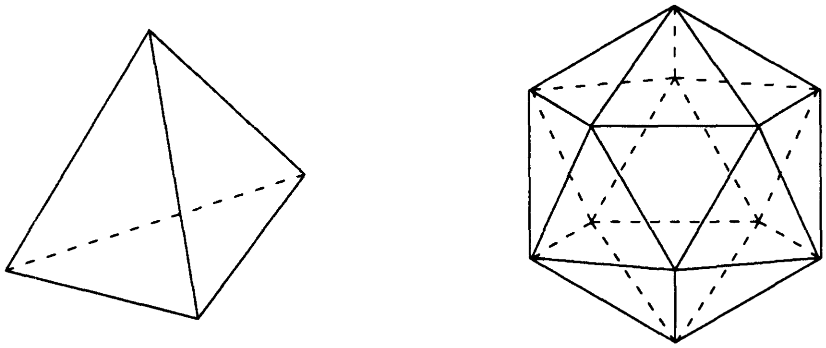

FIGURE I.1. $X(3)$ and $X(5)$.

Moreover, the simplices of $\Delta(p)$ are easy to specify in terms of the geometry of lattices. Say that a lattice is *rectangular* if it has an orthogonal basis. Then the edges of $\Delta(p)$ consist of all rectangular p-marked lattices, and the triangles contain all remaining lattices. In the terminology of modular symbols, the edges correspond to the "unimodular symbols."

We wish to use this triangulation and the techniques of combinatorial topology to study the action of the Hecke correspondences on $H^1(\mathscr{Y}(p);\mathbb{C})$. However, in doing so we encounter an immediate obstacle: the Hecke correspondences do not act simplicially on $\Delta(p)$. Given the above description of the simplices of $\Delta(p)$, this is clear, because if a lattice L rectangular, an index ℓ sublattice L' need not be rectangular:

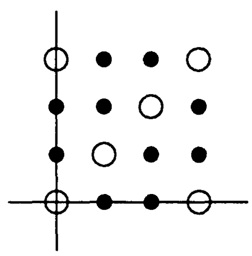

FIGURE I.2. $\ell = 3$.

To address this, we take the following tack. Using s and t, we lift $\Delta(p)$ to two cell complexes $\Delta_s(p)$ and $\Delta_t(p)$ on $\mathscr{C}_\ell(p)$. As an example, consider the case $p = 3$ and $\ell = 2$. Each connected component of $\mathscr{C}_2(3)$ has genus zero:

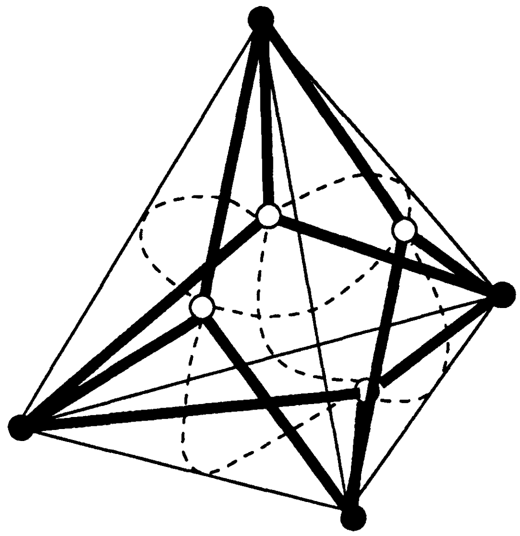

FIGURE I.3.

The picture is drawn using different types of lines to distinguish $\Delta_s(3)$ and $\Delta_t(3)$. The 1-skeleton of $\Delta_s(3)$ consists of the thin solid lines and the thick solid lines, and the 1-skeleton of $\Delta_t(3)$ consists of the dashed lines and the thick solid lines. Note that there are eight vertices, eighteen edges, and twelve triangles. This agrees with the fact that s and t are two-to-one over the set {cusps} and three-to-one over $\mathscr{Y}(p)$. All the vertices, whether hollow or solid, are common to $\Delta_s(3)$ and $\Delta_t(3)$. We leave to the reader the pleasant exercise to determine s and t.

In this setting, the action of the Hecke correspondence becomes

(a) Lift a cycle using s to a cycle in $\Delta_s(p)$.
(b) Use a homotopy to push this cycle from $\Delta_s(p)$ to $\Delta_t(p)$.
(c) Push the cycle back down to $\mathscr{X}(p)$ using t.

We are thus confronted with our basic problem: can we understand the action of the Hecke correspondence on $H^1(\mathscr{Y}(p); \mathbb{C})$ by understanding the relationship between the two cell complexes $\Delta_s(p)$ and $\Delta_t(p)$ on $\mathscr{C}_\ell(p)$?

4. The Main Construction

To attack this problem, we investigate the geometry of $\Delta_s(p)$ and $\Delta_t(p)$. We find that there are certain 1-cells in $\Delta_s(p)$ and $\Delta_t(p)$ that map to 1-cells under both s and t. We call these the *common edges* of $\mathscr{C}_\ell(p)$. In the figure above, the common edges are the thick solid lines. Fixing ℓ, we cut $\mathscr{C}_\ell(p)$ along the common edges and let $p \to \infty$ to obtain $\mathscr{C}_\ell$, the *universal Hecke correspondence*. Returning to the example, when we cut the figure along the thick lines we obtain six copies of

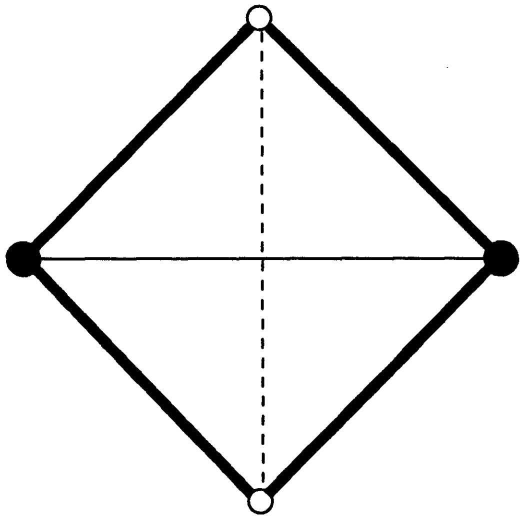

FIGURE I.4.

In general, $\mathscr{C}_\ell$ is a contractible space, independent of p, out of which we may build every Hecke correspondence $\mathscr{C}_\ell(p)$ using identifications that depend on p alone. Furthermore, $\mathscr{C}_\ell$ contains two cellular structures Δ_s and Δ_t which, under these identifications, pass to $\Delta_s(p)$ and $\Delta_t(p)$. In essence, $\mathscr{C}_\ell$ encodes all the geometry of the Hecke correspondence that is independent of the level structure p.

5. Results

In this thesis we explicitly construct $\mathscr{C}_\ell$ for all prime ℓ. Using $\mathscr{C}_\ell$ we describe an algorithm (the *Roadmap algorithm*) to compute the action of the Hecke correspondence on cohomology which we show to be equivalent to the Euclidean algorithm and thus to the classical modular symbol algorithm.

As an application of our construction we develop an algorithm to construct classes in the *Eisenstein cohomology* of $\mathscr{Y}(p)$. Let {cusps} denote the set of points $\mathscr{X}(p)-\mathscr{Y}(p)$. Consider the long exact sequence in homology with complex coefficients induced from the inclusion $\{\text{cusps}\} \hookrightarrow \mathscr{X}(p)$:

$$0 \to H_1(\mathscr{X}(p)) \to H_1(\mathscr{X}(p), \{\text{cusps}\}) \to H_0(\{\text{cusps}\}) \to H_0(\mathscr{X}(p)) \to 0.$$

Use $H_1(\mathscr{X}(p), \{\text{cusps}\}) = H_1^{cl}(\mathscr{Y}(p))$ (homology with closed supports), and Poincare duality to identify $H_1(\mathscr{X}(p))$ with $H^1(\mathscr{X}(p))$, and $H_1^{cl}(\mathscr{Y}(p))$ with $H^1(\mathscr{Y}(p))$. We obtain a sequence

$$0 \to H^1(\mathscr{X}(p)) \to H^1(\mathscr{Y}(p)) \to H_0(\{\text{cusps}\}) \to H_0(\mathscr{X}(p)) \to 0.$$

According to the Manin-Drinfeld theorem (cf. [Lan76]), there is a splitting of this sequence $E\colon H_0(\{\text{cusps}\}) \to H^1(\mathscr{Y}(p))$ that (a) is equivariant with respect to the action of the Hecke correspondences and (b) is defined over $\mathbb{Q}$. The image of E is called the Eisenstein cohomology. One traditionally constructs this section in this context through a technique of Hecke (cf. [Sch70]). One writes an Eisenstein series with an additional parameter τ. This series evaluated at $\tau = 1$ defines a cohomology class, but unfortunately does not converge. Hence one invokes analytic continuation, and this yields the appropriate Eisenstein class. Needless to say, this technique obscures the fact that the section is defined over $\mathbb{Q}$.

In our work we construct certain Eisenstein classes called *Steinberg classes* (see V.4 for the definition). To do this, we note that the full symmetry group $G_p = GL_2(\mathbb{F}_p)$ of $\Delta(p)$ induces an action on $H^1(\mathscr{Y}(p);\mathbb{C})$, and this action commutes with the action of the Hecke correspondences. We call this group the group of *nonabelian Hecke operators*; although each symmetry commutes with all Hecke correspondences, they do not commute with themselves. We decompose the chain complex associated to $\Delta(p)$ into G_p-isotypics, construct explicit bases for these representations, and then using the Roadmap algorithm determine the Hecke action on these basis elements. The result is a system of linear equations, independent of p, whose solution yields explicit cycles that are Eisenstein cohomology classes. Since the construction uses only elementary linear algebra and combinatorics, it is transparent that the section is defined over $\mathbb{Q}$.

6. Plan of the Paper

Chapter II introduces the space of p-marked lattices $\mathscr{Y}(p)$ and the Voronoï decomposition $\Delta(p)$. In II.1 we discuss the topology of $\mathscr{Y}(p)$ as a homogeneous space. In II.2 we specialize to lattices in $\mathbb{R}^2$ and discuss the compactification $\mathscr{X}(p)$ of $\mathscr{Y}(p)$. In II.3 and II.4 we introduce the Voronoï decomposition $\Delta(p)$, and in II.5 we discuss its combinatorics.

Chapter III discusses Hecke correspondences. In III.1 we discuss sublattices of the integral lattice, and in III.2 we define Hecke correspondences and the correspondence space $\mathscr{C}_\ell(p)$. Finally, in III.3 we discuss lifting $\Delta(p)$ to two complexes $\Delta_s(p)$ and $\Delta_t(p)$ on $\mathscr{C}_\ell(p)$.

Chapter IV contains the main construction of the paper, the universal Hecke correspondence $\mathscr{C}_\ell$. In IV.1 and IV.2 we discuss two examples to motivate the combinatorial construction in IV.3. The main theorem about $\mathscr{C}_\ell$ and its properties is stated and proved in IV.4. We conclude the chapter in IV.5 by discussing an algorithm that uses $\mathscr{C}_\ell$ to compute the action of the Hecke correspondence on $H^1(\mathscr{Y}(p);\mathbb{C})$, namely the Roadmap Algorithm.

Chapter V discusses the application of the UHC to the computation of some classes in the Eisenstein cohomology. In V.1 we define the group of nonabelian Hecke operators $G_p = GL_2(\mathbb{F}_p)$ and review its representation theory. In V.2 we describe the computation that decomposes the chain complex associated to $\Delta(p)$ into G_p-irreducibles, and in particular we describe the isotypics appearing in the Eisenstein cohomology. In V.3 and V.4 we discuss bases for certain G_p-isotypics in the chain complex, and in V.5 we describe the Hecke action on these bases. Finally, in V.6 we describe the system of linear equations that computes the Eisenstein section on the Steinberg cohomology classes.

CHAPTER II

Preliminaries

In this chapter we introduce configuration spaces of lattices and describe their topology. Standard references for this material are [Lan76], [Ser73], and [Shi71]. Our presentation draws heavily from [Mac90].

1. Spaces of Lattices

We will use the following notation:

- G will denote the special linear group $SL_n(\mathbb{R})$.
- K will denote the maximal compact subgroup of G, the special orthogonal group $SO_n(\mathbb{R})$.
- Γ will denote the discrete subgroup $SL_n(\mathbb{Z})$.

DEFINITION II.1. A *lattice* $L \subset \mathbb{R}^n$ is a $\mathbb{Z}$-module with any of the following equivalent properties:

(a) L is discrete and $\mathbb{R}^n/L$ is compact.
(b) L is discrete and generates $\mathbb{R}^n$ as a vector space.
(c) There exists a basis of $\mathbb{R}^n$ as a vector space that is also a basis of L as a $\mathbb{Z}$-module.

EXAMPLE II.1. $\mathbb{Z}^n \subset \mathbb{R}^n$ is a lattice, which we call the *standard lattice.* If $n = 2$, we call this the *square lattice.*

EXAMPLE II.2. Suppose we tile $\mathbb{R}^2$ with equilateral triangles with unit side length. Then the vertices of these triangles form a lattice in $\mathbb{R}^2$, which we call the *triangular lattice.*

Two lattices L, L' are *homothetic* if there exists $\lambda \in \mathbb{R}_{>0}$ such that $L = \lambda L'$. Two lattices L, L' are *equivalent* if there exists a $\rho \in K$ such that L is homothetic to $\rho L'$.

DEFINITION II.2. Let $\mathscr{Y}_{(n)}$ denote the set of all lattices in $\mathbb{R}^n$ modulo equivalence.

We topologize $\mathscr{Y}_{(n)}$ through the following:

PROPOSITION II.1. *There exists a homeomorphism* $\Gamma\backslash G/K \xrightarrow{\sim} \mathscr{Y}_{(n)}$.

PROOF. By using homotheties, we may assume that every point in $\mathscr{Y}_{(n)}$ is represented by a lattice of volume one. The group G acts transitively on $\mathscr{Y}_{(n)}$, since it acts transitively on the set of all bases of $\mathbb{R}^n$ of volume one. Since Γ stabilizes the standard lattice, we have a homeomorphism between $\Gamma\backslash G$ and the space of all lattices. Finally, since K acts on bases and hence on lattices by rotations, we may identify elements of $\Gamma\backslash G/K$ with lattices of volume one modulo rotations. □

In some sense, the points of $\mathscr{Y}_{(n)}$ are not homogeneous, because certain lattices have larger automorphism groups than do others. For example, the triangular lattice has an automorphism of order six, whereas the square lattice does not. To eliminate this discrepancy, we introduce the concept of *marked lattices* [Mac90].

DEFINITION II.3. A *marked lattice* is a triple $(L, m, \mathscr{S})$, where

(a) L is a lattice,
(b) $\mathscr{S}$ is a finite set, and
(c) $m\colon L \to \mathscr{S}$ is a surjective map, invariant with respect to translations by some sublattice of L.

Two marked lattices $(L, m, \mathscr{S})$ and $(L', m', \mathscr{S}')$ are *equivalent* if $\mathscr{S} = \mathscr{S}'$ and if there exists a lattice equivalence $\Phi\colon L \to L'$ with $m = \Phi \circ m'$.

DEFINITION II.4. Let p be a prime. A *p-marked lattice* is a marked lattice $(L, m, \mathscr{S})$ such that

(1) $\mathscr{S} = (\mathbb{Z}/p)^n$ and
(2) m is linear.

If the image of any basis of L has determinant d mod p, we say that L is *p-marked of determinant d.*

EXAMPLE II.3. Let L be the standard lattice $\mathbb{Z}^n \subset \mathbb{R}^n$ with basis

$$\{(1,0,\dots,0),(0,1,0,\dots,0),\dots,(0,\dots,0,1)\}$$

The marking $m_{\text{std}}\colon \mathbb{Z}^n \to (\mathbb{Z}/p)^n$ given by reduction of coordinates mod p is called the *standard p-marking of determinant one.* If we mark the last basis vector by

$$(0,\dots,0,1) \longmapsto (0,\dots,0,d \bmod p),$$

then this marking is called the *standard p-marking of determinant d.*

We denote a p-marked lattice simply by a pair (L, m).

To draw a picture of a p-marked lattice, we draw a lattice with a distinguished basis $\{\mathbf{v}_1,\dots,\mathbf{v}_n\}$, and we label each $\mathbf{v}_i$ with a column vector in $(\mathbb{Z}/p)^n$.

EXAMPLE II.4. The following are equivalent 5-marked square lattices. In both pictures, the origin is the point in the lower left-hand corner.

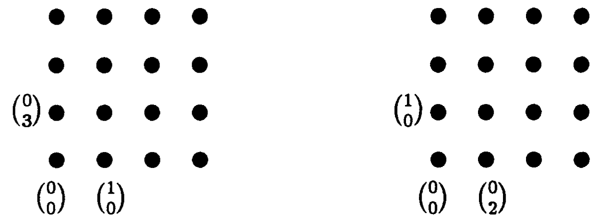

FIGURE II.1. Two 5-marked square lattices

DEFINITION II.5. Let $Y^d_{(n)}(p)$ denote the set of all p-marked lattices in $\mathbb{R}^n$ of determinant d modulo equivalence.

Now we wish to topologize $Y^d_{(n)}(p)$ in the same group-theoretic manner that we topologized $\mathscr{Y}_{(n)}$. The argument is similar, but this time Γ does not stabilize the standard p-marked lattice. However, there exists a unique maximal subgroup $\Gamma(p)$ of Γ that does.

DEFINITION II.6. Given a prime p, the *principal congruence subgroup of level* p is defined to be

$$\Gamma(p) := \{\gamma \in \Gamma \mid \gamma = \mathrm{Id}_n \bmod p\},$$

where Id_n denotes the $n \times n$ identity matrix.

PROPOSITION II.2. *The following statements are true:*

(a) There exists an exact sequence

$$1 \to \Gamma(p) \to \Gamma \to SL_n(\mathbb{Z}/p) \to 1.$$

(b) For $p \geq 3$, the group $\Gamma(p)$ is torsion-free.

PROOF. For the proof of the first statement, see [Shi71]. The proof of the second statement is due to Minkowski [Min87]. □

As an immediate corollary of (a) we have

COROLLARY II.1. *Let $d \in (\mathbb{Z}/p)^\times$. Then the group $\Gamma(p)$ acts trivially on the standard p-marked lattice of determinant d.*

Putting this all together, we conclude:

PROPOSITION II.3. *There exists a homeomorphism*

$$\Gamma(p)\backslash G/K \xrightarrow{\sim} Y^d_{(n)}(p).$$

For our applications we shall need all possible determinants of p-marked lattices, and thus we define

DEFINITION II.7. The space $\mathscr{Y}_{(n)}(p)$ of equivalence classes of p-marked lattices is

$$\mathscr{Y}_{(n)}(p) := \coprod_{d \in (\mathbb{Z}/p)^\times} Y^d_{(n)}(p) = \coprod_{d \in (\mathbb{Z}/p)^\times} \Gamma(p)\backslash G/K.$$

In general, we shall always use Roman letters for connected components and script letters for the disjoint union of connected components.

From now on we will only consider the case $p \geq 3$. Since $\Gamma(p)$ is torsion-free for these p, it follows that all p-marked lattices (L, m) have the same automorphism groups. In particular it follows that the space $\mathcal{Y}_{(n)}(p)$ is a noncompact manifold.

REMARK II.1. In the homeomorphisms defined above, we correspond equivalence classes of unmarked lattices with double cosets $\Gamma x K$, and p-marked lattices with double cosets $\Gamma(p)xK$ where x is a matrix in G. The geometric idea behind these homeomorphisms is that the lattice in $\mathcal{Y}_{(n)}$ corresponds to the lattice generated by x. This is true, but because we act by our discrete groups Γ and $\Gamma(p)$ on the left, we actually generate lattices in the *rows* of x. We caution the reader to this fact, as this is different from the usual notion of the matrix x representing a basis of $\mathbb{R}^n$ with its columns.

2. Modular Curves

Set $n = 2$, so that $G = SL_2(\mathbb{R})$, $K = SO_2(\mathbb{R})$, and $\Gamma = SL_2(\mathbb{Z})$. We will also drop the dimension subscript from $\mathcal{Y}_{(n)}$, $\mathcal{Y}_{(n)}(p)$, and $Y^d_{(n)}(p)$. In this case, the spaces $\Gamma(p)\backslash G/K$ are known as *modular curves.* We review in this section the basic concepts associated with modular curves, especially the technique of compactifying them by adding cusps.

Recall that the upper half plane $\mathbf{H}$ is defined as the set of all $z \in \mathbb{C}$ such that z has positive imaginary part $\Im(z)$. The group G acts on $\mathbf{H}$ by fractional-linear transformations. Under this action, the element $g = \left(\begin{smallmatrix} a & b \\ c & d \end{smallmatrix}\right) \in G$ acts on $z \in \mathbf{H}$ via

$$g \cdot z := \frac{az + b}{cz + d}.$$

Note that this action of G takes $\mathbf{H}$ to $\mathbf{H}$, because

$$\Im(g \cdot z) = \frac{\Im(z)}{|cz + d|^2} > 0 \quad \text{if } \Im(z) > 0.$$

It is easy to see that this action is transitive, and that the stabilizer of i is K. Thus we have a homeomorphism $G/K \xrightarrow{\sim} \mathbf{H}$ given by $gK \longmapsto g \cdot i$. We will always use this choice of homeomorphism to identify G/K and $\mathbf{H}$.

Since $\Gamma(p)$ is a subgroup of G, it also acts on $\mathbf{H}$. We call the quotient $\Gamma(p)\backslash\mathbf{H}$ the *(noncompact) modular curve of level p*, and denote it by $Y(p)$. One can show that this quotient is in fact the set of complex points of a smooth quasi-projective curve.

EXAMPLE II.5. The space $Y(3)$ is homeomorphic to a Riemann sphere minus four points, and $Y(5)$ is homeomorphic to a Riemann sphere minus twelve points. For larger primes we encounter spaces of nonzero genus. For example, $Y(7)$ is homeomorphic to a surface of genus three minus twenty-four points.

By Proposition II.3, we know that points in $Y(p)$ correspond to p-marked lattices of any determinant d, and so as before we add a superscript to $Y(p)$ to indicate that we consider p-marked lattices of some fixed determinant. Accordingly, we call the disjoint union

$$\mathscr{Y}(p) := \coprod_{d \in (\mathbb{Z}/p)^\times} Y^d(p).$$

the *full (noncompact) modular curve of level p*. The reader is warned that these notations are not standard (cf. Remark II.3).

Now we compactify $Y(p)$. The key idea is that instead of dealing with each $Y(p)$ individually, we add suitable "points at infinity" to $\mathbf{H}$ and compactify all $Y(p)$ simultaneously. First, we enlarge $\mathbf{H}$ by forming the disjoint union $\mathbf{H}^* := \mathbf{H} \cup \mathbb{Q} \cup \{\infty\}$. To picture these points, think of $\mathbb{Q}$ as being a subset of the real axis of $\mathbb{C}$, and the point ∞ as lying infinitely far up the imaginary axis. We topologize $\mathbf{H}^*$ using the *Satake topology*. Given a point $q \in \mathbb{Q}$, we take as a fundamental system of open neighborhoods the sets S given by

$$S := \{q\} \cup \{\text{the interior of a disk tangent to the real axis at } q\}.$$

For the point ∞, we take the family of open half planes H where

$$H := \{z \in \mathbf{H} \mid \Im(z) > \text{constant}\}.$$

The following picture illustrates these sets for ∞ and a fixed q:

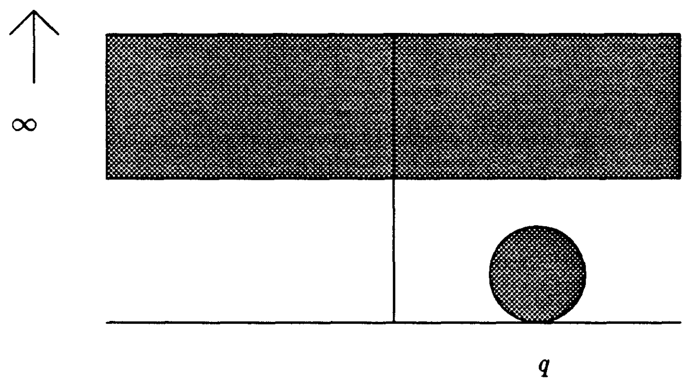

FIGURE II.2.

The action of G and hence of $\Gamma(p)$ extends to an action on $\mathbf{H}^* - \mathbf{H}$, and thus we may form the quotient $\Gamma(p)\backslash\mathbf{H}^*$. The virtue of the Satake topology is that with the quotient topology, $\Gamma(p)\backslash\mathbf{H}^*$ is actually a compact manifold. We call this quotient the *(compact) modular curve of level p* and denote it by $X(p)$. As above in the case of $Y(p)$, we use a superscript to indicate a choice of determinant, and we define the *full modular curve* $\mathscr{X}(p)$ by

$$\mathscr{X}(p) := \coprod_{d \in (\mathbb{Z}/p)^\times} X^d(p).$$

EXAMPLE II.6. As one would expect, $X(3)$ is a Riemann sphere, and $X(7)$ is a surface of genus three.

Elements of the set $X(p) - Y(p)$ are called *cusps*. Clearly, the set of cusps is nothing more than the set of orbits of the $\Gamma(p)$ in $\mathbb{Q} \cup \{\infty\}$. Indeed, we have the following convenient description. Let $\Xi(p)$ be the set of nonzero column vectors in $(\mathbb{Z}/p)^2$ modulo the relation that $v \sim -v$.

PROPOSITION II.4. *There is a bijection between $X(p) - Y(p)$ and $\Xi(p)$. Writing $a/b \in \mathbb{Q}$ in lowest terms, with the convention that $1/0 = \infty$, the correspondence is*

$$\frac{a}{b} \longmapsto \begin{pmatrix} a \\ b \end{pmatrix} \bmod p.$$

PROOF. See [Shi71]. □

COROLLARY II.2. *$X(p)$ has $(p^2-1)/2$ cusps, and $\mathscr{X}(p)$ has $(p-1)(p^2-1)/2$ cusps.*

In II.5 we shall see how the cusps correspond to "p-marked lattices at infinity."

REMARK II.2. Notice cusps are labeled by *column* vectors. Because of the content of Remark II.1, this is not just a formal distinction.

REMARK II.3. The extra components of the full modular curve are usually described in the literature in terms of *adeles*. Following MacPherson [Mac90], we have chosen a more elementary description.

3. Rational Polyhedral Cones

Our next goal is to construct a simplicial decomposition of $\mathscr{X}(p)$. This has been done in many different contexts and in many different levels of generality, notably by [Vor08] and by Ash in [AMRT75]. Here we develop this reduction theory only to the extent for our investigation. Our exposition in this and the following section follows [Ash77] and [McC87]

Given a real vector space V, an *open cone* C is a subset satisfying the following:

(a) If $x \in C$ and $\lambda \in \mathbb{R}_{>0}$, then $\lambda x \in C$.
(b) C contains no straight lines.
(c) C does not contain the origin.

An open cone C is called *rational polyhedral* if there exists a finite set of points $\{x_i\} \subset V(\mathbb{Q})$ such that C is the interior of the convex hull of the rays $\{(\mathbb{R}_{>0})x_i\}$. We say that C is *spanned* by this set of rays.

Now let V be the three-dimensional real vector space of all 2×2 symmetric matrices over $\mathbb{R}$, and let Q^+ be the open cone of positive-definite matrices. We think of Q^+ as being the space of positive-definite quadratic forms in the obvious way. Let $\mathbb{P}Q^+$ be the projectivization of Q^+, in other words the set of all positive-definite quadratic forms modulo scalars. It is well known that there exists a homeomorphism

$$\mathbf{H} = G/K \longrightarrow \mathbb{P}Q^+$$

given by $xK \longmapsto x \cdot x^t$. Note that this homeomorphism allows us to define an action of Γ on $\mathbb{P}Q^+$. We will identify a distinguished family of rational polyhedral cones in Q^+ that will induce a decomposition of $\mathbb{P}Q^+$. We will see that Γ acts equivariantly on this decomposition, and so we will obtain decompositions of $Y(p)$, $X(p)$, $\mathscr{Y}(p)$, and $\mathscr{X}(p)$.

Let Ξ be the set of primitive column vectors in $\mathbb{Z}^2$ modulo the relation that $v \sim -v$. Any $v \in \Xi$ determines a ray $\rho(v) \subset Q$ by

$$v \longmapsto (\mathbb{R}_{>0})v \cdot v^t.$$

Note that $\rho(v) \not\subset Q^+$, because the associated quadratic forms are indefinite.

Let v, $w \in \Xi$. We say that the pair (v, w) is *admissible* if there exist lifts $\bar{v}$, $\bar{w}$ in $\mathbb{Z}^2$ such that $\det(\bar{v}, \bar{w}) = 1$. Any admissible pair (v, w) determines a rational polyhedral cone in Q^+ by

$$(v, w) \longmapsto \alpha(v, w) := \{\text{span of } \rho(v) \text{ and } \rho(w).\}$$

Note that $\alpha(v, w)$ really is a subset of Q^+.

We may also form a similar construction for triples. Let v, w, $x \in \Xi$. We say that (v, w, x) is admissible iff each pair is admissible. Admissible triples also determine rational polyhedral cones $\beta(v, w, x) \subset Q^+$:

$$(v, w, x) \longmapsto \beta(v, w, x) := \{\text{span of } \rho(v),\ \rho(w), \text{ and } \rho(x).\}$$

Finally, let Δ denote the set of all $\alpha(v, w)$ and $\beta(v, w, x)$, as the arguments vary over all admissible pairs and triples of Ξ.

The left action of Γ on Ξ induces a left action on Δ in the obvious manner. We have the following proposition:

PROPOSITION II.5. *Δ is a locally finite decomposition of Q^+ into convex sets that satisfies the following properties:*

(a) Every point of Q^+ is contained in a unique cone of Δ.
(b) Given an admissible triple (v, w, x),

$$\overline{\beta(v, w, x)} = \beta(v, w, x) \cup \alpha(v, w) \cup \alpha(w, x) \cup \alpha(v, x).$$

Here the bar denotes closure in Q^+.
(c) There are two Γ orbits in Δ, one containing all the $\alpha(v, w)$, and the other containing all the $\beta(v, w, x)$.

Here is a picture of part of Δ. We have identified Q with $\mathbb{R}^3$ by

$$\begin{pmatrix} z + x & y \\ y & z - x \end{pmatrix} \longmapsto (x, y, z).$$

With these coordinates, Q^+ is the interior of the upper half of the double cone $x^2 + y^2 = z^2$. This is the right circular cone depicted. We have chopped off most of the cone to show some of the inner structure of Δ. Each shaded triangle is part of an $\alpha(v, w)$. They group together in threes to form the boundary of the $\beta(v, w, x)$. To add more cones to Δ, glue eight pyramids to the eight triangles on the outside, and so forth. Ultimately, the cones fill in all of Q^+.

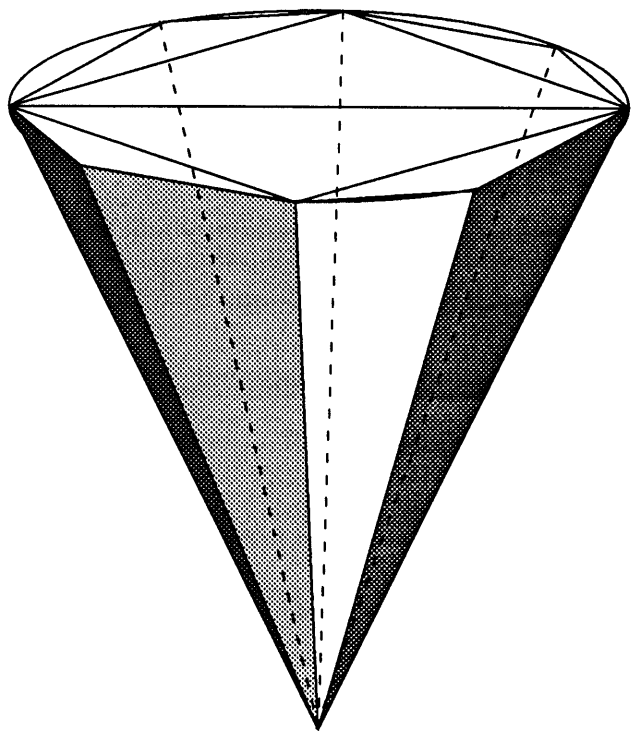

FIGURE II.3. The polyhedral decomposition of Q^+.

4. The Voronoï Decomposition

Now we wish to pass from a decomposition of Q^+ to a decomposition of $\mathbb{P}Q^+ = \mathbf{H} = G/K$.

PROPOSITION II.6. *The natural map* $Q^+ \longrightarrow \mathbb{P}Q^+$ *takes the cones* $\alpha(v,w)$ *to topological 1-cells and the cones* $\beta(v,w,x)$ *to topological 2-cells. Hence* Δ *descends to a locally finite decomposition of* $\mathbb{P}Q^+$ *into cells.*

PROOF. This is clear. □

DEFINITION II.8. This decomposition of $\mathbb{P}Q^+$ is called the *Voronoï decomposition*. By abuse of notation, we also denote it by Δ.

We present two pictures of Δ. Figure II.4 depicts an affine section of three dimensional cone of positive-definite matrices shown in Figure II.3. The cones α and β become the edges and triangles. The cusps $\mathbb{Q}\cup\{\infty\}$ are distributed densely around the outside of the disk; we have indicated eight of them in the figure. The second picture shows these cells as subsets of $\mathbf{H}$. Note that the map $xK \mapsto x \cdot x^t$ takes line segments to circular arcs. Note also that the Voronoï decomposition of $\mathbf{H}$ is different from the usual decomposition of $\mathbf{H}$ into fundamental domains of $PSL_2(\mathbb{Z})$ (cf. [Ser73]).

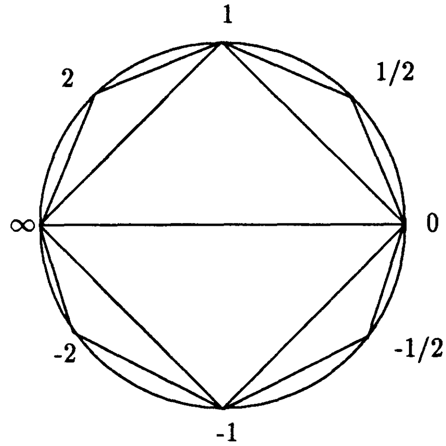

FIGURE II.4. An affine section of Q^+.

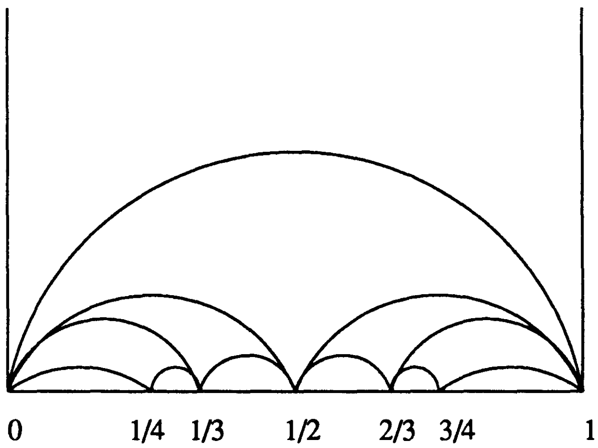

FIGURE II.5. The Voronoï decomposition in **H**.

Since Δ is Γ-equivariant by construction, it induces a decomposition $\Delta(p)$ of $Y(p)$ for all p. When we pass from $Y(p)$ to $X(p)$, we add the missing vertices to $\Delta(p)$, and the result is a simplicial decomposition of $X(p)$.

EXAMPLE II.7. With the Voronoï decomposition, the curve $X(3)$ becomes a tetrahedron, and $X(5)$ becomes an icosahedron. On the surface of genus three $X(7)$, the Voronoï decomposition is a triangulation with 56 triangles, 84 edges, and 24 vertices.

Finally, note that since all the connected components of $\mathscr{Y}(p)$ and $\mathscr{X}(p)$ are homeomorphic to each other, we may extend $\Delta(p)$ to a decomposition of all of $\mathscr{Y}(p)$ and $\mathscr{X}(p)$. By abuse of notation, we will refer to the Voronoï decomposition of any of these four spaces by $\Delta(p)$. Hopefully our meaning will be clear from context.

To complete this section, we must mention that although the Voronoï decomposition is a decomposition into topological cells, it is unfortunately not a regular cell complex in a strict sense. Consider, for example, the Voronoï complex associated to $Y(p)$. If we try to use the associated chain complex to compute homology, we conclude that $H_0(Y(p);\mathbb{C}) = 0$, since there are no zero-cells in $\Delta(p)$. This is certainly false, as $H_0(Y(p),\mathbb{C}) = \mathbb{C}$.

The resolution of our dilemma is that the Voronoï complex is actually what is known in the literature as a *regular cocell complex* (cf. [McC87]). Starting with $\Delta(p)$, we form a chain complex $(C^\bullet, \delta)$ indexed by *codimension* instead of dimension. The coboundary map

$$C^0 \xrightarrow{\delta} C^1$$

is just the obvious boundary map with appropriate signs. The cohomology of this complex is then the cohomology of $Y(p)$.

Although this is an easy point, it often causes confusion when discussing the Voronoï complex and its applications to modular varieties. The only important point for our study is that when we write a cycle with complex coefficients supported on the 1-skeleton of $\Delta(p)$, we are unambiguously specifying a class in $H^1(Y(p);\mathbb{C})$. There is no "extra" duality necessary.

5. Lattice Geometry of the Voronoï Cells

To complete our preliminary foray into the geometry of $\mathcal{Y}(p)$, we want to investigate the geometry of the lattices that appear in the Voronoï cells. In the process we will develop an indexing scheme that will aid us later. This scheme is an adaptation of ideas present in [McC87]

Recall that the cells in the Voronoï decomposition Δ of $\mathbf{H}$ correspond to $\alpha(v,w)$ and $\beta(v,w,x)$, where the arguments vary over all possible admissible pairs and triples of vectors in Ξ. We may define the barycenters of these cells in the obvious manner. Our first goal of this section is to prove the following:

PROPOSITION II.7. *In the curve $Y^d(p)$, the barycenters of the 1-cells correspond to equivalence classes of p-marked square lattices of determinant d. Similarly, the barycenters of the 2-cells correspond to equivalence classes of p-marked triangular lattices of determinant d.*

PROOF. Let v, w, $x \in \Xi$ be the three classes of

$$\begin{pmatrix}1\\0\end{pmatrix}, \quad \begin{pmatrix}0\\1\end{pmatrix}, \quad \text{and} \quad \begin{pmatrix}1\\1\end{pmatrix}.$$

The triple (v,w,x) is obviously admissible, and hence every 2-cell in $Y^d(p)$ comes from a Γ image of $\beta(v,w,x)$, and every 1-cell comes from a Γ image of $\alpha(v,w)$ (cf. Proposition II.5). Denote the barycenters of α and β by α_* respectively β_*. We will first show that the basis associated to β_* is a basis of the hexagonal lattice, and that the basis associated to α_* is a basis of the square lattice.

This is easy to verify using the fact that the homeomorphism

$$G/K \xrightarrow{\sim} \mathbb{P}Q^+$$

is defined via

$$xK \longmapsto x \cdot x^t.$$

We can construct a section to this map; given a matrix $x \in Q^+$, we can construct a matrix y so that $x = y \cdot y^t$. Since the ray in Q^+ passing through α_* is all multiples of the identity matrix, the section takes

$$\alpha_* \longmapsto \begin{pmatrix} \sqrt{1} & 0 \\ 0 & \sqrt{1} \end{pmatrix}.$$

This is clearly a basis of the square lattice. Similarly, the ray passing through β_* is all multiples of

$$\begin{pmatrix} 2 & -1 \\ -1 & 2 \end{pmatrix},$$

and this time the section takes

$$\beta_* \longmapsto \begin{pmatrix} \frac{1}{\sqrt{2}} & \sqrt{\frac{3}{2}} \\ \frac{1}{\sqrt{2}} & -\sqrt{\frac{3}{2}} \end{pmatrix}.$$

To see that this is a basis of the triangular lattice, we must recall that by Remark II.1 we actually generate lattices in the rows. A simple computation shows that the rows of the above matrix are a basis for the triangular lattice.

Since every 1- and 2-cell is a Γ image of α and β, all the barycenters correspond to bases of the square and triangular lattices. Hence, we have shown that the barycenters of the cells in $Y^d(p)$ correspond to distinct equivalences classes of p-marked square and triangular lattices. The converse, that all equivalence classes arise in this way, is easy. □

COROLLARY II.3. *The genus of* $X^d(p)$ *is* $1 + (p-6)(p^2-1)/24$.

PROOF. This is a standard result, but we want to prove it using Proposition II.7 and counting p-marked lattices. The number of distinct p-markings any lattice can have is

$$|SL_2(\mathbb{F}_p)| = p(p^2-1).$$

Square lattices are equivalent in groups of four, and triangular lattices are equivalent in groups of six. Hence

$$\begin{aligned} \text{number of 1-cells in } X^d(p) &= p(p^2-1)/4, \\ \text{number of 2-cells in } X^d(p) &= p(p^2-1)/6. \end{aligned}$$

By Proposition II.4, the number of 0-cells in $X^d(p)$ is $(p^2-1)/2$. Now we can compute the Euler characteristic χ, and can use the fact that $2 - 2g = \chi$, where g is the genus. □

COROLLARY II.4. *Any point in a 1-cell of* $\Delta(p)$ *is a p-marked rectangular lattice, i.e. a lattice with a basis consisting of orthogonal vectors.*

PROOF. Let v, $w \in \Xi$ be as above. Then all quadratic forms in $\alpha(v, w)$ are of the form

$$\begin{pmatrix} \lambda_1 & 0 \\ 0 & \lambda_2 \end{pmatrix},$$

where $\lambda_i \in \mathbb{R}_{>0}$. The section above obviously takes these quadratic forms to orthogonal bases. $\square$

Now we wish to develop an indexing scheme for the 1-skeleton of $\Delta(p)$ in $\mathscr{X}(p)$ based on the principle of representing a 1-cell σ by the p-marked square lattice $L(\sigma)$ at its barycenter. Fix a connected component $X^d(p)$.

Recall that the set of cusps in $X^d(p)$ is equivalent to the set of pairs $(v; d)$ where

$$v \in \Xi(p) := \{(\mathbb{Z}/p)^2 - (0,0)^t\}/\{\pm 1\}$$

and $d \in (\mathbb{Z}/p)^\times$. (Cf. Proposition II.4.) Also, since $\Delta(p)$ is a simplicial decomposition of $X^d(p)$, every oriented 1-cell σ is uniquely determined by the ordered pair of cusps (ξ, ξ') that are its endpoints. Combining these facts, we shall write

$$\sigma = (v, v'; d) \quad \text{where } v, v' \in \Xi(p) \text{ and } \det(v, v') = \pm d \bmod p.$$

The condition that $\det(v, v') = \pm d \bmod p$ follows from the fact that $Y^d(p) \subset X^d(p)$ is the space of all p-marked lattices of determinant d, and the sign ambiguity arises because there is a sign ambiguity built into $\Xi(p)$.

Now given σ, we want to attach to the datum $(v, v'; d)$ a picture of a p-marked square lattice of determinant d. First we choose lifts $\bar{v}, \bar{v}' \in (\mathbb{Z}/p)^2$ so that $\det(\bar{v}, \bar{v}') = d \bmod p$. Then we draw $(\mathbb{Z}^2, m)$, where $m(1,0) = \bar{v}$ and $m(0,1) = \bar{v}'$.

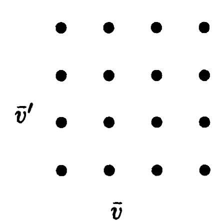

FIGURE II.6.

This is the lattice we shall call $L(\sigma)$.

Now we can bring the cusps ξ and ξ' into the picture. By Corollary II.4, every point in σ is a rectangular lattice. To represent motion within σ, we add the x- and y-axes to $L(\sigma)$, and we expand and contract these axes while preserving $\operatorname{vol} L(\sigma) = 1$:

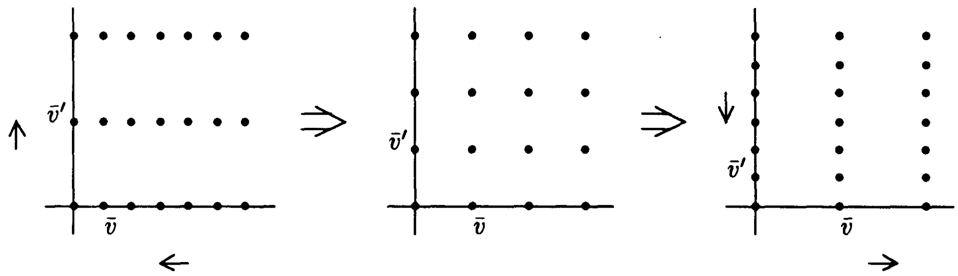

FIGURE II.7. Moving within $\sigma = (v, v'; d)$.

Consider moving towards the cusp $\xi = (v; d)$. In $L(\sigma)$ this corresponds to expanding the y-axis and contracting the x-axis, so that $L(\sigma)$ becomes a tall, thin rectangular lattice. Eventually all we see is a rank-one lattice in the x-axis, marked by the point $\bar{v} \in (\mathbb{Z}/p)^2$.

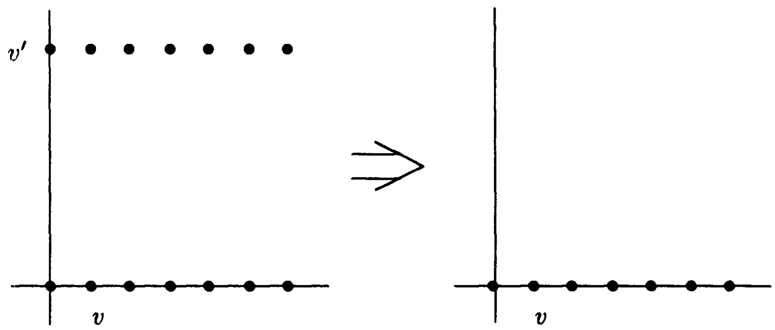

FIGURE II.8. The lattice at infinity.

This is the sense in which cusps correspond to p-marked lattices at infinity.

Similarly, to move towards the cusp $\xi' = (v'; d)$ we expand the x-axis and contract the y-axis. Eventually only the y-axis remains in the picture. Since this notion of stretching lattices will become important in later chapters, we make a formal definition:

DEFINITION II.9. The coordinate axes in the picture of $L(\sigma)$ are called the *stretching axes* of σ.

To conclude this investigation of the geometry of the 1-cells, we define *adjacency operators*:

DEFINITION II.10. Let $S^{\pm 1}$ respectively $S_{\pm 1}$ be the four matrices

$$\begin{pmatrix} 1 & \pm 1 \\ 0 & 1 \end{pmatrix} \quad \text{and} \quad \begin{pmatrix} 1 & 0 \\ \pm 1 & 1 \end{pmatrix}.$$

Let $\sigma = (v, v'; d)$ be a 1-cell in $\Delta(p)$. The matrices $S^{\pm 1}$ and $S_{\pm 1}$ act on σ from the right. They are called adjacency operators because they fix one endpoint of σ and move to an adjacent 1-cell. The action on $L(\sigma)$ is to shear along either the x- of y-axis. The result is a new p-marked square lattice corresponding to the barycenters of adjacent 1-cells in $X^d(p)$, as in the following figure.

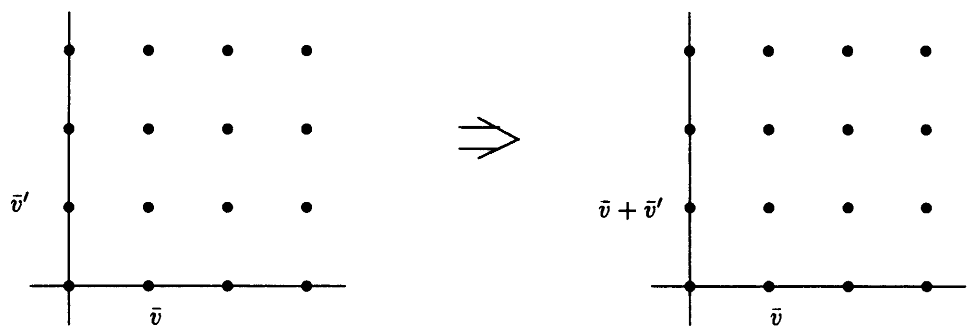

FIGURE II.9. Moving to an adjacent 1-cell.

CHAPTER III

Hecke Correspondences

In this chapter we describe the *Hecke correspondences*, which are the tools used to extract number-theoretic information from $H^1(\mathscr{Y}(p); \mathbb{C})$. Again, references for most of the material in this section are [Lan76], [Ser73], and [Shi71]. As before we follow the geometric style of [Mac90].

1. Sublattices

Consider the square lattice $\mathbb{Z}^2 \subset \mathbb{R}^2$ with fixed basis $\{(1,0),(0,1)\}$. Let ℓ be a prime, and let $\{L_k\}$ be the set of index ℓ sublattices of $\mathbb{Z}^2$. We claim that there are $\ell+1$ of these sublattices, and that they may be parameterized in a natural way by $\mathbb{P}^1(\mathbb{F}_\ell)$, the projective line over the finite field $\mathbb{F}_\ell$. To see this, first note that $(\mathbb{Z}^2)/\ell(\mathbb{Z}^2)$ has an obvious identification with the finite plane $(\mathbb{Z}/\ell)^2$. Then under the projection

$$\{(\mathbb{Z}/\ell)^2 - (0,0)\} \longrightarrow \mathbb{P}^1(\mathbb{F}_\ell),$$

each sublattice L_k is carried to a unique point of $\mathbb{P}^1(\mathbb{F}_\ell)$.

To be as explicit as possible, first write for $\mathbb{P}^1(\mathbb{F}_\ell)$ the set

$$\{\infty, 0, 1, \ldots, \ell - 1\}.$$

Then if $k \neq \infty$, we correspond

$$\{\text{the sublattice generated by } (-k,1) \text{ and } (\ell,0)\} \Longleftrightarrow \{k \in \mathbb{P}^1(\mathbb{F}_\ell)\},$$

and otherwise

$$\{\text{the sublattice generated by } (1,0) \text{ and } (0,\ell)\} \Longleftrightarrow \{\infty \in \mathbb{P}^1(\mathbb{F}_\ell)\}.$$

Definition III.1. The element $k \in \mathbb{P}^1(\mathbb{F}_\ell)$ associated to an index ℓ sublattice of $\mathbb{Z}^2$ is called the *type* of the sublattice.

We always use subscripts to indicate the type of a sublattice.

Example III.1. There are two distinguished sublattices L_∞ and L_0 that occur for every value of ℓ. We call these the *horizontal* and *vertical* sublattices:

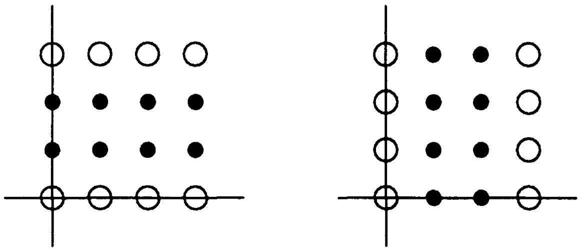

FIGURE III.1. Horizontal and vertical sublattices for $\ell = 3$

Now we describe a different invariant associated to L_k. Let $S(t)$ denote the one-parameter family of linear transformations

$$\begin{pmatrix} t & 0 \\ 0 & t^{-1} \end{pmatrix} \qquad \text{where } t \in \mathbb{R}_{>0}$$

acting on L_k from the right. This family expands and contracts L_k along the coordinate axes. Recall that a lattice is called rectangular if it has an orthogonal basis.

DEFINITION III.2. The *valence* $v(L_k)$ is the number of times that $S(t)L_k$ becomes rectangular as t varies over $\mathbb{R}_{>0}$.

The range of the valence function is the set $\mathbb{Z}_{>0}\bigcup\{\infty\}$. Using the correspondence between points of $\mathbb{P}^1(\mathbb{F}_\ell)$ and sublattices of index ℓ, we will also allow the domain of the valence function to include $\mathbb{P}^1(\mathbb{F}_\ell)$. We summarize some simple properties of v.

PROPOSITION III.1. *The valence function satisfies the following:*

(a) $v(L_k) = \infty$ *iff* $k = 0$ *or* $k = \infty$.
(b) $v(L_k) = v(L_{-k})$.
(c) $v(L_k) = v(L_{1/k})$.

PROOF. For (a), the sublattices L_0 and L_∞ are the horizontal and vertical stripe sublattices of Example III.1. Thus $v(L_k)$ is obviously infinite in these cases. The converse, that $v(L_k)$ is finite otherwise, will be addressed in Corollary IV.1 For (b) and (c), note that L_{-k} (respectively $L_{1/k}$) is obtained from L_k by reflection in the 45° line (resp. by a 90° rotation). □

2. Correspondences and Hecke Operators

We begin by defining correspondences.

DEFINITION III.3. Let X be a space. A *correspondence* on X is a diagram

$$(s,t)\colon C \rightrightarrows X$$

where C is an auxiliary space, called the *correspondence space*, and s and t are two maps, called respectively the *source* and *target* maps. Two correspondences $(s_i,t_i)\colon C_i \rightrightarrows X, i = 1,2$ are isomorphic if there exists an invertible map $\Phi\colon C_1 \to C_2$ such that $s_2 \circ \Phi = s_1$ and $t_2 \circ \Phi = t_1$.

Now let $\ell \neq p$ be a prime, and define the space $\mathscr{C}_\ell^0(p) \subset \mathscr{Y}(p) \times \mathscr{Y}(p)$ by

$$\mathscr{C}_\ell^0(p) := \{((L,m),(L',m')) \mid [L:L'] = \ell \text{ and } m' = m|_{L'}.\}$$

Construct two maps s and t from $\mathscr{C}_\ell^0(p)$ to $\mathscr{Y}(p)$ by projecting on the first and second factors, respectively.

Definition III.4. The diagram

$$(s,t)\colon \mathscr{C}_\ell^0(p) \rightrightarrows \mathscr{Y}(p)$$

is called a *Hecke correspondence.*

Note that lifting by s and then projecting by t takes a marked lattice (L,m) into the set of its index ℓ sublattices. This is the same as the action of the classical Hecke operator T_ℓ (cf. [Ser73]).

Proposition III.2. *The space $\mathscr{C}_\ell^0(p)$ is a noncompact surface with $p-1$ connected components.*

Proof. Clearly $\mathscr{C}_\ell^0(p)$ is a noncompact manifold, and must have at least $p-1$ connected components since $\mathscr{Y}(p)$ does. We will show that $\mathscr{C}_\ell(p)$ has exactly $p-1$ connected components. This will follow if we can construct a path from any point $((L,m),(L',m'))$ to $((\mathbb{Z}^2, m_{\text{std}}), (\mathbb{Z}^2_\infty, m_\infty)$, where $(\mathbb{Z}^2, m_{\text{std}})$ is the standard lattice of a given determinant (cf. Example II.3).

To see that this is possible, first take any path from (L,m) to $(\mathbb{Z}^2, m_{\text{std}})$. The sublattice (L',m') will be taken to some sublattice of $\mathbb{Z}^2$. Since ℓ is prime, we can apply adjacency operators $S^\pm$ and $S_\pm$ and move through all possible index ℓ sublattices of $\mathbb{Z}^2$. Furthermore, since ℓ is prime to p, we may move to $(\mathbb{Z}^2_\infty, m_\infty)$. Hence $\mathscr{C}_\ell^0(p)$ has exactly $p-1$ connected components. □

We will write this decomposition into connected components as

$$\mathscr{C}_\ell^0(p) = \coprod_{d \in (\mathbb{Z}/p)^\times} C_\ell^d(p),$$

where each component fits into a diagram of the form

$$Y^d(p) \xleftarrow{s} C_\ell^d(p) \xrightarrow{t} Y^{\ell d}(p).$$

Although we have defined the Hecke correspondence only over $\mathscr{Y}(p)$, we claim that we can also extend it over $\mathscr{X}(p)$:

Proposition III.3. *The Hecke correspondence extends continuously to a correspondence*

$$(s,t)\colon \mathscr{C}_\ell(p) \rightrightarrows \mathscr{X}(p),$$

where $\mathscr{C}_\ell(p)$ is a compact manifold.

PROOF. We investigate what happens as we move from a barycenter of a 1-cell to either of its endpoints, and then conclude that there is a unique way to compactify the correspondence continuously.

Let $\sigma = (v, v'; d)$ be an oriented 1-cell of $\Delta(p)$ and let $\xi = (v; d)$ and $\xi' = (v'; d)$ be its two endpoints. Recall that we represent σ by drawing a p-marked square lattice $L(\sigma)$ with coordinate axes.

Let $\{L(\sigma)_k \mid k \in \mathbb{P}^1(\mathbb{F}_\ell)\}$ be the set of index ℓ sublattices of $L(\sigma)$. Notice that the notation makes sense, because we have chosen a fixed way to draw $L(\sigma)$. Suppose we move towards the cusp ξ by letting the y-axis stretch to ∞. We see that the ℓ sublattices

$$L(\sigma)_0, \ \ldots, L(\sigma)_{\ell-1}$$

restrict to an index ℓ sublattice of the x axis, and the sublattice

$$L(\sigma)_\infty$$

restricts to an index one sublattice of the x axis.

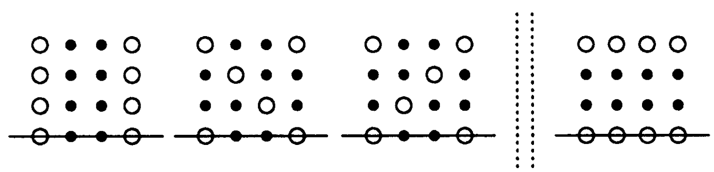

FIGURE III.2. Three of index three, and one of index one ($\ell = 3$).

Similarly, when we approach the cusp ξ' the ℓ sublattices

$$L(\sigma)_1, \ldots, L(\sigma)_\infty$$

restrict to an index ℓ sublattice of the y-axis and

$$L(\sigma)_0$$

restricts to an index one sublattice of the y-axis. and so we conclude that to extend s continuously to any cusp ξ, the set $s^{-1}(\xi)$ must contain two elements. A similar argument works for t, and so we extend the correspondence to $\mathscr{X}(p)$ by requiring both maps s, t to be two-to-one over the cusps. □

By abuse of notation, we will call this extended correspondence the Hecke correspondence. We shall write the diagram

$$(s, t)\colon \mathscr{C}_\ell(p) \rightrightarrows \mathscr{Y}(p)$$

and shall mean that the maps are to be restricted to $\mathscr{C}_\ell^0(p)$.

Given a cusp ξ, we will always write for the two inverse images

$$\{\xi_1, \xi_\ell\}$$

where the subscript denotes the index of the induced rank-one sublattice at the cusp.

3. Lifting the Voronoï Complex

Consider the Hecke correspondence

$$(s,t)\colon \mathscr{C}_\ell(p) \rightrightarrows \mathscr{X}(p).$$

Let $\Delta(p)$ be the Voronoï decomposition of $\mathscr{X}(p)$. We want to lift $\Delta(p)$ to $\mathscr{C}_\ell(p)$ using s and t.

DEFINITION III.5. Let $\Delta_s(p)$ be the decomposition of $\mathscr{C}_\ell(p)$ into cells given by

$$\Delta_s(p) := s^{-1}\Delta(p).$$

Similarly, let $\Delta_t(p)$ be the decomposition of $\mathscr{C}_\ell(p)$ given by

$$\Delta_t(p) := t^{-1}\Delta(p).$$

PROPOSITION III.4. *Both $\Delta_s(p)$ and $\Delta_t(p)$ are regular cell complexes.*

PROOF. Over $\mathscr{Y}(p)$ this is true since $\Delta(p)$ is a regular cell complex and s and t are covering maps. It is easy to check that extension over $\mathscr{X}(p)$ does not change this. □

Although $\Delta(p)$ is a simplicial complex, in general $\Delta_s(p)$ and $\Delta_t(p)$ will not be simplicial. This is clear, since usually different 1-cells upstairs will share the same vertices.

PROPOSITION III.5. *The genus of $C_\ell^d(p)$ is* $1 + \ell(p+1)(p^2-1)/24 - p^2/2$.

PROOF. This is a simple calculation, since we know the numbers of cells in both $\Delta_s(p)$ and $\Delta_t(p)$. □

Now we investigate some of the geometry these two cell complexes on the correspondence space. Choose an oriented 1-cell $\sigma = (v, v'; d) \in \Delta(p)$, and represent σ by a p-marked square lattice $L(\sigma)$ with coordinate axes. We draw a lift of σ by choosing a sublattice of type k:

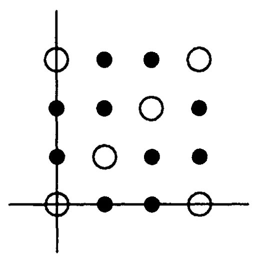

FIGURE III.3. A lift by s ($\ell = 3$, $k = 2$)

We denote this 1-cell in $\Delta_s(p)$ by $(v, v'; d)_k$. Notice that the sublattice will not be rectangular in general; this reflects the fact that the Hecke correspondence does not act cellularly on $\Delta(p)$.

Now consider a lift of σ by t. We draw $L(\sigma)$, this time using hollow dots, and then fill in a lattice $L'(\sigma)$ so that $L(\sigma) \subset L'(\sigma)$ is a sublattice of index ℓ.

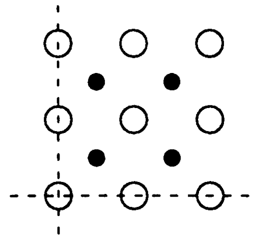

FIGURE III.4. A lift by t ($\ell = 2$)

Again, in general $L'(\sigma)$ will not be rectangular. We use no special notation for lifting 1-cells by t, since we will always lift by s and project by t. However, we use dashed coordinate axes to describe how to move within $t^{-1}(\sigma)$, as in the figure. The coordinate axes given with the lattice always determine how to move within the lifted cell. We illustrate what we mean with an example.

EXAMPLE III.2. Suppose $\ell = 5$. Then there exists a sublattice of the square lattice which is itself square. In $\mathscr{C}_\ell(p)$, this implies that there is a 1-cell $\sigma_s \in \Delta_s(p)$ and a 1-cell $\sigma_t \in \Delta_t(p)$ that intersect in their barycenters:

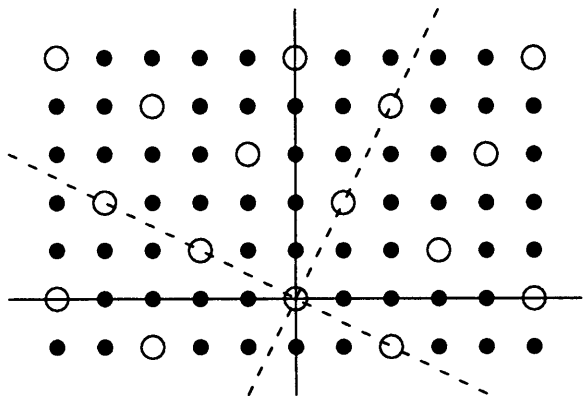

FIGURE III.5. A square sublattice of index 5

Notice that as we stretch the solid axes to remain in σ_s, we leave σ_t, for the hollowsublattice ceases to be rectangular. Similarly, as we stretch the dashed axes to remain in σ_t, we leave σ_s. Thus we conclude that σ_s and σ_t intersect transversely in $\mathscr{C}_\ell(p)$.

EXAMPLE III.3. Consider the horizontal and vertical stripe sublattices of Example III.1. In these cases, the stretching axes for the hollow sublattices are also the x- and y- axes, which means that the cells with these lattices at their barycenters must map cellularly under both s and t. We call these 1-cells *common edges*, since they are common to both $\Delta_s(p)$ and $\Delta_t(p)$. Furthermore, we can describe the action of t on these cells in terms of our indexing scheme:

$$t\colon (v, v'; d)_0 \longmapsto (\ell v, v'; \ell d)$$
$$t\colon (v, v'; d)_\infty \longmapsto (v, \ell v'; \ell d)$$

The figures in this chapter use our conventions for drawing lattices and sublattices. Since these will be used repeatedly in this paper, we summarize them:

Important conventions for lattices and cusps.

Given the point $((L, m), (L', m'))$, we will always draw L using solid dots and L' using hollow dots. Let ξ be a cusp and let $s^{-1}(\xi) = \{\xi_1, \xi_\ell\}$. Since the induced sublattice at ξ_1 is completely hollow, we shall call this the hollow cusp. Similarly, since the induced sublattice at the cusp ξ_ℓ is mostly solid, we shall call this the solid cusp.

CHAPTER IV

The Universal Hecke Correspondence

In this chapter we present the main construction of this thesis, the universal Hecke correspondence $\mathscr{C}_\ell$. This is a space such that for any Hecke correspondence, the correspondence space $\mathscr{C}_\ell(p)$ is constructed from a finite collection of $\mathscr{C}_\ell$'s, with identifications that depend only on p.

The basic problem is simple. We begin with a Hecke correspondence

$$(s,t)\colon \mathscr{C}_\ell(p) \rightrightarrows \mathscr{X}(p)$$

defined on a full modular curve $\mathscr{X}(p)$. As in III.3, using s and t we construct the lifts $\Delta_s(p)$ and $\Delta_t(p)$. Neither of the maps

$$s\colon \Delta_t(p) \to \Delta(p) \quad \text{nor} \quad t\colon \Delta_s(p) \to \Delta(p)$$

is cellular. Understanding the geometry of $\Delta_s(p)$ and $\Delta_t(p)$ is the key to understanding the action of this Hecke correspondence on the cohomology of $\mathscr{Y}(p)$ and $\mathscr{X}(p)$.

So how do we accomplish this? To study the geometry of $\Delta_s(p)$ and $\Delta_t(p)$, we investigate the lattices in $\mathscr{C}_\ell(p)$. Recall (cf. Example III.3) that there are *common edges* of $\Delta_s(p)$ and $\Delta_t(p)$: these are 1-cells that map cellularly under both s and t. We decompose $\mathscr{C}_\ell(p)$ by cutting along these common edges, and the result is a finite disjoint union of homeomorphic surfaces with boundary. Then the space $\mathscr{C}_\ell$ will be the universal covering space of any of these pieces.

Of course, to understand explicitly the action of the correspondence on cohomology, it is not sufficient to build $\mathscr{C}_\ell$ as an abstract covering space. Hence we present a combinatorial model for $\mathscr{C}_\ell$ in IV.3. Unfortunately, without any examples, this model seems obscure, and so we engage in what appears to be a leisurely discussion of examples. In IV.1 we describe the simplest example, namely the production of $\mathscr{C}_2$ from the correspondence $\mathscr{C}_2(3) \rightrightarrows \mathscr{X}(3)$. Then in IV.2 we present another example, the production of $\mathscr{C}_5$ from the correspondence $\mathscr{C}_5(3) \rightrightarrows \mathscr{X}(3)$. These two examples exhibit most of the complexity of the general case. The main theorem of the thesis is stated and proved in IV.4. Finally in IV.5 we show how the geometry of $\mathscr{C}_\ell$ leads to an algorithm to compute the action of the Hecke correspondence on cohomology.

1. Example I ($p = 3, \ell = 2$)

Let $\mathscr{X}(3)$ be the full compact modular curve of level three. Recall that every point $(L, m) \in \mathscr{Y}(3) \subset \mathscr{X}(3)$ is a 3-marked lattice. Globally $\mathscr{X}(3)$ is a disjoint union of two Riemann spheres, $X^1(3)$ and $X^2(3)$, and with the Voronoï decomposition $\Delta(3)$ each connected component becomes a tetrahedron. Moreover, the cusps are the eight points

$$\left(\begin{pmatrix}1\\0\end{pmatrix};d\right), \quad \left(\begin{pmatrix}0\\1\end{pmatrix};d\right), \quad \left(\begin{pmatrix}1\\1\end{pmatrix};d\right), \quad \text{and} \quad \left(\begin{pmatrix}2\\1\end{pmatrix};d\right),$$

where $d = 1, 2$ and the four column vectors are the four classes in $\Xi(3)$. Recall that to specify a 1-cell $\sigma \in \Delta(3)$, we draw a 3-marked lattice and add coordinate axes (5).

The two connected components $X^1(3)$ and $X^2(3)$ are homeomorphic, but they have opposite orientations:

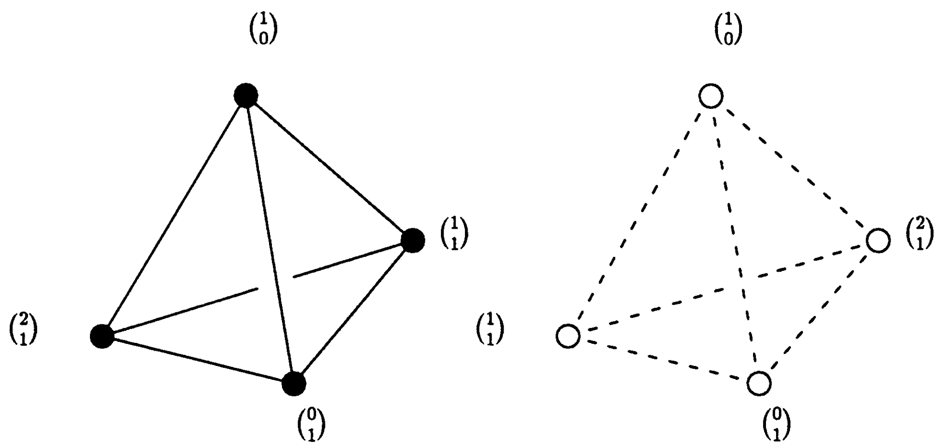

FIGURE IV.1.

The figure adheres to our convention (cf p. 35). We draw edges in $X^1(3)$ using solid lines (since $X^1(3)$ will be the image of s), and we draw edges in $X^2(3)$ using dashed lines (since $X^2(3)$ will be the image of t).

In this example, we consider the Hecke correspondence of index two:

$$(s, t)\colon \mathscr{C}_2(3) \rightrightarrows \mathscr{X}(3).$$

Recall that points in $\mathscr{C}_2(3)$ are indexed by the datum $((L, m); (L', m'))$, where $L' \subset L$ is an index 2 sublattice. The space $\mathscr{C}_2(3)$ also has two components, $C_2^1(3)$ and $C_2^2(3)$, and the Hecke correspondence breaks apart into a disjoint union of two diagrams. For convenience, we focus on the diagram

$$X^1(3) \xleftarrow{s} C_2^1(3) \xrightarrow{t} X^2(3).$$

Thus, our immediate problem is to understand the geometry of $C_2^1(3)$.

By Proposition III.5, the genus of $C_2^1(3)$ is zero, and we want to analyze explicitly the induced decomposition $\Delta_s(3)$ of $C_2^1(3)$ To do this we start with a path γ around a cusp $\xi \in X^1(3)$. Using s, we lift γ to two paths in $C_2^1(3)$, one circling ξ_1, and one circling ξ_2. (The meaning of these subscripts is discussed at the end of III.2.) To be explicit, we take as a cusp $\xi = (\binom{1}{0}; 1)$, and take γ to connect the barycenters of the three edges that meet ξ:

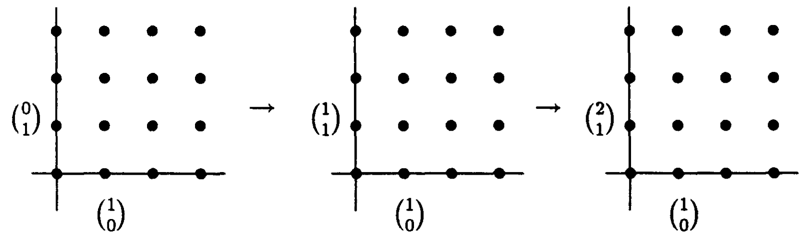

FIGURE IV.2. A path connecting three barycenters in $X^1(3)$.

The path γ can be describes shearing the lattice at the left of the figure along the x axis using the one-parameter family of linear transformations

$$\begin{pmatrix} 1 & -t \\ 0 & 1 \end{pmatrix}, \quad \text{where } t \in [0,3].$$

Note that combinatorially we are just applying the adjacency operator

$$S^+ = \begin{pmatrix} 1 & 1 \\ 0 & 1 \end{pmatrix}$$

to the 1-cell represented by the lattice at the left of the figure.

First lift γ to a path around ξ_1:

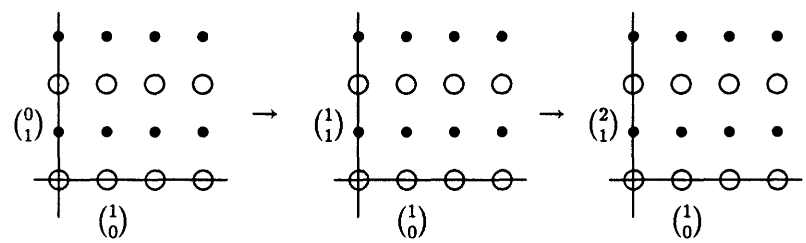

FIGURE IV.3. Three barycenters in $C_2^1(3)$.

This lift passes through three 3-marked square lattices with index 2 sublattice, and therefore we conclude that the decomposition $\Delta_s(3)$ contains three 1-cells that meet the vertex ξ_1.

Now we lift γ to a path around ξ_2:

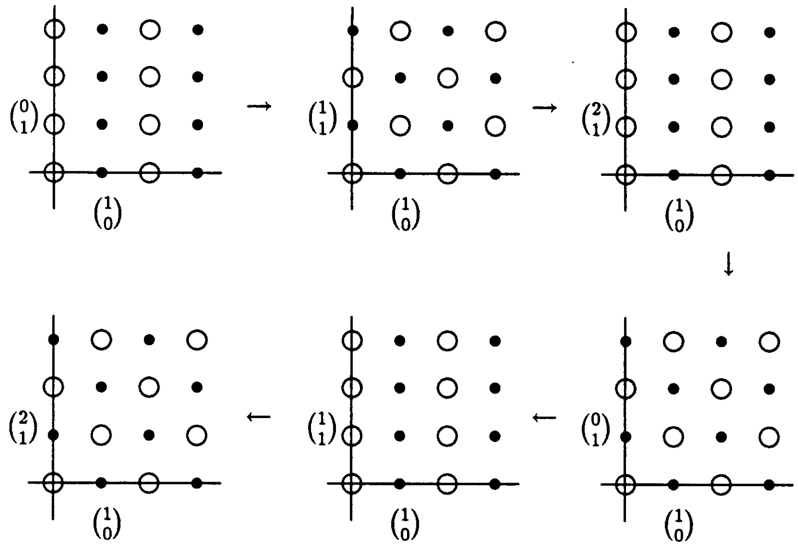

FIGURE IV.4. Six barycenters upstairs

This time, however, the lift of γ passes through *six* 3-marked square lattices with index 2 sublattice. Hence $\Delta_s(3)$ must contain six 1-cells that meet ξ_2. This argument is clearly independent of the choice of the initial cusp ξ and so it remains to find a cell decomposition of the sphere with

- twelve 2-cells,
- eighteen 1-cells, and
- eight 0-cells, where
- four 0-cells meet three 1-cells, and
- four 0-cells meet six 1-cells.

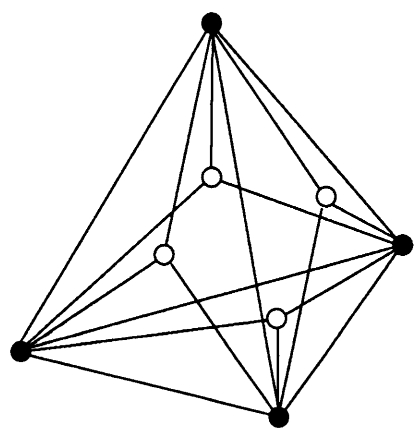

FIGURE IV.5.

This is $\Delta_s(3)$ in $C_2^1(3)$.

Now, to complete the picture, we must find $\Delta_t(3)$. First, we look for the common edges. We know that these correspond to the horizontal and vertical stripe sublattices of $L(\sigma)$ (cf. Example III.3) Considering the two lifts of γ, we see that the four hollow cusps meet only common edges, while every other edge the four solid cusps meet is a common edge. We indicate the common edges in the following picture by thick 1-cells.

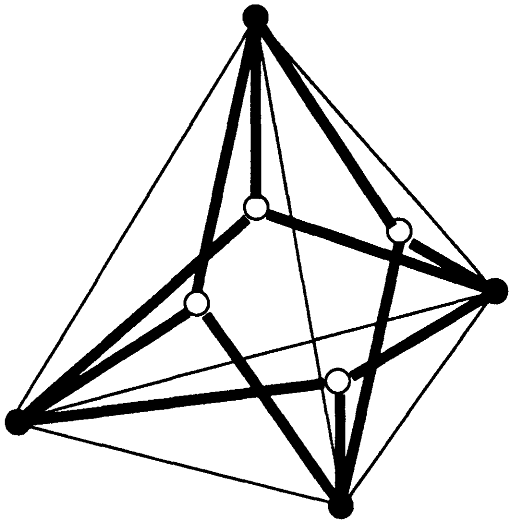

FIGURE IV.6.

To complete our analysis, we must account for the remaining 1-cells in $\Delta_t(3)$. There are six of these 1-cells; they correspond to the sublattices of type 1. Again, we focus attention on one such 1-cell, represented by the figure

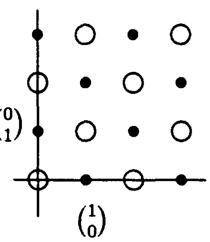

FIGURE IV.7.

First, note that the image of this point under t is 3-marked square lattice, and hence is the barycenter of a 1-cell σ' in $X^2(3)$. From Figure 1, we see that $\sigma' = (\binom{1}{1}, \binom{2}{1}; 2)$. and so our dashed 1-cell meets the hollow cusps $(\binom{1}{1}; 2)$ and $(\binom{2}{1}; 2)$. Furthermore, note that when we expand and contract the x and y axes, Figure 1 is the *only* time that both the solid and hollow lattices are rectangular. In other words, this is the only time that these two 1-cells in $\Delta_s(3)$ and $\Delta_t(3)$ intersect. The picture is identical for the five remaining 1-cells in $\Delta_t(3)$, which means that the only possible picture for $C_2^1(3)$ is the following:

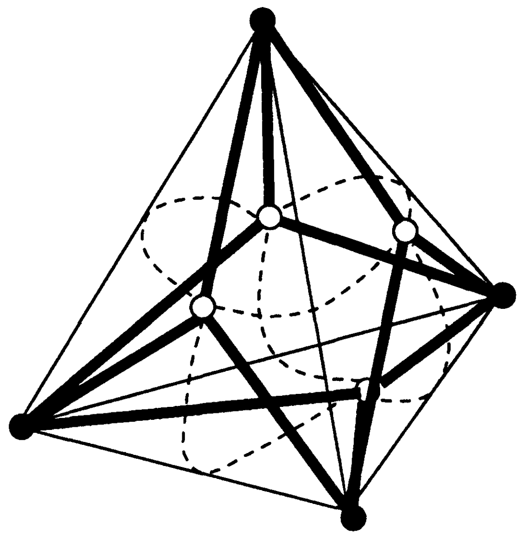

FIGURE IV.8.

Notice that this figure is completely symmetric in $\Delta_s(3)$ and $\Delta_t(3)$.

To complete the discussion, as promised we decompose $C_2^1(3)$ along the common edges. The result is six copies of the following object:

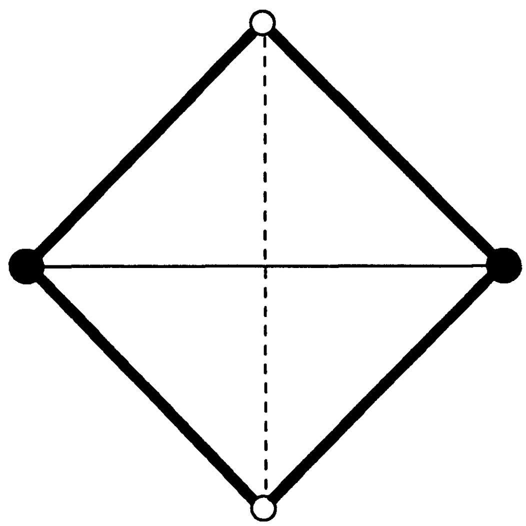

FIGURE IV.9.

This is the space that we shall call the universal Hecke correspondence $\mathscr{C}_2$. The instructions necessary to assemble $C_2^1(3)$ from copies of this space only depend on arithmetic modulo 2.

2. Example II ($p = 3, \ell = 5$)

Now let $\ell = 5$, and consider the Hecke correspondence

$$(s,t)\colon \mathscr{C}_5(3) \rightrightarrows \mathscr{X}(3).$$

Again we look at the following portion of the correspondence:

$$X^1(3) \longleftarrow C_5^1(3) \longrightarrow X^2(3).$$

This time using the genus formula, we find that $C_5^1(3)$ is a surface of genus three.

We proceed exactly as before, by lifting a path γ around a cusp $\xi \in X^1(3)$ to two paths in $C_5^1(3)$. As before we take a path connecting the barycenters of the 1-cells incident to ξ and find that

- ξ_1 meets three 1-cells in $\Delta_s(3)$, and
- ξ_5 meets fifteen 1-cells in $\Delta_s(3)$.

Now we look for the common edges. Again we find that γ_1 meets only common edges, but this time every fifth 1-cell that γ_5 meets is a common edge. After a somewhat longer period of experimentation than for $\ell = 2$, we arrive at the following picture:

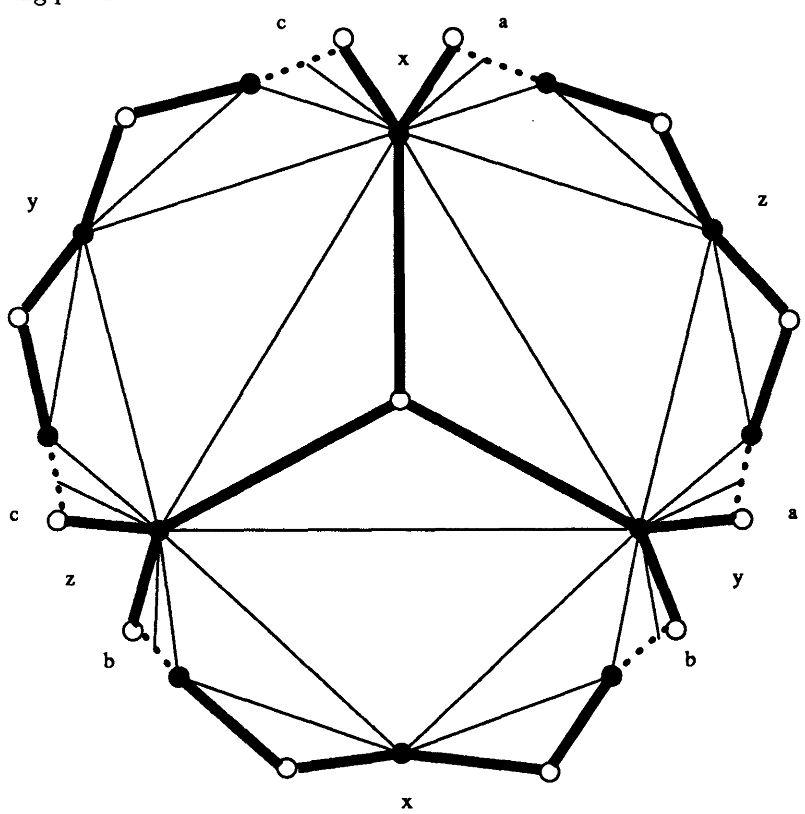

FIGURE IV.10.

Notice that there are identifications along the boundary. To reconstruct the space, identify pairwise the solid vertices labeled x, y, and z, and glue the dotted edges labeled a, b, and c pairwise together. There are a few remaining identifications, and it is a pleasant to zip the surface up into a closed manifold. The interested reader may verify that this is indeed a surface of genus three.

Now we must find $\Delta_t(3)$. Our key tool is the following lemma:

LEMMA IV.1. (RECONSTRUCTION LEMMA) *Fix p and ℓ as usual. If given any σ in $\Delta_s(p)$ we know the number of times σ intersects the 1-skeleton of $\Delta_t(p)$ as subspaces of $\mathscr{C}_\ell(p)$, then we may uniquely reconstruct the 1-skeleton of $\Delta_t(p)$ as a subspace of $\mathscr{C}_\ell(p)$.*

We defer the proof of this lemma until IV.4, but we want to apply it to this example. The point is that the intersection information is exactly contained in the valence function.

For example, let $\sigma_0 = (v, v'; d)_0$ be the following 1-cell in $\Delta_s(3)$:

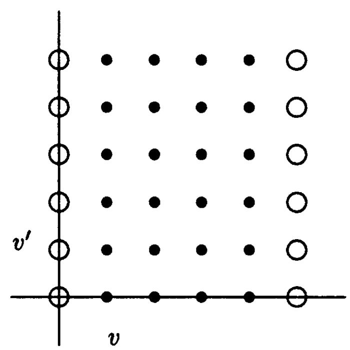

FIGURE IV.11.

Recall that S^+ is the adjacency operator

$$\begin{pmatrix} 1 & 1 \\ 0 & 1 \end{pmatrix}.$$

Apply S^+ to σ_0 until we reach another common edge. Since this operator acts by shearing to the left along the x-axis, we observe that

$$\text{the type of } L(\sigma_0) \cdot S^{+k} \text{ is } k \in \mathbb{P}^1(\mathbb{F}_5).$$

Since $v(L_k) = v(L_{\pm 1/k})$, to compute all the valences we only need to compute $v(L_1)$ and $v(L_2)$. First consider L_1. We claim that $v(L_1) = 4$, and the four times the sublattice becomes rectangular correspond to the four bases $(\mathbf{v}_1, \mathbf{v})$, $(\mathbf{v}_2, \mathbf{v})$, $(\mathbf{v}_3, \mathbf{v})$, and $(\mathbf{v}_4, \mathbf{v})$ shown below.

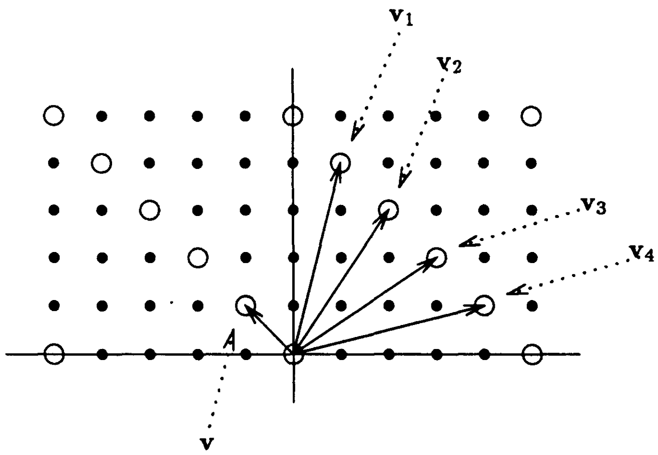

FIGURE IV.12.

We shall later develop an algorithm to enumerate these bases, but merely note that the only possible bases that can work must have a vector in the first and fourth quadrants. The reader may convince himself that these are the only four possibilities.

Now have a look at L_2:

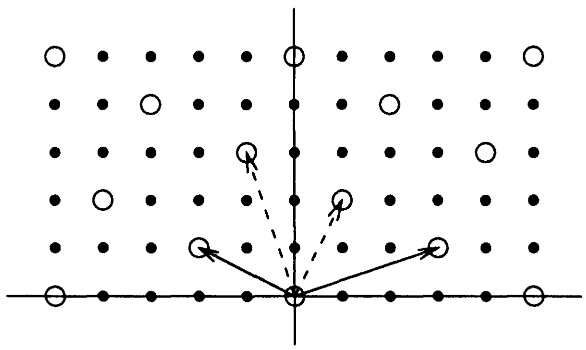

FIGURE IV.13.

This picture appears in Example III.2; it corresponds to a solid 1-cell and a dashed 1-cell intersecting in their barycenters. The figure itself is one of three times that L_2 becomes rectangular, and the other two bases are indicated.

Now we may put everything together. Start with a 1-cell σ' in $\Delta_s(3)$. If we repeatedly apply S^+ to σ', we find that $v(L(\sigma') \cdot S^{+i})$ steps through either of the sequences

$$\{\infty, 4, 3, 3, 4, \infty, 4, 3, 3, 4, \ldots\} \quad \text{or} \quad \{\infty, \infty, \infty, \infty, \infty, \ldots\},$$

depending on whether the cusp fixed by S^+ is ξ_1 or ξ_5. This means that there are two types of triangles in $\Delta_s(3)$, which we may fill in with dashed arcs:

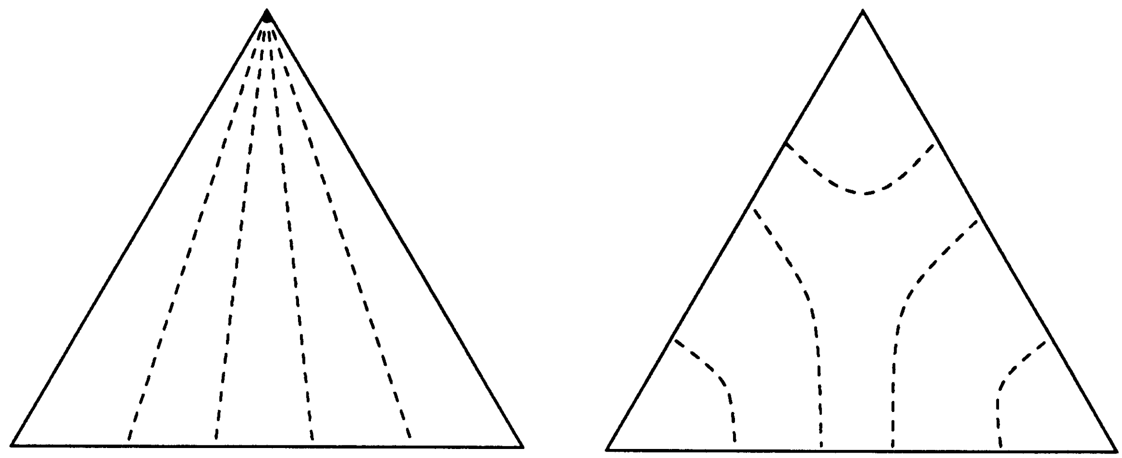

FIGURE IV.14.

Finally, we may return to our global picture of $C_5^1(3)$:

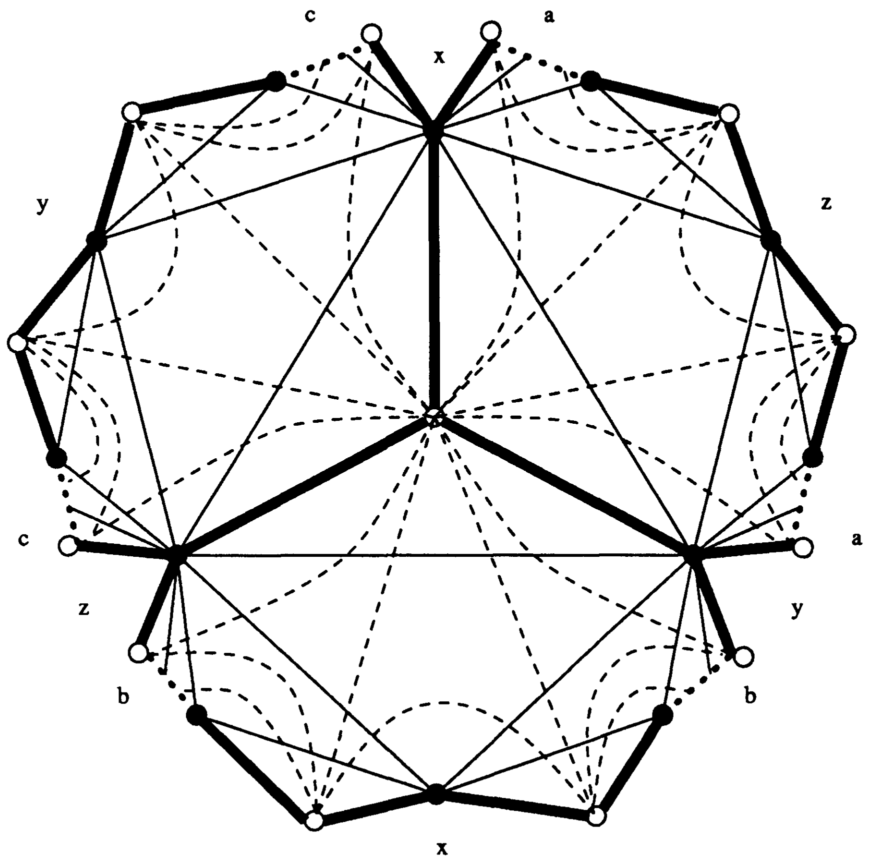

FIGURE IV.15.

If we decompose this space along the common edges, we obtain a disjoint union of three strips, and we may pass to their universal cover:

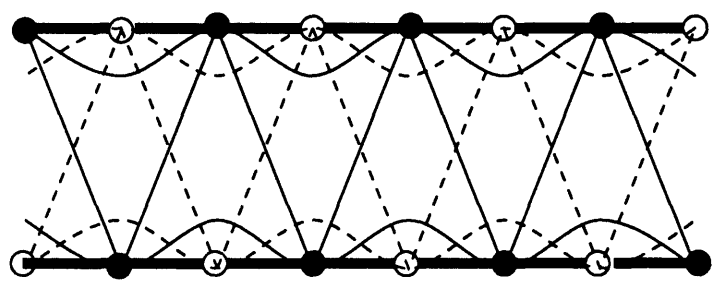

FIGURE IV.16.

This is the space that we shall call $\mathscr{C}_5$.

3. The Construction

Now we distill the essential features of the previous two examples and describe the construction of $\mathscr{C}_\ell$. The basic idea is to construct a space with the structure of a simplicial complex that has the valence data attached to its edges. Then using the reconstruction lemma we build another simplicial complex structure on the space.

Since sublattices are equivalent to point in a finite projective space, we begin with the finite projective line $\mathbb{P}^1(\mathbb{F}_\ell)$. Recall that we explicitly write the points in $\mathbb{P}^1(\mathbb{F}_\ell)$ as the set $\mathbb{F}_\ell \cup \{\infty\}$:

$$\{\infty, 0, 1, \dots, \ell - 1\}.$$

We extend addition and multiplication from $\mathbb{F}_\ell$ to $\mathbb{P}^1(\mathbb{F}_\ell)$ by defining

- $\infty + k = \infty$ for all $k \in \mathbb{P}^1(\mathbb{F}_\ell)$, and
- $\infty \cdot k = \infty$ for all $k \in \mathbb{P}^1(\mathbb{F}_\ell)$.

Before constructing $\mathscr{C}_\ell$, we must standardize some terminology. Let T be a triangle, and let $\bar{T}$ be the barycentric subdivision of T. In $\bar{T}$, the original triangle T is called the *outer triangle*, and the six smaller triangles are called the *inner triangles*. Similarly, the edges of T are called *outer edges*, and the additional edges of $\bar{T}$ are called *inner edges*. Two inner triangles are called an *edge pair* if two of their edges form an outer edge. A *labeling* for $\bar{T}$ is a function $\{\text{inner triangles of } \bar{T}\} \to \mathbb{P}^1(\mathbb{F}_\ell)$.

DEFINITION IV.1. Let $k \in \mathbb{P}^1(\mathbb{F}_\ell)$. A *brick* B_k is a barycentrically subdivided triangle T, with a labeling, subject to the following restrictions:

(a) As we proceed clockwise around the barycenter of the triangle, the labels must follow the sequence

$$k \to k+1 \to -\frac{1}{k+1} \to \frac{k}{k+1} \to -\frac{k+1}{k} \to -\frac{1}{k} \to k.$$

(b) If two inner triangles form an edge pair, then their labels must be negative reciprocals.

EXAMPLE IV.1. The figure on the left is a brick for $\ell = 5$, but the figure on the right is not.

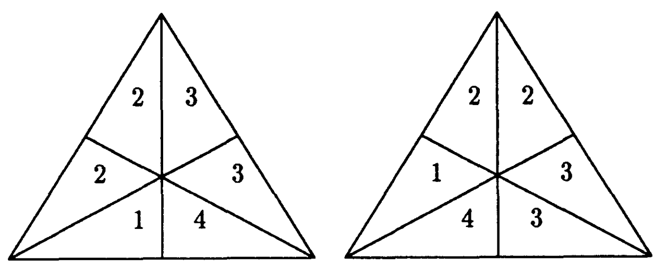

FIGURE IV.17.

EXAMPLE IV.2. For every ℓ, there is a distinguished brick B_∞, shown below.

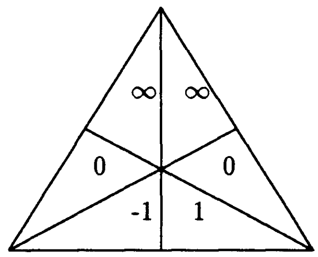

FIGURE IV.18.

Two bricks are considered equivalent if one may be rotated into the other. Hence many initial values of a in the definition will give rise to equivalent bricks. We will always take "brick" to mean "equivalence class of bricks." We say that two bricks B_k and $B_{k'}$ are *sequential* if $k' = k + 1$.

To each oriented outer edge of B_k, we may associate a sublattice of the square lattice. If the edge $\overline{ab}$ is oriented from a to b, and passes first along the inner triangle labeled k and then along $-1/k$, we associate to $\overline{ab}$ the sublattice of type k. Similarly, if the edge is oriented from b to a, then we take the sublattice of type $-1/k$. In light of this we can attach a valence to each outer edge. This is independent of orientation since $v(k) = v(-1/k)$.

Finally, bricks have one additional structure: we divide the vertices of a brick into two types. All outer vertices of all bricks B are called *solid*, unless $B = B_\infty$. In this case, the vertex opposite the $(1, -1)$ edge pair is called *hollow*, while the other two vertices are called *solid*.

EXAMPLE IV.3. Here we see the two bricks for $\ell = 5$ labeled with valences and with the correct structure on the vertices.

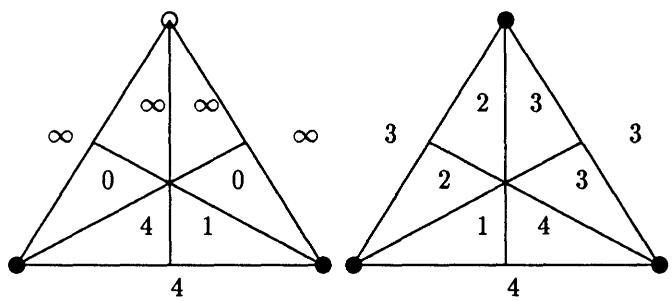

FIGURE IV.19.

What is the point of these bricks? They are the fundamental building blocks for $\mathscr{C}_\ell$.

ALGORITHM IV.1. (THE CONSTRUCTION OF $\mathscr{C}_\ell$.)

Step 1: Begin with an endless supply of bricks for ℓ.

Step 2: Identify sequential bricks B_k and B_{k+1} together along outer edges. We glue B_k to B_{k+1} so that they appear as follows:

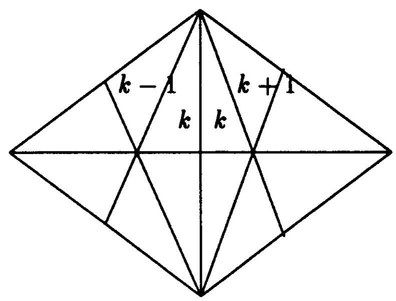

FIGURE IV.20.

Continue gluing bricks indefinitely. **Exception:** No brick maybe glued to B_∞ except along the $\{1,-1\}$ edge pair.

Step 3: For the moment, ignore all structures of the bricks except the edge valences and the types of vertices. For each brick $B \neq B_\infty$, fill the interior with dashed arcs so that N arcs end in each edge of valence N. (The valence function insures that there exists a way to do this, and by our geometric arguments of section blah if any solution exists it is unique.) For B_∞, where the valences are $\{\infty, \infty, \ell - 1\}$, draw $\ell - 1$ dashed arcs starting from the edge with valence $\ell - 1$ and ending at the hollow vertex. Connect these dashed arcs across the brick edges to form 1-cells.

EXAMPLE IV.4. Here we do the process for the case $\ell = 5$.

Step 1: There are two distinct bricks in this case. (cf. Figure IV.3)

Step 2: After we glue bricks indefinitely, we obtain the following object:

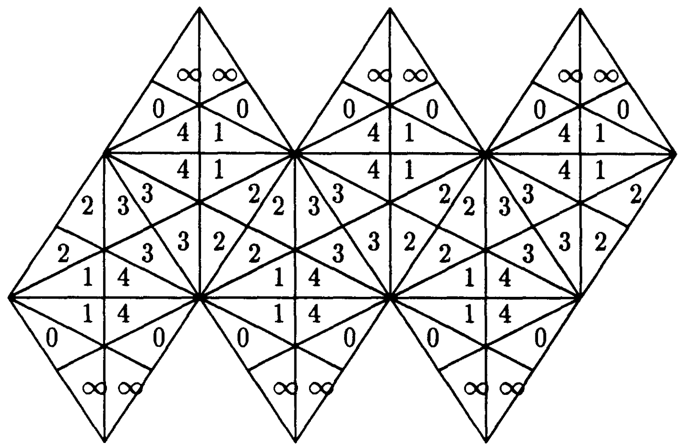

FIGURE IV.21.

Step 3: When we connect the dashed arcs and add the appropriate vertices, we have the following:

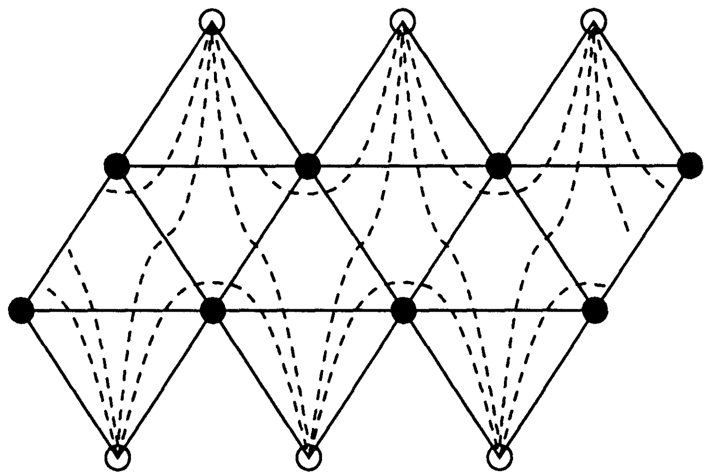

FIGURE IV.22.

Hence we construct the same $\mathscr{C}_5$ that we found before.

DEFINITION IV.2. The object constructed in steps 1–3 above is the *universal Hecke correspondence* (UHC) $\mathscr{C}_\ell$.

A menagerie of UHCs is presented in Appendix A.

The UHC $\mathscr{C}_\ell$ has two distinct cellular structures:

DEFINITION IV.3. Let Δ_s denote the cell complex on $\mathscr{C}_\ell$ with

- 0-skeleton the solid and hollow vertices,

- 1-skeleton the outer edges of all the bricks including those of valence ∞, and
- 2-skeleton the underlying triangles of all the bricks.

Similarly, let Δ_t denote the cell complex on $\mathscr{C}_\ell$ with

- 0-skeleton the solid and hollow vertices,
- 1-skeleton the dashed arcs constructed in Step 3 and the edges of valence ∞, and
- 2-skeleton the subsets of $\mathscr{C}_\ell$ whose boundaries are the dashed arcs.

4. The Main Theorem

The main virtue of the UHC is expressed by the following theorem.

THEOREM IV.1. *Let p and ℓ be distinct primes. Consider the Hecke correspondence T_ℓ:*

$$(s,t)\colon \mathscr{C}_\ell(p) \rightrightarrows \mathscr{X}(p).$$

Let $\Delta(p)$ be the Voronoï decomposition of $\mathscr{X}(p)$, and let $\Delta_s(p)$ and $\Delta_t(p)$ be the lifts of $\Delta(p)$ by s and t. Cut $\mathscr{C}_\ell(p)$ along its common edges, and let $C_\ell(p)$ be one of the remaining connected components. Let $\mathscr{C}_\ell$ be the universal Hecke correspondence constructed in IV.3. *Then we may construct a continuous map $\pi(p)$ such that:*

(a) The map

$$\pi(p)\colon \mathscr{C}_\ell \longrightarrow C_\ell(p)$$

is a covering map.

(b) The map $\pi(p)$ is cellular in two different ways:

$$\pi(p)\colon \Delta_s \longrightarrow \Delta_s(p) \cap C_\ell(p)$$
$$\pi(p)\colon \Delta_t \longrightarrow \Delta_t(p) \cap C_\ell(p)$$

The proof of the theorem is broken into several parts. The first step is to prove part (a).

PROOF OF PART (A).

Decompose $\mathscr{C}_\ell(p)$ along its common edges, and let $C_\ell(p)$ be any connected piece that remains. We will show that we can construct a covering from $\mathscr{C}_\ell$ to $C_\ell(p)$.

Simply choose any 2-cell τ in $C_\ell(p)$ that meets two common edges, and pick a brick B_τ in $\mathscr{C}_\ell$ that is equivalent to B_∞. We label the vertices in B_τ as they are labeled in B_∞:

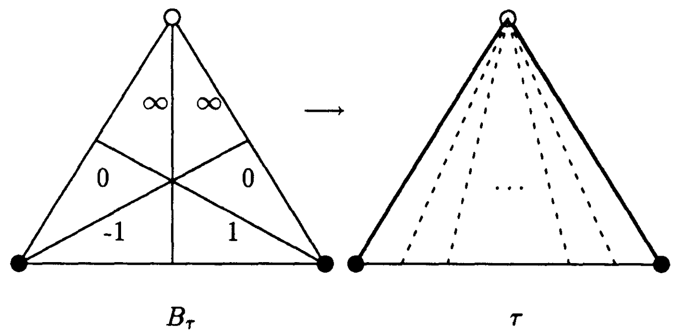

FIGURE IV.23.

We initially define our map to take B_τ to τ in the obvious way.

Once we have chosen these three labels for the vertices of B_τ, we may uniquely label the remaining vertices of $\mathscr{C}_\ell$ by using the rules described in II.??. Or, equivalently, we may apply appropriate adjacency operators to B_τ to see how the propagate the labeling. Either way, there is no obstruction to propagating the labels on the vertices of $\mathscr{C}_\ell$. Since the local structures of these spaces are identical, this constructs a map from $\mathscr{C}_\ell$ to $C_\ell(p)$ which is a covering on its image. □

Before we prove part (b), we need to prove the Reconstruction Lemma of the previous section. We recall the statement of the lemma.

LEMMA. (RECONSTRUCTION LEMMA) *Fix p and ℓ. If we know the valence $v(\sigma)$ of all 1-cells $\sigma \in \Delta_s(p)$, then we may uniquely reconstruct $\Delta_t(p)$.*

PROOF. We begin by summarizing a few geometric facts about $\Delta_s(p)$ and $\Delta_t(p)$. Let $\tau \in \Delta_s(p)$ be a 2-cell, and let $\sigma, \sigma' \in \Delta_t(p)$ be 1-cells.

(a) If σ' is not a common edge, then σ' has endpoints at hollow cusps.
(b) No pair σ, σ' ever intersects in the interior of τ, and no σ has an endpoint in the interior of τ.
(c) If σ enters τ through a 1-cell, then it cannot leave τ through the same 1-cell.

The only statement that requires any proof is item (c). The instant σ crosses a 1-cell of $\Delta_s(p)$ corresponds to the following type of picture:

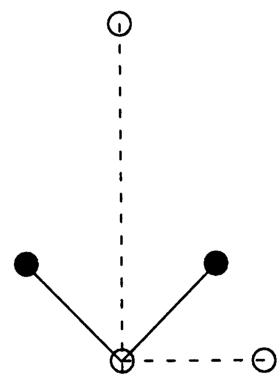

FIGURE IV.24.

The edge that σ has just crossed has as endpoints the two solid lattice points. As we continue to move within σ by expanding or contracting the coordinate axes, the solid axes cease to be perpendicular, and clearly will never be perpendicular again. This means it is impossible that σ ever crosses the same solid 1-cell.

Notice that this argument also implies that if σ is not a common edge, then as a subspace of $\mathscr{C}_\ell(p)$ it intersects the 1-skeleton of $\Delta_s(p)$ transversely.

Now, to complete the proof of the lemma, we claim that every 2-cell $\tau \in \Delta_s(p)$ must resemble one of the following two possibilities:

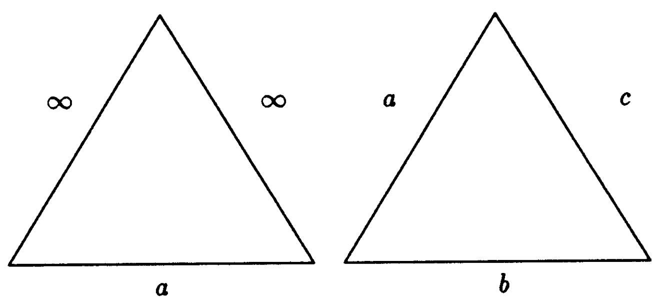

FIGURE IV.25.

Certainly all three edges cannot be labeled with ∞, because one adjacency operator applied to a stripe lattice must take it to one that is not a stripe lattice, and similarly if one edge is labeled with ∞ then another edge must also be labeled so. Finally, in either of the two possibilities, we can reconstruct the dashed 1-cells uniquely. In the left figure, we simply draw a dashed lines from the apex to the base, and on the right we may use some trivial linear algebra. □

This means that the construction of Δ_t in $\mathscr{C}_\ell$ makes sense.

Now we conclude the proof of the theorem.

PROOF OF PART (B). We need to prove that $\pi(p)$ is cellular on both Δ_s and Δ_t.

First note that π is clearly cellular on Δ_s, since we constructed it to be so.

But we claim that π is also clearly cellular on Δ_t. By the Reconstruction Lemma, the valence data in $\mathscr{C}_\ell$ determines a a unique way to construct Δ_t. The same data is obviously present in $\Delta_t(p)$, which means that locally Δ_t and $\Delta_t(p)$ are combinatorially equivalent. Hence, at worst all we have to do is slightly perturb π to insure that it is cellular on Δ_t. □

5. The Cohomology Algorithm

In this section we describe an algorithm for computing the action of the Hecke correspondence on $H^1(\mathscr{X}(p);\mathbb{C})$ and $H^1(\mathscr{Y}(p);\mathbb{C})$, the *Roadmap Algorithm.*

How does one compute the action of T_ℓ on cohomology? What is needed is a method to take a 1-cell $\sigma \in \Delta_s(p)$ and push it into the 1-skeleton of $\Delta_t(p)$. Since these pushes need to be done only locally, and $\mathscr{C}_\ell$ contains the local geometry of $\Delta_s(p)$ and $\Delta_t(p)$ for all p, we can do this if we can do it for every type of 1-cell in $\Delta_s \subset \mathscr{C}_\ell$.

So how do we do this? Let $F[r,l]$ be the free monoid with identity on the letters r and l. The idea is to associate to each oriented $\sigma \in \Delta_s$ a word $R(\sigma) \in F[r,l]$. We start at one end of σ and move. Initially σ leaves a vertex of a 2-cell $\tau \in \Delta_t$ and exits the opposite 1-cell. As σ moves into the neighboring 2-cell τ', it must make a decision: σ must turn left, turn right, or terminate in the opposite vertex:

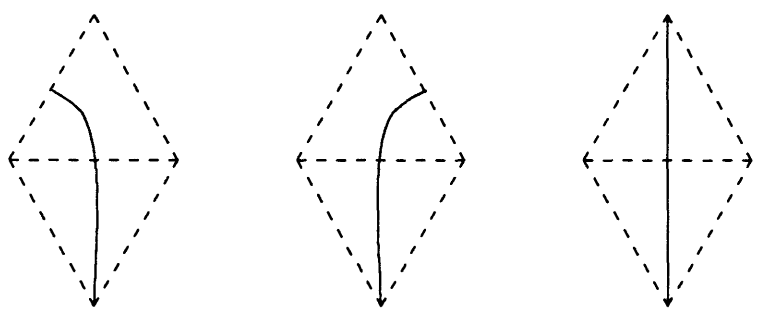

FIGURE IV.26. Turn left, right, or exit.

By keeping track of these local turns, we get a word in r and l. For example, to the following 1-cell we associate the word $r^2l^2r^2$.

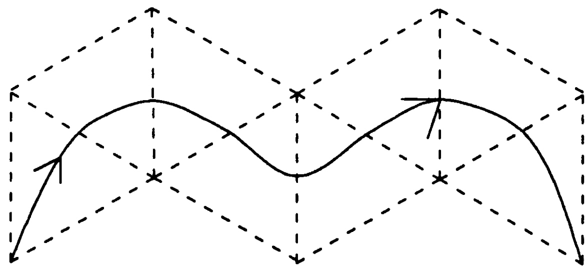

FIGURE IV.27. An edge with roadmap $r^2l^2r^2$.

DEFINITION IV.4. The word $R(\sigma) \in F[r, l]$ associated to an oriented 1-cell $\sigma \in \Delta_s$ is called the *roadmap* of σ.

Note that calling a direction "right" or "left" does not quite make sense without specifying global orientation, but saying that the two directions are distinct does. We will see momentarily how to make sense of these directions when we adapt the algorithm to act on our indexing scheme.

The importance of the roadmap is the following:

PROPOSITION IV.1. *The roadmap $R(\sigma)$ determines a homology of σ into Δ_t.*

PROOF. Let τ be the first 2-cell in Δ_t that σ enters. We shall see momentarily (cf. the proof below) that we are able to determine all the vertices of τ, and can thus determine all the 1-cells of τ. Suppose without loss of generality that the first letter that appears in $R(\sigma)$ is r, so that σ turns right after exiting τ. Then the first 1-cell in the image of the homology will be the right edge of τ.

Now two things may happen. Either σ terminates, continues to turn right, or turns left. If σ terminates, then we add the obvious 1-cell to complete the homology. If σ continues to turn right, we add no new edge to the homology. If σ turns left, though, then we must add a 1-cell to the homology, namely the 1-cell σ' over which σ has just changed directions. By applying the rules in §??, we can determine the endpoints of σ'.

Now continue in this manner, only adding 1-cells to the homology if σ changes from r to l or l to r. Eventually σ will terminate at a cusp, and we will have a accumulated a list of 1-cells to which σ is homologous. □

Thus $R(\sigma)$ tells us how to push σ into Δ_t. In fact, we may compute $R(\sigma)$ and the valence $v(\sigma)$ simultaneously.

ALGORITHM IV.2. (THE ROADMAP/VALENCE ALGORITHM)

Initialization: Take $k \in \mathbb{P}^1(\mathbb{F}_\ell)$ not equal to 0 of ∞. Begin with an oriented 1-cell $\sigma_k \in \Delta_s$ represented by the lattice $L_k \subset \mathbb{Z}^2$. Take as an initial basis for L_k the pair $\{(\ell - k, 1), (-k, 1)\}$. Initialize $R(\sigma_k)$ to the identity in the free group on r and l and $v(\sigma_k)$ to be one.

Main Loop: Perform the Euclidean algorithm on the pair $(\ell - k, k)$ by successively subtracting the minimum of the two from the other until the pair becomes $(1, 1)$. At each stage:

(a) If you subtract the left from the right, multiply $R(\sigma_k)$ on the right by r and increment $v(\sigma_k)$.
(b) If you subtract the right from the left, multiply $R(\sigma_k)$ on the right by l and increment $v(\sigma_k)$.

End: When the algorithm terminates, $R(\sigma_k)$ is the roadmap for σ_k and $v(\sigma_k)$ is the valence.

PROOF. Let L_k be the sublattice of the square lattice of type k representing σ_k. Let ξ_x be the vertex represented by the x-axis, and let ξ_y be the cusp represented by the y-axis. Assume that σ_k is oriented so that we move from ξ_x to ξ_y.

As a first step, we will show that we can find a basis of L_k that becomes rectangular, and that it is in fact the basis in the initialization step above. Begin on σ_k very close to ξ_x. This means that only the x-axis is visible in the picture of L_k; all other lattice points have moved "out of frame". Move away from ξ_x, so the that the first row of points above the x-axis becomes visible. Any basis b of L_k with both vectors on this first row will become rectangular first. This is true because any other basis with vectors that lie above this will make an angle strictly less that of b. Clearly b is $\{(\ell - k, 1), (-k, 1)\}$. Since this initial basis will become rectangular, we set $v(\sigma_k)$ to be one.

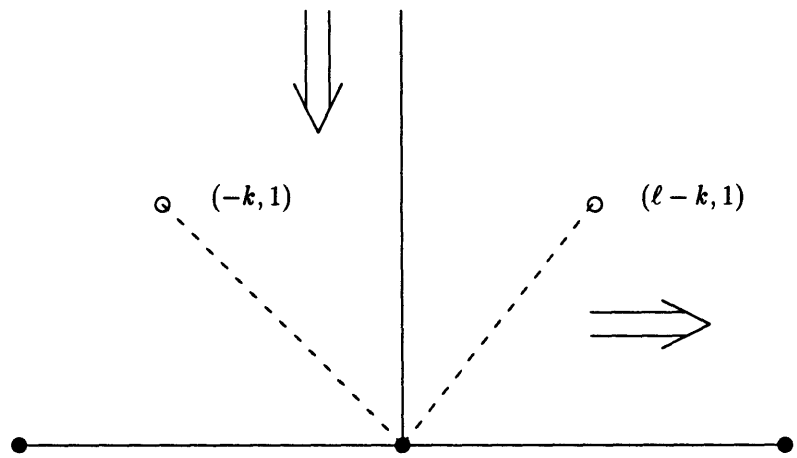

FIGURE IV.28. The first basis becomes rectangular.

Continue moving in σ_k by contracting along the y-axis. As soon as this first basis ceases to be rectangular, we have entered a new 2-cell of Δ_ℓ. The next basis that becomes rectangular must be adjacent to our first basis, because adjacent bases correspond to the other two sides of this 2-cell. We move to this new basis by adding either the first basis vector to the second or the second basis vector to the first. This has the effect of performing the an iteration of the Euclidean algorithm in the absolute values of the x coordinates of our basis vectors.

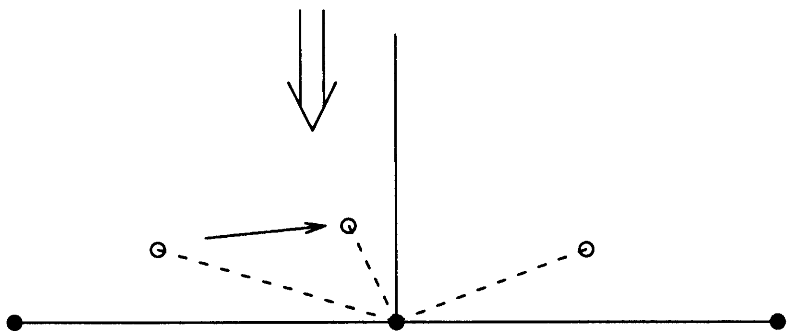

FIGURE IV.29. Moving to an adjacent basis.

Thus, each time we perform an iteration of the algorithm, we increment $v(\sigma_k)$ and multiply $R(\sigma_k)$ by a generator. The generator changes as the minimum of the two x coordinates changes, since we move in a different direction in this case.

It only remains to see that the algorithm terminates. We claim that this happens when the basis vectors are as close to the y-axis as possible. This is clear: any pair of vectors that is further away will have no chance of becoming orthogonal as the y-axis is contracted. But the vectors in the basis are as close the the y-axis as possible when the absolute values of their x coordinates are equal to one. This is precisely when the Euclidean algorithm terminates. Thus the algorithm terminates, and successfully computes both $v(\sigma)$ and $R(\sigma)$. □

We are finally able to resolve an unproven statement in Proposition III.1.

COROLLARY IV.1. *Let L_k be a sublattice of $\mathbb{Z}^2$ of type k. If $k \neq 0$ or ∞, then $v(L_k)$ is finite.*

PROOF. This follows since Algorithm IV.4 terminates in these cases. □

To conclude this chapter, we show how the roadmap algorithm can be combined with the indexing scheme developed in chapters II and III to yield a computational method for computing with modular curves.

We begin with an oriented 1-cell $\sigma = (v, v'; d) \in \mathscr{X}(p)$. We choose lifts $\bar{v}, \bar{v}' \in (\mathbb{Z}/p)^2$ of $v, v' \in \Xi(p)$ so that $\det(\bar{v}, \bar{v}') = d \bmod p$. Then we construct the lattice $L(\sigma)$:

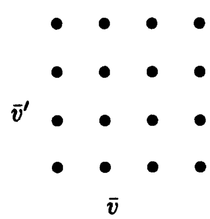

FIGURE IV.30. $L(\sigma)$.

Our goal is to write the action of the Hecke correspondence as

$$t \circ s^{-1} \colon (v, v'; d) \longmapsto \sum_{i=0}^{m-1} (v_i, v_{i+1}; \ell d).$$

We can meet our goal if we can describe the projection

$$t \colon (v, v'; d)_k \longmapsto \sum_{i=0}^{m-1} (v_i, v_{i+1}; \ell d)$$

for each type of sublattice of index ℓ. Since Example III.3 does this for $k = 0, \infty$, we study the other cases.

Fix a type $k \neq 0$ or ∞, and consider the corresponding 1-cell $\sigma_k = (v, v'; d)_k \in \Delta_s(p)$. Consider the following picture of $L(\sigma)_k$:

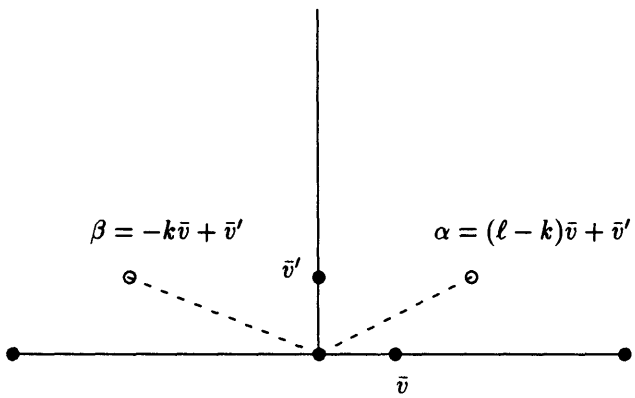

FIGURE IV.31. $L(\sigma)_k$.

In $\mathscr{C}_\ell(p)$, this corresponds to the following picture:

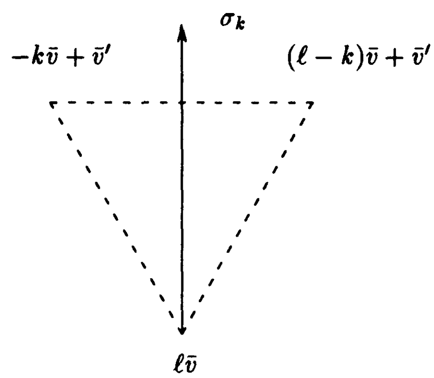

FIGURE IV.32.

Notice that we may immediately conclude that $v_0 = \ell\bar{v}$.

Assume without loss of generality that $\ell - k < k$. This means that the vector labeled α is closer to the y-axis than the vector β is. In other words:

(a) $v_1 = (\ell - k)\bar{v} + \bar{v}'$ and
(b) The first letter in $R(\sigma_k)$ is r.

At this point we have determined the first 1-cell in the image, $(v_0, v_1; \ell d)$.

Now abbreviate $R(\sigma_k) = r^{a_1} l^{a_2} \cdots$ to the tuple $(a_1, \ldots, a_s)$. We claim that

$$v_2 = (a_1 + 1)v_1 - v_0.$$

Consider the following picture:

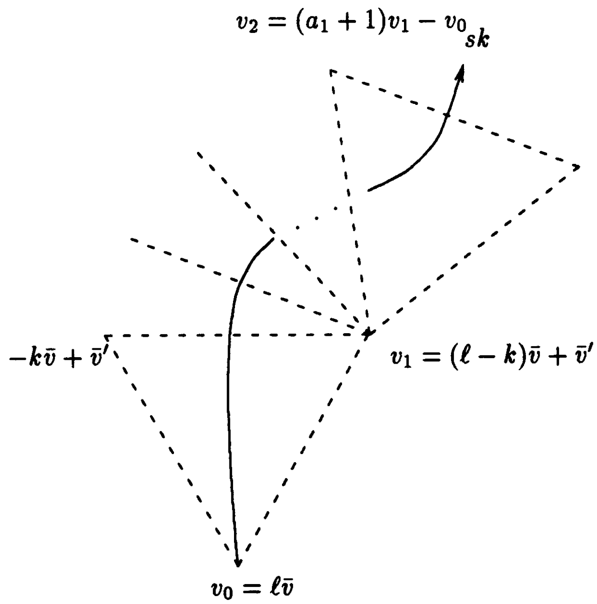

FIGURE IV.33.

Altogether, $a_1 + 1$ dashed 1-cells are crossed before σ_k changes directions. We must actually add $-v_0$ since $-k\bar{v} + \bar{v}' = v_1 - v_0$.

We claim that the remaining 1-cells in the image can be found using the formula

$$v_{i+1} = a_i v_i + v_{i-1} \quad \text{for } i + 1 < m.$$

This is also easy to see by induction. Consider the following figure:

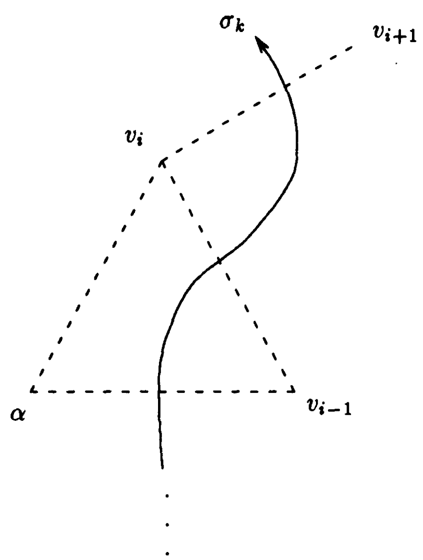

FIGURE IV.34.

Assume that σ_k changes directions over (v_i, v_{i-1}) and (v_{i+1}, v_i). By induction we assume $v_i = a_{i-1}v_{i-1} + v_{i-2}$, and we want to show $v_{i+1} = a_i v_i + v_{i-1}$. Notice that the vertex labeled α must be equal to $(a_{i-1}-1)v_{i-1}+v_{i-2}$. Since we change directions over (v_i, v_{i-1}), we change pivot vectors, and we begin adding multiples of v_i to v_{i-1}. Since we add v_i to v_{i-1} once for every 1-cell that σ_k crosses between (v_i, v_{i-1}) and (v_{i+1}, v_i), we add in fact $a_i v_i$ to v_{i-1}. Hence $v_{i+1} = a_i v_i + v_{i-1}$.

This means that we can determine all the images of σ_k after pushing into the 1-skeleton of $\Delta_t(p)$ and mapping by t. We summarize the result as follows:

PROPOSITION IV.2. *Let the notation be as above. Using the roadmap algorithm, we have that*

$$t\colon (v, v'; d) \longmapsto \sum_{i=0}^{m-1} (v_i, v_{i+1}; \ell d)$$

where:

(a) $v_0 = \ell\bar{v}$ *and* $v_m = \ell\bar{v}'$.
(b) If the first letter of $R(\sigma_k)$ *is* r, *then* $v_1 = (\ell - k)\bar{v} + \bar{v}'$. *Otherwise,* $v_1 = -k\bar{v} + \bar{v}'$.
(c) $v_2 = (a_1 + 1)v_1 + v_0$ *and* $v_{i+1} = a_i v_i + v_{i-1}$ *for* $2 < i + 1 < m$.

CHAPTER V

Combinatorial Eisenstein Cohomology

In this chapter we describe our combinatorial technique for constructing Eisenstein cohomology classes. Recall from the introduction that we have an exact sequence

$$0 \to H^1(\mathscr{X}(p)) \to H^1(\mathscr{Y}(p)) \to H_0(\{\text{cusps}\}) \to H_0(\mathscr{X}(p)) \to 0,$$

and that according to the Manin-Drinfeld theorem, there is a splitting of this sequence $E\colon H_0(\{\text{cusps}\}) \to H^1(\mathscr{Y}(p))$ that (a) is equivariant with respect to the action of the Hecke correspondences and (b) is defined over $\mathbb{Q}$. The image of the splitting in $H^1(\mathscr{Y}(p); \mathbb{C})$ is called the Eisenstein cohomology.

Our technique of constructing this piece of the cohomology is to first note that there exists a large symmetry group that acts on the above exact sequence, the group of *nonabelian Hecke operators.* These operators arise from symmetries of the Voronoï complex $\Delta(p)$, and they commute with the action of the Hecke correspondences. We describe these operators in V.1. In section V.2 we describe the decomposition of the above exact sequence into irreducible representations of the nonabelian Hecke operators, which has as a corollary a topological proof of a slight generalization of a result of Hecke. In V.3 we construct a geometric basis in $H_0(\{\text{cusps}\})$ for these irreducible representations and use the basis to compute the eigenvalues of the Hecke operators on Eisenstein cohomology. Next in V.4 we specialize to special classes called the *Steinberg* classes, and compute a geometric basis for them in $H^1(\mathscr{Y}(p))$. In V.5 we show how to compute the Hecke action on these bases, and finally in V.6 we describe a system of linear equations, independent of the level p, that computes E on the Steinberg classes.

1. Nonabelian Hecke Operators

Let G_p be the finite group $GL_2(\mathbb{F}_p)$. This group acts on the full modular curve $\mathscr{Y}(p)$ as follows: the element $g \in G_p$ takes $(L, m) \in \mathscr{Y}(p)$ to the point (L, gm).

DEFINITION V.1. The group G_p is called the group of *nonabelian Hecke operators* attached to $\mathscr{Y}(p)$.

PROPOSITION V.1. *The action of G_p commutes with the action of any Hecke correspondence.*

PROOF. Denote the Hecke correspondence by T_ℓ. Intuitively, this is true because T_ℓ acts on lattices and G_p acts on markings. Formally, let $g \in G_p$. Then

$$(T_\ell \circ g)(L, m) = \{g(L_i, m_i)\} = \{(L_i, gm_i)\}$$

and

$$(g \circ T_\ell)(L, m) = T_\ell(L, gm) = \{(L_i, (gm)|L_i)\} = \{(L_i, g(m|L_i))\} = \{(L_i, gm_i)\}.$$

□

The classical algebra of Hecke operators is generated by the T_ℓ and another operator R_ℓ that sends $L \longmapsto \ell L$ (cf. [Ser73]). In fact, the center of G_p corresponds to these lattice dilation operators.

We may actually define an action of G_p on the compactification $\mathscr{X}(p)$:

PROPOSITION V.2. *The action of G_p extends continuously to $\mathscr{X}(p)$. If $\xi = (v; d)$, then*

$$g(v; d) = (gv; (\det g)d).$$

PROOF. This is clear given our description of the cusps in II.5. □

Now let

$$0 \to C^0 \to C^1 \to C^2 \to 0$$

be the chain complex over $\mathbb{C}$ associated to the Voronoï complex $\Delta(p)$ of $\mathscr{X}(p)$. Recall (II.4) that we use superscripts because the Voronoï complex is actually a cocell complex, in which cells are indexed by their codimension. Hence C^0 denotes the $\mathbb{C}$-vector space generated by the 2-cells of $\Delta(p)$, and so forth. The coboundary map $C^i \to C^{i+1}$ is just the usual boundary map.

The action of G_p commutes with the coboundary operator of this complex, and so G_p acts on cohomology. Since the actions of G_p and each T_ℓ commute, the decomposition of cohomology into T_ℓ-eigenspaces and G_p-irreducibles must be compatible. Therefore, to understand the Hecke action, we want to decompose C^* into G_p-irreducibles. We will describe how to do this later, but first we must fix notation concerning the representation theory of G_p. This material is standard and can be found in many sources. Our discussion follows [FH91].

Conjugacy Classes. There are four types of conjugacy classes in G_p.

(a) Classes parameterized by the *center*, consisting of elements of the form

$$\begin{pmatrix} x & 0 \\ 0 & x \end{pmatrix} \quad \text{where } x \in \mathbb{F}_p^\times.$$

Each conjugacy class has one element, and there are $p - 1$ such classes.

(b) Classes parameterized by the *semisimple elements*, consisting of elements of the form

$$\begin{pmatrix} x & 1 \\ 0 & x \end{pmatrix} \quad \text{where } x \in \mathbb{F}_p^\times.$$

Each conjugacy class has p^2-1 elements, and there are $p-1$ such classes.

(c) Classes parameterized by the *isotropic torus*, consisting of elements of the form

$$\begin{pmatrix} x & 0 \\ 0 & y \end{pmatrix} \quad \text{where } x, y \in \mathbb{F}_p^\times, \text{ and } x \neq y.$$

Each conjugacy class has p^2+p elements, and there are $(p-1)(p-2)/2$ such classes.

(d) Classes parameterized by the *anisotropic torus*, consisting of elements which over the algebraic closure $\overline{\mathbb{F}}_p$ diagonalize to

$$\begin{pmatrix} \zeta & 0 \\ 0 & \zeta^p \end{pmatrix} \quad \text{where } \zeta \in \mathbb{F}_{p^2}^\times \text{ and } \zeta \notin \mathbb{F}_p^\times.$$

Each conjugacy class has p^2-p elements, and there are $p(p-1)/2$ such classes.

Representations. There are four types of representations. In what follows, α and β are complex characters of $\mathbb{F}_p^\times$, and ϕ is complex character of $\mathbb{F}_{p^2}^\times$.

(a) *Trivial and twisted trivial representations.* Let U denote the trivial representation of G_p, and let U_α denote the representation defined by $U_\alpha(g) := \alpha(\det(g))$.

(b) *Steinberg and twisted Steinberg representations.* The permutation representation of G_p on the projective line $\mathbb{P}^1(\mathbb{F}_p)$ splits as direct sum $U \oplus V$, where V is irreducible of dimension p. Using the twisted trivial representations we may also construct the representations $V_\alpha := V \otimes U_\alpha$.

(c) *Principal series representations.* Let $B \subset G_p$, be the Borel subgroup consisting of upper-triangular matrices, and consider the representation defined by

$$\alpha\beta\colon \begin{pmatrix} a & b \\ 0 & d \end{pmatrix} \longmapsto \alpha(a)\beta(d).$$

Then the induced representation $W_{\alpha,\beta} := \operatorname{Ind}_B^G \alpha\beta$ is irreducible if $\alpha \neq \beta$, and otherwise splits as $W_{\alpha,\alpha} = V_\alpha \oplus U_\alpha$.

(d) *Discrete series representations.* These are representations X_ϕ associated to characters of $\mathbb{F}_{p^2}^\times$. We say no more about these representations because they do not appear in the Eisenstein cohomology.

Finally, the group G_p has the following character table:

G_p	Ctr.	SS.	Iso. T.	Aniso. T.
U_α	$\alpha(x^2)$	$\alpha(x^2)$	$\alpha(xy)$	$\alpha(\zeta^p)$
V_α	$p\alpha(x^2)$	0	$\alpha(xy)$	$-\alpha(\zeta^p)$
$W_{\alpha,\beta}$	$(p+1)\alpha(x)\beta(x)$	$\alpha(x)\beta(x)$	$\alpha(x)\beta(y)+\alpha(y)\beta(x)$	0
X_ϕ	$(p-1)\phi(x)$	$-\phi(x)$	0	$-(\phi(\zeta)+\phi(\zeta^p))$

2. The Decomposition

Let χ_k denote the character of G_p acting on C^k. Let C'^k denote the portion of the chain complex supported in the identity component $X^1(p)$. We want to compute χ_k, but as a first step we look at the action of $PSL_2(\mathbb{F}_p)$ on C'^k. Once we know the character of this action we can easily deduce that of G_p.

Recall that $PSL_2(\mathbb{F}_p)$ has a unique conjugacy class c_2' of elements of order two, a unique conjugacy class c_3' of elements of order three, and two conjugacy classes c_p' and $\hat{c}_p'$ of elements of order p. We take as representatives of these classes the following four matrices x_2', x_3', x_p', and $\hat{x}_p'$:

$$\begin{pmatrix} 0 & -1 \\ 1 & 0 \end{pmatrix}, \quad \begin{pmatrix} 1 & -1 \\ 1 & 0 \end{pmatrix}, \quad \begin{pmatrix} 1 & 1 \\ 0 & 1 \end{pmatrix}, \quad \text{and} \quad \begin{pmatrix} 1 & \epsilon \\ 0 & 1 \end{pmatrix}.$$

Here ϵ denotes an element of $\mathbb{F}_p$ that is not a square.

LEMMA V.1. *Let χ_k' denote the character of $PSL_2(\mathbb{F}_p)$ acting on C'^k. Then*

(a) χ_2' equals $(p-1)/2$ on both c_p' and $\hat{c}_p'$,

(b) χ_1' equals $-(p-1)/2$ on c_2' if $p = 1 \bmod 4$, and equals $-(p+1)/2$ on c_2' if $p = 3 \bmod 4$, and

(c) χ_0' equals $(p-1)/3$ on c_3' if $p = 1 \bmod 3$, and equals $(p+1)/3$ on c_3' if $p = 2 \bmod 3$.

Furthermore, except for the conjugacy class of the identity, these characters are zero.

PROOF. First we discuss χ_2'. Consider the special cusp $\xi = (\binom{1}{0}; 1 \in X^1(p)$. Obviously any element of $PSL_2(\mathbb{F}_p)$ that stabilizes ξ must be of the form

$$\begin{pmatrix} 1 & * \\ 0 & 1 \end{pmatrix}.$$

Hence only elements of c_p' and $\hat{c}_p'$ and the identity stabilize cusps. But note also that the elements x_p' and $\hat{x}_p'$ actually stabilize the $(p-1)/2$ cusps $(\binom{*}{0}; 1)$ This proves part (a).

Now consider χ_1', and consider the special edge $e = (\binom{1}{0}, \binom{0}{1}; 1)$. Any element that acts nontrivially on e and stabilizes e must act by flipping the endpoints of e, i.e. must take e to $-e$. The only element that does this is the special element x_2'; hence a stabilizer of an edge must be the identity or an element of order two. To finish, we need to compute how many edges are stabilized by a given element of order two. By symmetry, every such element must stabilize the same number of edges, and so

$$\frac{\#\text{ edges flipped}}{\text{elt. of order two}} = \frac{\#\text{ edges}}{\#\text{ elts. of order two}}.$$

The result follows from the standard formulas for the number of elements of order two in $PSL_2(\mathbb{F}_p)$ and the formula used in the proof of Proposition II.II.3.

Finally, we must consider χ'_0. A argument similar to the one used for edges works here. This time, a stabilizer of a triangle that acts nontrivially must be of order three, and by symmetry the same number of triangles is stabilized by each element of order three. The only difference is that an element of order three and its square stabilize the same number of triangles. Thus

$$\frac{\#\text{ triangles stabilized}}{\text{elt. of order three}} = \frac{\#\text{ triangles}}{(\#\text{ elts. of order three})/2}.$$

Again, the result follows from standard formulæ. □

Now we can lift the previous result to G_p. Let x_4, x_6, x_3, x_p, and x'_p denote the following elements of G_p:

$$\begin{pmatrix} 0 & -1 \\ 1 & 0 \end{pmatrix}, \begin{pmatrix} 1 & -1 \\ 1 & 0 \end{pmatrix}, \begin{pmatrix} 0 & -1 \\ 1 & -1 \end{pmatrix}, \begin{pmatrix} 1 & 1 \\ 0 & 1 \end{pmatrix}, \text{and} \begin{pmatrix} -1 & 1 \\ 0 & -1 \end{pmatrix}.$$

As before, the subscripts denote order, and we let c_4, c_6, c_3, c_p, and c'_p denote their conjugacy classes. The classes c_4, c_6, and c_3 will be classes of type (c) or (d), depending on whether x_4, x_6, or x_3 are diagonalizable over $\mathbb{F}_p$.

PROPOSITION V.3. *Let χ_k be the character of G_p acting on C^k. Then*

(a) χ_2 equals $(p-1)^2/2$ on both c_p and c'_p,
(b) χ_1 equals $-(p-1)^2/2$ on c_2 if $p = 1 \bmod 4$, and equals $-(p^2-1)/2$ on c_2 if $p = 3 \bmod 4$, and
(c) χ_0 equals $(p-1)^2/3$ on c_3 and c_6 if $p = 1 \bmod 3$, and equals $(p^2-1)/3$ on c_3 and c_6 if $p = 2 \bmod 3$.

Furthermore, except for the conjugacy classes of Id *and* $-$Id, *these characters are zero.*

PROOF. All verifications are simple once one realizes that these are the elements that descend to the elements x'_2, x'_3, and both x'_p and $\hat{x}'_p$. The numbers in the statement are the values in the statement for $PSL_2(\mathbb{F}_p)$ multiplied by the number of connected components. □

From the knowledge of χ_k we may decompose the action of G_p on the Voronoï chain complex, from there may compute the induced decomposition of cohomology. Since these are elementary and messy character-theoretic computations, we put the results in Appendix B, and content ourselves with stating the following:

PROPOSITION V.4. *Let H_{Eis} denote the Eisenstein cohomology of $\mathscr{X}(p)$. Then as a G_p-module H_{Eis} contains only induced representations. Furthermore, every Steinberg V_α occurs with multiplicity one, and every other induced representation $W_{\alpha,\beta}$ with $\alpha(-1) = \beta(-1)$ occurs with multiplicity two.*

DEFINITION V.2. The representations of G_p occurring in H_{Eis} are called *Eisenstein irreducibles.*

REMARK V.1. In the paper [Hec39], E. Hecke decomposed the space of weight-two modular forms of level p into $PSL_2(\mathbb{F}_p)$-irreducibles by considering deck transformations of the branched cover

$$X(p) \longrightarrow \mathbb{P}^1(\mathbb{C}).$$

His computations are equivalent to those in Lemma V.1. Since classes of $H^1(Y(p))$ may be identified with these forms via the De Rham isomorphism, our decomposition is a slight generalization of this result. (I am grateful to Avner Ash for pointing this out to me.)

3. Bases for the Eisenstein Irreducibles

Consider C^2, the portion of the chain complex generated by the vertices of the Voronoï decomposition. As usual, vertices $\xi \in \mathscr{X}(p)$ are represented by pairs $(v; d)$, where $v \in \Xi(p)$ and $d \in (\mathbb{Z}/p)^\times$. There is an obvious map

$$f : \Xi(p) \times (\mathbb{Z}/p)^\times \longrightarrow \mathbb{P}^1(\mathbb{F}_p)$$

defined by projecting the first factor and forgetting the second. We say two cusps ξ and ξ' are *associate* if $f(\xi) = f(\xi')$.

Recall that *star* of a cell σ in a cell complex is defined to be the set

$$St(\sigma) := \{\text{cells } \sigma' \mid \bar{\sigma}' \cap \sigma \neq \emptyset\},$$

and that that *link* of σ is defined by

$$Lk(\sigma) := \partial(\overline{St(\sigma)}).$$

Given any cusp ξ, define $\lambda(\xi) \in C^2$ by

$$\lambda(\xi) := p\xi - \sum_{\eta \in C^2 \cap Lk(\xi)} \eta.$$

The symbol λ is supposed to suggest "link". We define λ because the Eisenstein section E is only defined classes in kernel of $H_0(\{\text{cusps}\}) \to H_0(\mathscr{X}(p))$, and we shall need a convenient way to pass from a class supported on ξ to a class in the kernel near ξ. If ξ is represented by the datum $(v; d)$, then we shall also write $\lambda(v; d)$.

Now we shall construct projections from C^2 to the general induced representation $W_{\alpha,\beta}$. We assume as usual that α and β are two complex characters of $(\mathbb{Z}/p)^\times$ satisfying $\alpha(-1) = \beta(-1)$.

Let $\xi = (v; d) \in \mathscr{X}(p)$ be a cusp. Define two vectors $w_{\alpha,\beta}(\xi)$ and $w_{\beta,\alpha}(\xi)$ by

$$w_{\alpha,\beta}(\xi) := \frac{1}{2} \sum_{m,n \in (\mathbb{Z}/p)^\times} \alpha^{-1}(m)\lambda(\frac{\alpha}{\beta}(n)nv; m),$$

$$w_{\beta,\alpha}(\xi) := \frac{1}{2} \sum_{m,n \in (\mathbb{Z}/p)^\times} \beta^{-1}(m)\lambda(\frac{\beta}{\alpha}(n)nv; m).$$

As before, if $\xi = (v; d)$ then we shall also write $w_{\alpha,\beta}(v; d)$ for $w_{\alpha,\beta}(\xi)$. We shall prove in a moment that $w_{\alpha,\beta}(\xi) \in W_{\alpha,\beta}$, but to help the reader see the simple geometry behind these opaque formulas we present an example.

EXAMPLE V.1. We shall compute these vectors for the curve $\mathscr{X}(7)$. Fix a cusp ξ.

We may abstract each connected component of $\mathscr{X}(7)$ to the graph shown below. Each black dot represents an associate of ξ in this component, and the shaded dots represent the links of these associates. The full modular curve will consist of six copies of this object:

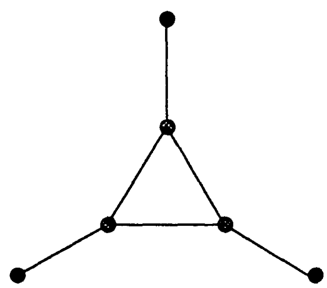

FIGURE V.1.

First consider the special case that $\alpha = \beta$ is the trivial character. In this case the vectors $w_{1,1}(\xi)$ should be in the Steinberg representation. In the d^{th} component, we obtain the following figure:

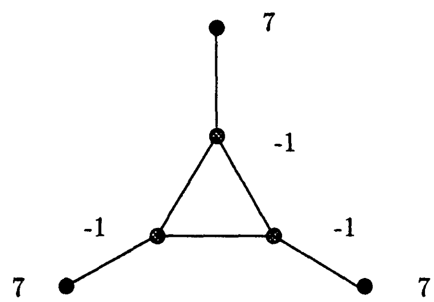

FIGURE V.2.

Notice that there is no character information, and that as ξ varies over the all cusps, we obtain $p+1$ distinct vectors whose sum is trivial. Since the action of G_p on these vectors is the same as the permutation representation of G_p on $\mathbb{P}^1(\mathbb{F}_p)$, this is indeed the Steinberg.

The next simplest case is when $\alpha = \beta$ is not trivial. Here is a picture of the d^{th} component:

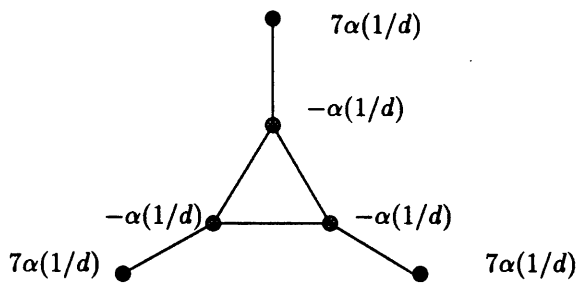

FIGURE V.3.

This time the picture is modified by twisting "horizontally" by α. In other words, we detect the character only in the determinants of the components. There is no separate modification within each component: the entire d^{th} component is multiplied by $\alpha^{-1}(d)$. Again, there are $p+1$ distinct vectors that arise, whose span over $\mathbb{C}$ has dimension p, and on which the action of G_p is the same as the Steinberg twisted by α.

Finally we consider the most general case, when $\alpha \neq \beta$. Consider the vector $w_{\alpha,\beta}(\xi)$. Again, we see the same horizontal twisting by α, but now we also see a "rotational" twisting by β/α within each connected component. Notice that the condition that $\alpha(-1) = \beta(-1)$ arises because on ξ is represented equally well by $(v; d)$ or $(-v; d)$.

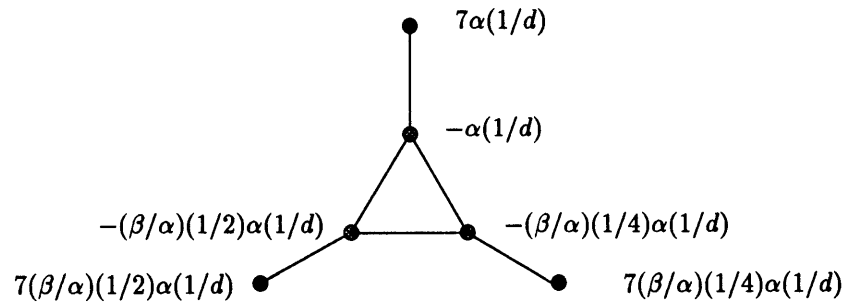

FIGURE V.4.

It is not difficult to verify that this time the $p+1$ vectors are linearly independent over $\mathbb{C}$, and that the action of G_p is via the representation $W_{\alpha,\beta}$. Notice also that under projection by $w_{\beta,\alpha}$ we obtain a different copy of $W_{\alpha,\beta}$, which is consistent with the results of Proposition V.4.

PROPOSITION V.5. *The maps $w_{\alpha,\beta}$ and $w_{\beta,\alpha}$ map C^2 onto the $W_{\alpha,\beta}$-isotypic of the G_p-action.*

PROOF. First note that as ξ ranges over all cusps of $\mathscr{X}(p)$, the $w_{\alpha,\beta}(\xi)$ generate a $p+1$ dimensional subspace over $\mathbb{C}$. In fact, to generate the space we need only consider the $p+1$ vectors corresponding to the cusps $\xi_{(0)} = \left(\binom{0}{1}; 1\right)$,

$\xi_{(1)} = \left(\binom{1}{1};1\right), \dots, \xi_{(p-1)} = \left(\binom{p-1}{1};1\right)$, and $\xi_{(\infty)} = \left(\binom{1}{0};1\right)$. (We write $\xi_{(k)}$ instead of ξ_k so that we do not conflict with the notation of Chapter III.)

Given an element $g \in G_p$, we shall write $g \cdot w_{\alpha,\beta}(\xi)$ for g acting on $w_{\alpha,\beta}(\xi)$.

(a) *Center.* Let $g = \left(\begin{smallmatrix} x & 0 \\ 0 & x \end{smallmatrix}\right)$. This element acts diagonally on every $w_{\alpha,\beta}(\xi_{(k)})$, and we compute that

$$g \cdot w_{\alpha,\beta}(\xi_{(k)}) = \alpha(x^2)\frac{\beta}{\alpha}(x)w_{\alpha,\beta}(\xi_{(k)}) = \alpha(x)\beta(x)w_{\alpha,\beta}(\xi_{(k)}).$$

Hence the trace of this element acting on the collection of $w_{\alpha,\beta}(\xi_{(k)})$ is $(p+1)\alpha(x)\beta(x)$, as required.

(b) *Semisimple elements.* Let $g = \left(\begin{smallmatrix} x & 1 \\ 0 & x \end{smallmatrix}\right)$. Then only $w_{\alpha,\beta}(\xi_{(\infty)})$ is carried into a multiple of itself, and that multiple is clearly $\alpha(x)\beta(x)$.

(c) *Isotropic Torus.* Let $g = \left(\begin{smallmatrix} x & 0 \\ 0 & y \end{smallmatrix}\right)$. Only the vectors $w_{\alpha,\beta}(\xi_{(\infty)})$ and $w_{\alpha,\beta}(\xi_{(0)})$ are acted upon diagonally, and we find that

$$g \cdot w_{\alpha,\beta}(\xi_{(\infty)}) = \alpha(xy)\frac{\beta}{\alpha}(x)w_{\alpha,\beta}(\xi_{(\infty)}) = \alpha(y)\beta(x)w_{\alpha,\beta}(\xi_{(\infty)})$$

and

$$g \cdot w_{\alpha,\beta}(\xi_{(0)}) = \alpha(xy)\frac{\beta}{\alpha}(x)w_{\alpha,\beta}(\xi_{(0)}) = \alpha(x)\beta(y)w_{\alpha,\beta}(\xi_{(0)}).$$

Hence the trace is $\alpha(x)\beta(y) + \alpha(y)\beta(x)$, as required.

(d) *Anisotropic Torus.* These elements do not act diagonally on any vectors $w_{\alpha,\beta}(\xi_{(k)})$. □

It is now easy to compute all of the Hecke eigenvalues on the Eisenstein classes.

PROPOSITION V.6. *Let p and ℓ be distinct primes, and let ξ be a cusp. Then*

$$T_\ell w_{\alpha,\beta}(\xi) = (\beta(\ell)\ell + \alpha(\ell))w_{\alpha,\beta}(\xi).$$

PROOF. This is a simple computation using the fact that

$$T_\ell(v;d) = \ell(\ell v;\ell d) + (v;\ell d).\quad \square$$

4. Bases in C^1 for the Twisted Steinbergs

DEFINITION V.3. The classes occurring in the Steinberg and twisted Steinberg representations in $H^1(\mathscr{Y}(p);\mathbb{C})$ are called *Steinberg classes.*

The next step in our construction is to describe a basis in C^1 for the Steinberg isotypics $V_\alpha \subset C^1$. First, we state the result from the character-theoretic computations alluded to above:

PROPOSITION V.7. *As a G_p-module, C^1 contains each twisted Steinberg V_α with with multiplicity $(p-1)/2$ if $p = 1 \bmod 4$ and multiplicity $(p+1)/2$ if $p = 3 \bmod 4$.*

By abuse of notation we shall also write V_α to mean the subspace of C^1 isomorphic to the twisted Steinberg V_α. We shall also abbreviate the projection map $w_{\alpha,\beta}$ to v_α.

The main result of this section is the following:

PROPOSITION V.8. *Fix a twisted Steinberg isotypic V_α. Then for each cusp ξ there exists a set of cocycles*

$$e_j \in H^1(\mathscr{X}(p), \{\text{cusps}\}) \quad \textit{where } j \in \mathbb{P}^1(\mathbb{F}_p)$$

satisfying:

(a) *Each $e_j \in V_\alpha$.*
(b) *The cocycles e_j are linearly independent, except for the relation that $e_j = -e_{-1/j}$.*
(c) *In cohomology, $e_j - e_{j-1} + e_{(j-1)/j} = 0$.*
(d) *For $j \neq 0$ or ∞, the class e_j is cuspidal. In other words, in this case $e_j \in H^1(\mathscr{X}(p))$.*
(e) *The homomorphism from the long exact sequence*

$$H^1(\mathscr{Y}(p)) = H^1(\mathscr{X}(p), \{\text{cusps}\}) \longrightarrow H_0(\{\text{cusps}\})$$

takes e_0 to $v_\alpha(\xi)$.

Furthermore, as ξ ranges over all cusps of $\mathscr{X}(p)$, the sets $\{e_j \mid j \in \mathbb{P}^1(\mathbb{F}_p)\}$ generate the entire V_α isotypic component.

The first step in the construction of $\{e_j\}$ is to define a metric μ on C^1 having values in $\mathbb{P}^1(\mathbb{F}_p)$. Given a fixed cusp and an oriented 1-cell, μ measures the distance between them. Since $\mathscr{X}(p)$ is orientable, around each cusp we choose a direction called "clockwise." To do this, we arbitrarily choose one of the directions around any cusp and use the group G_p to distribute our choice uniformly over the rest of $\mathscr{X}(p)$.

Now fix a cusp $\xi \in X^1(p)$ and let η be a cusp in the link of ξ. Let Σ denote the set of 1-cells in the star of η. Orient each $\sigma \subset \Sigma$ in the direction of η.

Suppose σ is the 1-cell from ξ to η. We define $\mu(\sigma) = 0$. Then we extend μ by saying that if σ is at distance j, then the 1-cell adjacent to σ in the clockwise direction is at distance $j+1$:

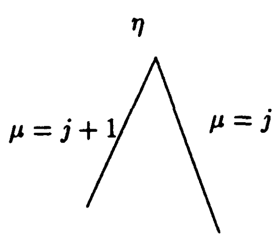

FIGURE V.5.

Using the group G_p, we can extend μ to all of C^1. *Convention:* If we reverse the orientation of the 1-cell at distance zero, the resulting 1-cell is said to have distance ∞.

LEMMA V.2. *Let $\sigma \in C^1$. Then if $\mu(\sigma) = j$, we have that $\mu(-\sigma) = -1/j$.*

PROOF. Consider the following picture, where we have used the notation $\xi = (v; d)$:

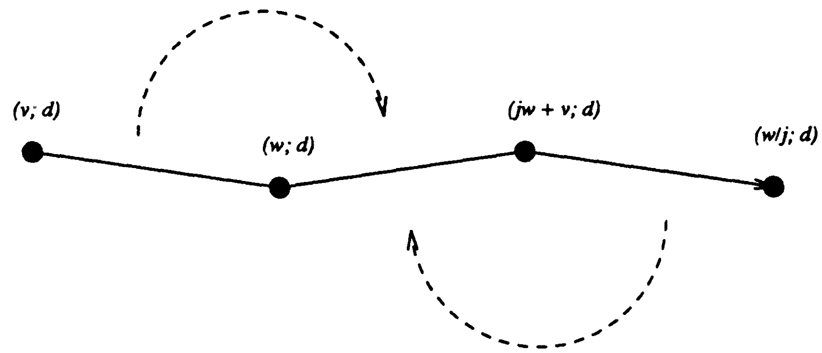

FIGURE V.6.

□

Now we are ready to construct the e_j.

DEFINITION V.4. Fix $\xi = (v; d)$. Let $\sigma_j^d \subset C^1$ denote the subset at distance j supported in the component $X^d(p)$.

The cocycle e_j is defined to be

$$e_j := \sum_{n \in (\mathbb{Z}/p)^\times} \alpha^{-1}(n)\sigma_j^{nd}.$$

PROOF OF PROPOSITION V.8. We address each item separately:

(a) To each 1-cell in e_j we may correspond a unique associate of ξ, namely, the associate from which e_j is distance j. Consider labeling each associate of ξ with the coefficient of the corresponding 1-cell in e_j. We obtain a vector v in C^2 which is clearly in V_α. Since the relationships used in building v clearly are preserved by the action of G_p, it follows that G_p acts on each e_j as the twisted Steinberg V_α.

(b) Obviously the cocycles are linearly independent, and the relation is an easy consequence of Lemma V.2.

(c) Let $\eta \in Lk\xi$. Consider the following 2-cell in the link of η that contains e_{j-1}:

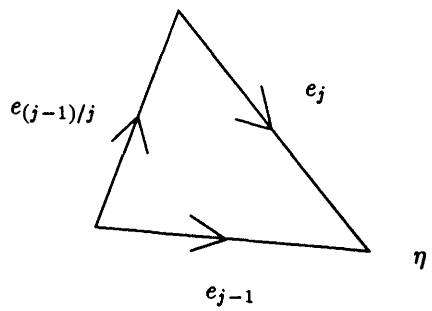

FIGURE V.7.

The reason that the top 1-cell is part of e_j is clear. To see that the left 1-cell is part of $e_{(j-1)/j}$, note that this 1-cell is one step clockwise from the 1-cell $e_{-1/j}$.

(d) If $j \neq 0$ or ∞, then at every cusp η that is not an associate of ξ, the cocycle e_j enters at distance j and exits at distance $-1/j$.

(e) This is clear.

Now, to complete the proof, note that every 1-cell σ is at distance j from a unique class of associate cusps, and $-\sigma$ is at distance j from another unique class of associate cusps. Thus, if we fix j and add together all the e_j's that arise by varying ξ, we obtain zero. This is the only relation that arises, and hence we conclude that the vector space generated by fixing j and varying σ has dimension p, and thus must be the twisted Steinberg. □

Note that Propositions V.7 and V.8 are consistent. Specifically, fix a cusp ξ. As j ranges over $\mathbb{P}^1(\mathbb{F}_p)$, we obtain $p+1$ cocycles e_j. The relation $e_j = e_{-1/j}$ means that we in fact have $(p+1)/2$ cocycles. If $p = 1 \bmod 4$, then there is a $i \in \mathbb{P}^1(\mathbb{F}_p)$ such that $i = -1/i$, which means that $e_i = 0$. Hence the representation V_α occurs with multiplicity $(p+1)/2$ if $p = 3 \bmod 4$ and with multiplicity $(p-1)/2$ if $p = 1 \bmod 4$.

5. The Hecke Action

Fix a cusp $\xi \in \mathscr{X}(p)$ and a character $\alpha\colon \mathbb{F}_p^\times \to \mathbb{C}^\times$. Let $\{e_j \mid j \in \mathbb{P}^1(\mathbb{F}_p)\}$ be the set of cocycles attached to ξ and α constructed in the previous section. If $\ell \neq p$ is a prime, then we would like to compute the action of the Hecke correspondence T_ℓ on the set $\{e_j\}$. We will do this by constructing a set of 2×2 integral matrices $\{\phi_i\}$so that

$$T_\ell(e_j) = \sum_i e_{\phi_i(j)},$$

where the action of ϕ_i on $j \in \mathbb{P}^1(\mathbb{F}_p)$ is given by fractional-linear transformations.

Let M be the set of all 2×2 integral matrices. Define a function $h\colon M \longrightarrow M$ by the following procedure. Let $m = \left(\begin{smallmatrix} a & b \\ c & d \end{smallmatrix}\right) \in M$.

(a) If $b = 0$, then $h(m) = m$. Otherwise, add or subtract the first row of m from the second until $|d| < |b|$.

(b) Change the sign of the bottom row, then exchange rows.

For example, if $m = \left(\begin{smallmatrix}1 & -5\\ 0 & 13\end{smallmatrix}\right)$, then $h(m) = \left(\begin{smallmatrix}-2 & -3\\ -1 & 5\end{smallmatrix}\right)$.

Given $m \in M$, define the *h-sequence* of m to be the sequence $\{m_0, \dots, m_n\}$, where

(a) $m_0 = m$.
(b) $m_{i+1} = h(m_i)$.

For example, the h-sequence of $\left(\begin{smallmatrix}1 & -5\\ 0 & 13\end{smallmatrix}\right)$ is the following:

$$\begin{pmatrix}1 & -5\\ 0 & 13\end{pmatrix}, \begin{pmatrix}-2 & -3\\ 1 & -5\end{pmatrix}, \begin{pmatrix}-3 & 2\\ -2 & -3\end{pmatrix}, \begin{pmatrix}5 & 1\\ -3 & 2\end{pmatrix}, \begin{pmatrix}13 & 0\\ 5 & 1\end{pmatrix}.$$

The main result of this section is the following:

PROPOSITION V.9. *Fix an odd prime $\ell \neq p$, a Steinberg V_α, and a cusp ξ. Construct the family of cocycles $\{e_j\}$. Define a set Φ of 2×2 integral matrices by*

$$\Phi := \left\{\begin{pmatrix}\ell & 0\\ 0 & 1\end{pmatrix}\right\} \sqcup \coprod_{k=-(\ell-1)/2}^{(\ell-1)/2} \left\{h\text{-sequence of} \begin{pmatrix}1 & k\\ 0 & \ell\end{pmatrix}\right\}.$$

(The union is disjoint.) Then

$$T_\ell(e_j) = \sum_{\phi \in \Phi} \alpha(\ell) e_{\phi(j)}.$$

PROOF. First, we observes that the character $\alpha(\ell)$ that arises because T_ℓ takes the det d component to the det ℓd components..

Let $\xi = (\left(\begin{smallmatrix}1\\ 0\end{smallmatrix}\right); 1)$, and construct the set $\{e_j\}$ with respect to ξ. Our method of proof is to compute directly the action on a particular representative of e_j, shown here:

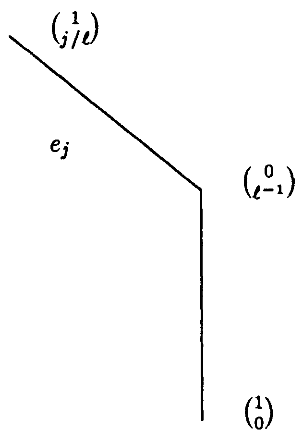

FIGURE V.8.

This edge is part of an e_j in the det ℓ^{-1} component; the Hecke images will lie in the det 1 component. First we examine the "stripe" images, which correspond to simply multiplying first one and then the other endpoint:

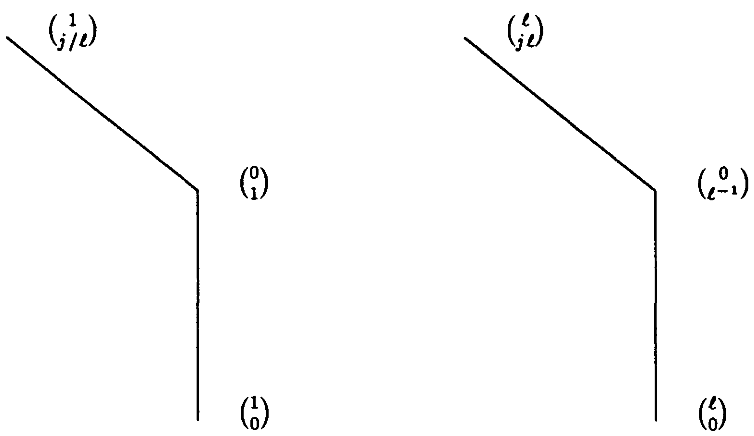

FIGURE V.9.

The first is a part of $e_{j/\ell}$, and the second is a part of $e_{\ell j}$. This accounts for the matrices

$$\begin{pmatrix} 1 & 0 \\ 0 & \ell \end{pmatrix} \text{ and } \begin{pmatrix} \ell & 0 \\ 0 & 1 \end{pmatrix}$$

in Φ. The remaining images terminate at $(\binom{\ell}{j};1)$ and $(\binom{0}{1};1)$, and these must be pushed back into the cell complex using the roadmap algorithm. Suppose we fix a type k of image and thus fix a roadmap with exponents $(a_1,\ldots,a_n)$. Near $(\binom{0}{1};1)$, we have the following picture:

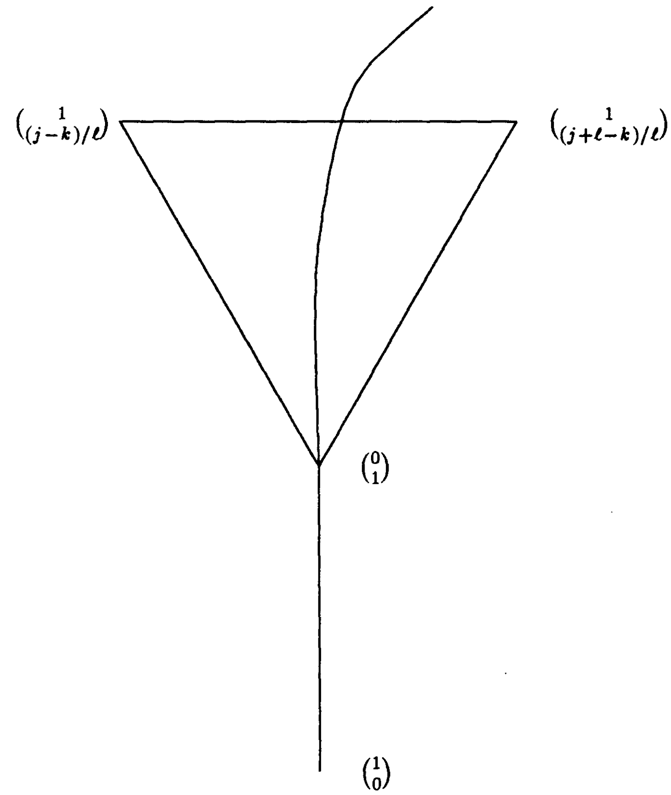

FIGURE V.10.

Here k is between 0 and ℓ. Suppose that $\ell - k < k$. Then using our algorithm we push this image to the right; in other words, our image contains a part of $e_{(j+\ell-k)\ell}$. On the other hand, if $k < \ell - k$, then the image contains a part of $e_{(j-k)/\ell}$. Since k can range over all possible values between 0 and ℓ, we have accounted for the matrices

$$\begin{pmatrix} 1 & -(\ell-1)/2 \\ 0 & \ell \end{pmatrix}, \ldots, \begin{pmatrix} 1 & (\ell-1)/2 \\ 0 & \ell \end{pmatrix}.$$

These index the h-sequences appearing in the statement.

To conclude the proof, we must show that the h-sequences of these matrices arise as we push the image back into the 1-skeleton. Assume without loss of generality that $\ell - k < k$, so that the initial matrix is

$$\begin{pmatrix} 1 & \ell - k \\ 0 & \ell \end{pmatrix}$$

Write the action of this matrix on j as $\phi_1(j)$. Write $e_{\phi_2(j)}$ for the next segment that appears in the image. Our immediate goal is to show that $\phi_2 = h(\phi_1)$.

We have the following picture:

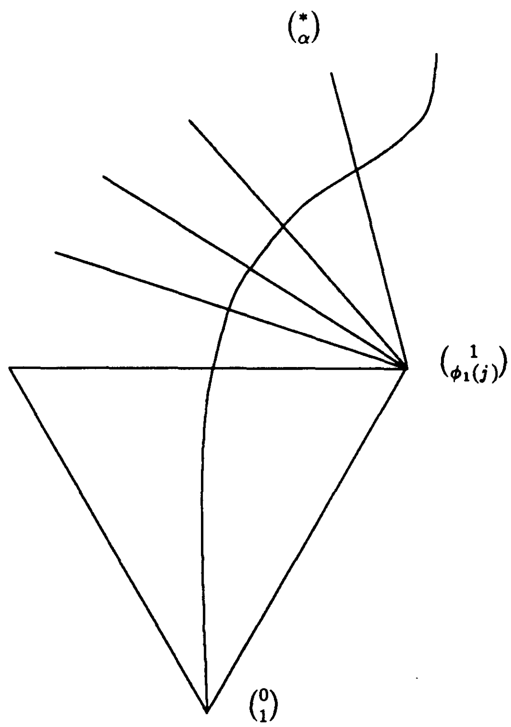

FIGURE V.11.

From our algorithm, we know that

$$\alpha = (a_1 + 1)\phi_1(j) - 1.$$

Now, by definition, $\phi_2(j)$ is the number of steps we must take to get from the associate of ξ in the link of $\binom{1}{\phi_1(j)}$ to get to $\binom{*}{\alpha}$. This associate is some vector of the form $\binom{*}{0}$, which means that

$$\phi_2(j)\phi_1(j) = \alpha$$

and so

$$\phi_2(j) = (a_1 + 1) - \phi_1(j)^{-1}.$$

Notice that when we perform the subtraction on the right, on matrices we are actually performing the steps used to define h. It is easy to see, recalling the construction of a_1, that we are in fact subtracting just the right multiple of the bottom from the top so that $\phi_2 = h(\phi_1)$.

We conclude the proof by induction. To aid in the proof, we define a sequence $= \lambda_1$ by the following picture:

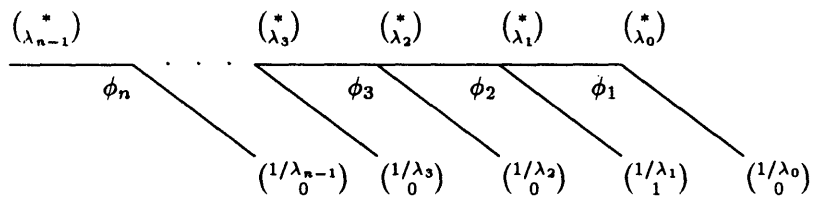

FIGURE V.12.

The meaning of the figure is this. The horizontal row is the result of pushing this image of $T_\ell(e_j)$ back into the cell complex. The vectors along the bottom are the associates of $(\binom{1}{0}; 1)$ from which we compute μ. (The determinant information has been suppressed since we know that we are in the det 1 component. The λ_i can be determined inductively using the roadmap algorithm and the results above:

$$\begin{aligned}\lambda_0 &= 1\\ \lambda_1 &= (j+k-\ell)/\ell\\ \lambda_2 &= (a_1+1)\lambda_1 - \lambda_0\\ \lambda_{i+1} &= a_i\lambda_i + \lambda_{i-1}, \quad \text{for } i > 1\end{aligned}$$

The point is that, for $i > 2$,

$$\mu(i\text{th edge}) = (-1)^i \frac{\lambda_i}{\lambda_{i-1}}.$$

This is clear, except for the sign, and this arises because we change directions back and forth from right to left and vice versa. Now we begin the induction. We fix m, and assume that

$$\phi_i = h(\phi_{i-1}) \quad \text{for } i \leq m.$$

Then

$$\begin{aligned}\phi_{m+1} &= (-1)^{m+1}\frac{\lambda_{m+1}}{\lambda_m}\\ &= (-1)^{m+1}\frac{a_m\lambda_m + \lambda_{m-1}}{\lambda_m}\\ &= (-1)^{m+1}a_m + \frac{\lambda_{m-1}}{\lambda_m}\\ &= (-1)^{m+1}a_m + (-1)^m\phi_m^{-1}.\end{aligned}$$

It remains to be seen that this last expression is $h(\phi_m)$. Again, at the matrix level we are flipping rows and reducing the top, and the extra sign arises from the direction changes. □

6. The Eisenstein Section

We are now ready to describe the linear system that determines the Eisenstein section E on the Steinberg classes. Fix a Steinberg $V_\alpha \subset C^2$, and a set of cusps

$$\{\xi_{(k)} \mid k \in \mathbb{P}^1(\mathbb{F}_p)\}$$

so that $v_\alpha(\xi_{(k)})$ generate V_α. By symmetry, we need only consider a fixed cusp ξ. To make notation simpler, we shall write v_ξ for $v_\alpha(\xi)$.

Recall that the Eisenstein section E must satisfy two properties:

(a) If $\delta\colon H^1(\mathscr{Y}(p)) \longrightarrow H_0(\{\text{cusps}\})$ is the map in the long exact sequence, then $\delta \circ E$ is the identity map.
(b) Given $v \in V_\alpha \subset H_0(\{\text{cusps}\})$, we must have that $T_\ell(E(v)) = \alpha(\ell)(\ell + 1)E(v)$.

The idea to build E is that the relative class e_0 approximates $E(v_\xi)$. This is a reasonable guess, since by Proposition V.8 $\delta(e_0) = v_\xi$, but unfortunately in most cases e_0 will not be a Hecke eigenclass. Since the action of T_ℓ preserves V_α, we modify this guess by writing

$$E(v_\xi) = \sum_{j \in \mathbb{P}^1(\mathbb{F}_p)} a_j e_j,$$

where $a_j \in \mathbb{C}$. (Note that $a_0 = 1$.) Since by Proposition V.8 the cocycles e_j are cuspidal if $j \neq 0$ or ∞, the composition $\delta \circ E$ is the identity on this expression. By Proposition V.9 we know how to compute the action of T_ℓ on each e_j, and so by linearity we know how to compute T_ℓ on the entire expression. Hence we may construct $E(v_\xi)$ if we can determine enough conditions on the a_j to specify them uniquely.

Before we begin to describe the system, we note that Example V.2 completely performs the process for the modular curve $\mathscr{X}(11)$, and the reader might find it helpful to read this example concurrently with the conditions.

Condition I. We immediately obtain conditions of the a_j by Proposition V.8. Part (b) of this proposition requires that

$$a_j = -a_{-1/j}.$$

In light of this, we shall write $\sum_j a_j e_j$ for $E(v_\xi)$, where the sum is taken an appropriate subset of $\mathbb{P}^1(\mathbb{F}_p)$.

Condition II. (Harmonic conditions). We must reconcile the fact that we want a Hecke eigenclass in $H^1(\mathscr{X}(p), \{\text{cusps}\})$, and all our computations are performed at the chain level. This means we have two choices:

(a) We may attempt to choose a cohomology basis from $\{e_j\}$ by using the relations in Proposition V.8.
(b) We may insist that each cellular representative for $E(v_\xi)$ be canonical, without choosing a specific basis in the $\{e_j\}$.

We choose the second approach by requiring that our representative be *harmonic*. Since this notion in the context of cell complexes is somewhat unfamiliar, we review it here. Let (Δ, ∂) be a cell complex, and let (Δ', ∂') be the dual cell complex. A cycle σ in the chain complex associated to Δ is said to harmonic if $\partial'(\sigma') = 0$. As in the usual use of the word harmonic, every cycle has a unique harmonic representative.

PROPOSITION V.10. *The cocycle* $e_0 + \sum_j a_j e_j$ *is harmonic iff*

$$a_j - a_{j-1} + a_{(j-1)/j} = 0.$$

PROOF. Simply consider the triangle in Figure 4 in the proof of Proposition V.8:

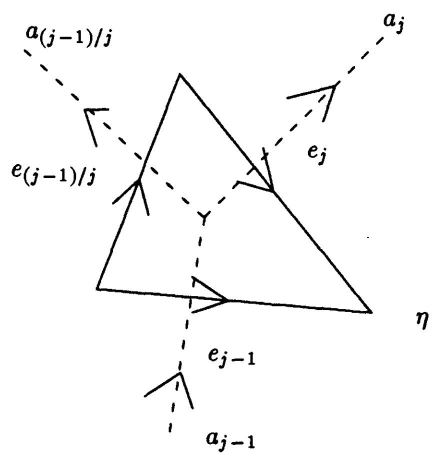

FIGURE V.13.

We have drawn the dual complex using dashed lines. The result is clear. □

We will say that a chain satisfying this property is a *harmonic chain*. We adopt this condition into our system.

Condition III. (Eigenclass conditions). The statement that $E(v_\xi)$ is a Hecke eigenclass of eigenvalue $\alpha(\ell)(\ell+1)$ translates into the conditions

$$\alpha(\ell)(\ell+1)a_j = \sum_i a_{\phi_i^{-1}(j)}.$$

Note the use of ϕ_i^{-1} in the subscript. These conditions are not quite correct, as the Hecke image of a harmonic chain will not in general be a harmonic chain. We fix this by adding multiples of boundaries

$$e_j - e_{j-1} + e_{(j-1)/j}.$$

Hence, for every boundary, add a new parameter $\omega^{(j)}$ to these conditions. For example, given the boundary $e_j - e_{j-1} + e_{(j-1)/j}$, modify the following three equations as indicated:

$$\alpha(\ell)(\ell+1)a_j = \sum_i a_{\phi_i^{-1}(j)} + \omega^{(j)},$$
$$\alpha(\ell)(\ell+1)a_{j-1} = \sum_i a_{\phi_i^{-1}(j-1)} - \omega^{(j)},$$
$$\alpha(\ell)(\ell+1)a_{(j-1)/j} = \sum_i a_{\phi_i^{-1}((j-1)/j)} + \omega^{(j)}.$$

This completes the conditions needed to build the system. For the convenience of the reader, we present an example.

EXAMPLE V.2. Consider the full modular curve $\mathscr{X}(11)$. By the calculations of II.5, $\mathscr{X}(11)$ is ten copies of a surface of genus twenty-six. In each connected component, $\Delta(p)$ has 60 vertices, 330 edges, and 220 triangles. Let us take as a fixed cusp $\xi = (\binom{1}{0}; 1)$. To simplify the example, we will build the Eisenstein section on classes in the genuine Steinberg representation. In other words, we shall take α to be the trivial character. The first figure depicts the intersection of each e_j with the closed star of $(\binom{0}{1}; 1)$, which is the vertex at the center of the 11-gons. The fixed cusp ξ is the vertex at the bottom of each 11-gon. In these pictures, one computes $\mu(e_j)$ as follows. Count around the edges emanating from $(\binom{0}{1}; 1)$ in the clockwise direction. The value of $\mu(e_j)$ is the number for which e_j is directed into $(\binom{0}{1}; 1)$. Note that by the condition $e_j = -e_{-1/j}$, a complete set of cocycles is given by $j = 0,\ 1,\ \pm 2$, and ± 3.

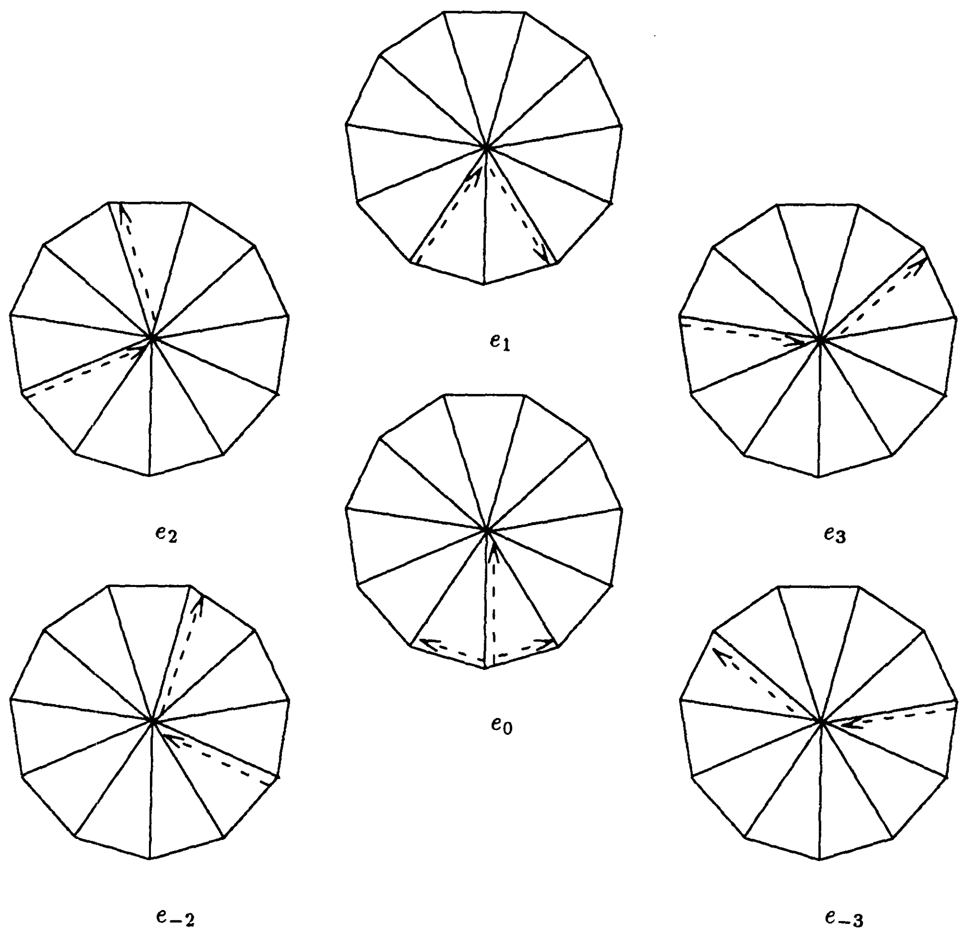

FIGURE V.14. The cocycles $\{e_j\}$ in the closed star of $(\binom{0}{1}; 1)$.

The next figure provides some intuition for how some of the cocycles sit globally in $X^1(11)$. The edges labeled a and a' are to be identified. The cocycles $e_{\pm 2}$ run parallel to each other in eleven disjoint strips, while the cocycles e_3 cut transversely across the strips.

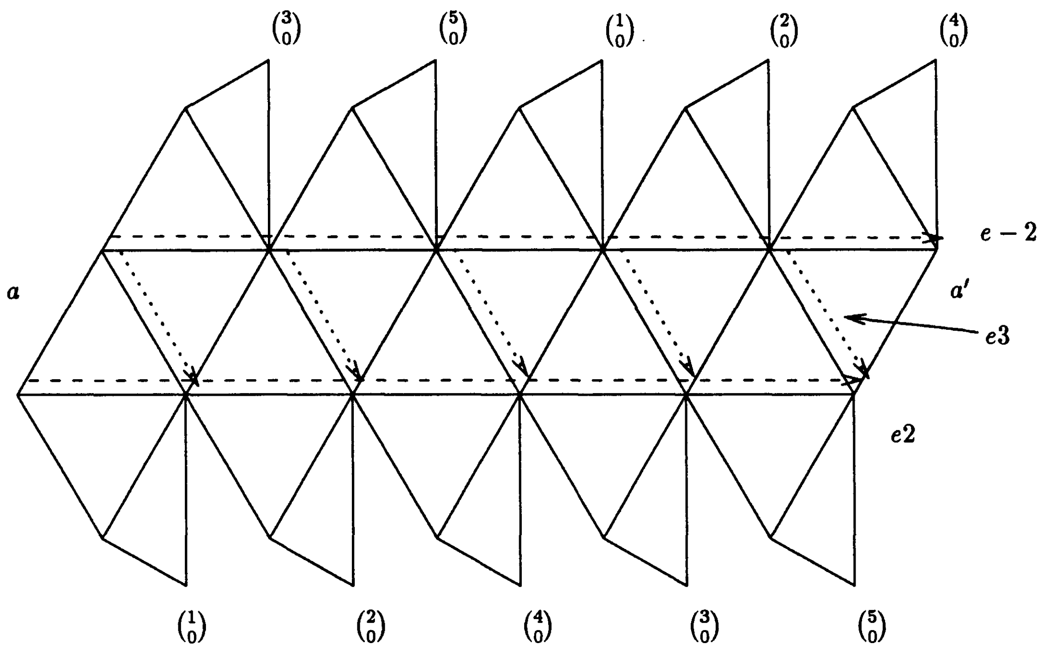

FIGURE V.15. A portion of $X^1(11)$.

Now assume that $E(\xi)$ has the form

$$e_0 + a_1e_1 + a_2e_2 + a_{-2}e_{-2} + a_3e_3 + a_{-3}e_{-3}.$$

The condition that this cocycle be harmonic yields three conditions on the coefficients:

$$\begin{aligned} a_1 &= 0 \\ a_2 - a_3 - a_{-3} &= 0 \\ a_3 + a_3 - a_{-2} &= 0 \end{aligned}$$

Now we apply a Hecke correspondence. For convenience we use the simplest correspondence allowed by Proposition V.9, namely T_3. Using the results of V.5 we conclude that

$$T_3(e_j) = e_{3j} + e_{j/3} + e_{(j+1)/3} + e_{(j-1)/3} + e_{3j/(j+1)} + +e_{-3j/(j-1)}.$$

In terms of our cocycles this becomes

$$\begin{aligned} T_3(e_0) &= 4e_0 - e_3 - e_{-3} \\ T_3(e_2) &= -e_{-2} \\ T_3(e_{-2}) &= -e_2 \\ T_3(e_3) &= -2e_2 + e_{-2} - e_{-3} \\ T_3(e_{-3}) &= -2e_{-2} + e_2 - e_3 \end{aligned}$$

Translating these into eigenclass conditions on the a_j's, we find

$$\begin{aligned} 4a_2 &= -a_{-2} - 2a_3 + a_{-3} \\ 4a_{-2} &= -a_2 - 2a_{-3} + a_3 \\ 4a_3 &= a_{-3} - 1 \\ 4a_{-3} &= a_3 - 1 \end{aligned}$$

Now we must add correction terms corresponding to the parameters $\omega^{(j)}$ described above. Since there are only two boundaries of importance, namely $e_2 - e_3 - e_{-3}$ and $e_3 + e_{-3} - e_{-2}$, we need to add only two parameters. The final linear system, composed of the coboundary and eigenclass conditions, is

$$\begin{aligned} a_2 - a_3 - a_{-3} &= 0 \\ a_3 + a_{-3} - a_{-2} &= 0 \\ 4a_2 &= -a_{-2} - 2a_3 + a_{-3} - \omega^{(1)} \\ 4a_{-2} &= -a_2 - 2a_{-3} + a_3 - \omega^{(2)} \\ 4a_3 &= a_{-3} - 1 + \omega^{(1)} + \omega^{(2)} \\ 4a_{-3} &= a_3 - 1 + \omega^{(1)} + \omega^{(2)} \end{aligned}$$

We solve this system to obtain

$$a_2 = a_{-2} = -2/25 \quad \text{and} \quad a_3 = a_{-3} = -1/25,$$

which means that

$$E(\xi) = e_0 - \frac{2}{25}(e_2 + e_{-2}) - \frac{1}{25}(e_3 + e_{-3}).$$

We summarize our system in the following theorem:

THEOREM V.1. *Fix two odd primes $p \neq \ell$. Fix a cusp $\xi \in \mathscr{X}(p)$ and a character $\alpha\colon \mathbb{F}_p^\times \to \mathbb{C}^\times$. Let $\{e_j\}$ be the set of cocycles constructed in Proposition V.8 that spans the twisted Steinberg $V_\alpha \subset H^1(\mathscr{X}(p), \{\text{cusps}\})$. Construct a system, of linear equations by allowing the parameter j to range over $\mathbb{P}^1(\mathbb{F}_p)$:*

(a) $a_j = -a_{-1/j}$.
(b) $a_j - a_{j-1} + a_{(j-1)/j} = 0$.
(c) $\alpha(\ell)(\ell+1)a_j = \sum_i a_{\phi_i^{-1}(j)}$.

Furthermore, for each equation in part (b) add a correction parameter $\omega^{(j)}$ to the appropriate equations in part (c), with the correct signs as described in the text.

Then if $\{a_j\}$ is the solution to this system, the Eisenstein section on v_ξ is given by

$$E(v_\xi) = e_0 + \sum_j a_j e_j.$$

PROOF. The real difficulty is the existence of the Eisenstein section, which we have taken for granted. Given that the section exists, and that these e_j's span the V_α-isotypic of $H^1(\mathscr{X}(p), \{\text{cusps}\})$, the above system for any given ℓ is the only possibility for $E(v_\xi)$. Finally, since the algebra of Hecke correspondences is commutative, it suffices to compute the system for one ℓ. □

In Appendix C, we list some example Eisenstein classes. We conclude with a few remarks.

REMARK V.2. The astute reader will notice many symmetries in the above system that could be used to afford a cleaner presentation. In particular, the size of the system could be halved through introducing a new basis cocycle corresponding to $e_j + e_{-j}$. We have chosen not to do this because doing so complicates the statement of how T_ℓ acts on the basis.

REMARK V.3. Although harmonic classes are canonical representatives of cohomology classes, it would be much better to find a better basis. The main reason is that the coefficients a_j contain important arithmetic information, and this information is best detected by using a basis that is in fact an integral basis. At present we are unable to choose a geometrically satisfying integral basis, so we are forced to use harmonic classes.

APPENDIX A

A Collection of Universal Hecke Correspondences

In this appendix we present pictures of the simplest universal Hecke correspondences, $\mathscr{C}_2$, $\mathscr{C}_3$, $\mathscr{C}_5$, and $\mathscr{C}_7$. The pictures follow the conventions established in Chapter IV.

Notes for the figures:

- For $\ell \geq 5$, the spaces are noncompact.
- The space $\mathscr{C}_7$ has the universal tree of valence three as a deformation retract.
- The solid and dashed 1-cells in $\mathscr{C}_2$ and $\mathscr{C}_5$ that intersect in their barycenters correspond to sublattices of the square lattice that are square.
- The barycenters solid and dashed 2-cells in $\mathscr{C}_3$ and $\mathscr{C}_7$ that intersect symmetrically correspond to sublattices of the triangular lattice that are triangular.

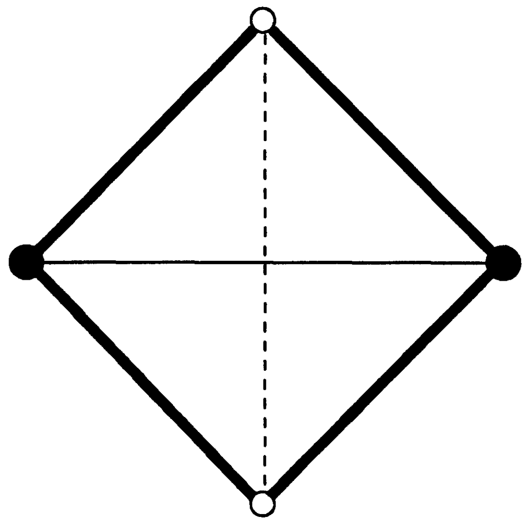

FIGURE A.1. $\mathscr{C}_2$

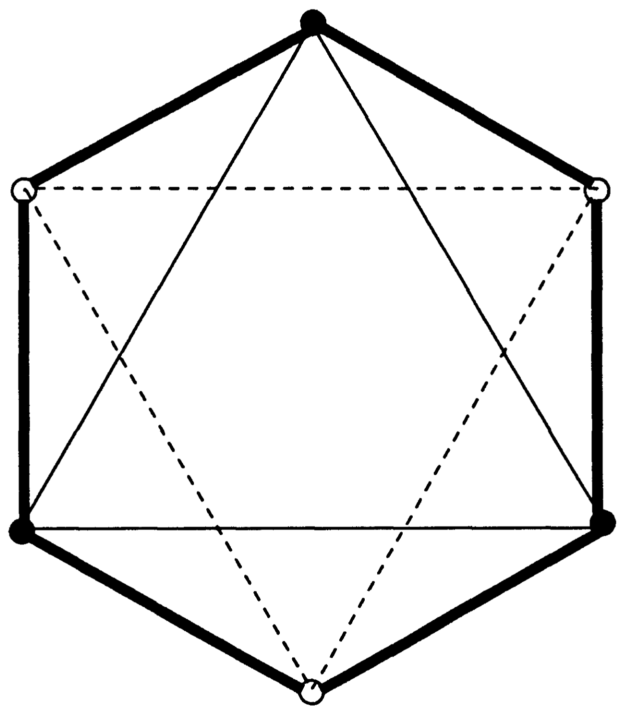

FIGURE A.2. $\mathscr{C}_3$

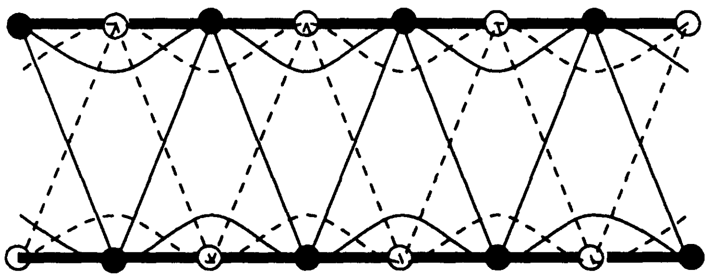

FIGURE A.3. $\mathscr{C}_5$

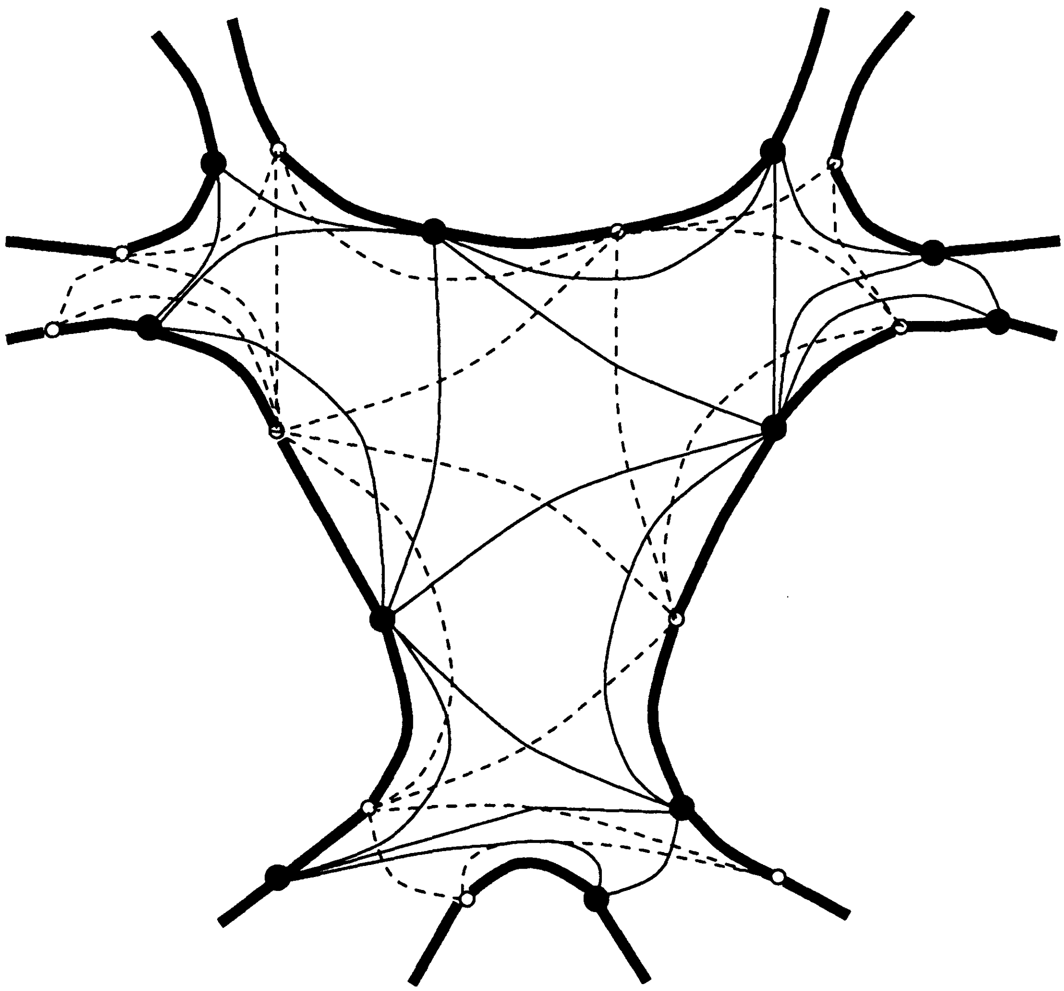

FIGURE A.4. $\mathscr{C}_7$

APPENDIX B

Decomposition of Cohomology

In this appendix we present the results of the character theoretic computations alluded to in V.2. We present the result at the level of cohomology; the corresponding result at the level of the chain complex is not difficult.

Notes for the decomposition table:

- α and β denote complex characters of $(\mathbb{F}_p)^\times$.
- ϕ denotes a complex character of $(\mathbb{F}_{p^2})^\times$ such that $\phi^p \neq \phi$.
- x denotes a primitive fourth root of unity in either $(\mathbb{F}_p)^\times$ or $(\mathbb{F}_{p^2})^\times$.
- a denotes a primitive sixth root of unity in either $(\mathbb{F}_p)^\times$ or $(\mathbb{F}_{p^2})^\times$, and b denotes a^2.
- ω denotes a complex cube root of unity.
- Representations of type $W_{\alpha,\beta}$ are the standard induced representations.
- Representations of type V_α are the twisted Steinberg representations.
- Representations of type X_ϕ are those associated to the anisotropic tori of $GL(2, \mathbb{F}_p)$.

$p = 1 \bmod 12$

Type V_α (dimension $= p$)

Restrictions	*Number of Distinct Types*	*Multiplicity of Each Type*
none	$p-1$	$(p-7)/6$

Type $W_{\alpha,\beta}$ (dimension $= p+1$)

Restrictions	*Number of Distinct Types*	*Multiplicity of Each Type*
$\alpha(-1) = \beta(-1)$ $\alpha(x) = \beta(x)$ $\alpha(a) = \beta(a)$	$(p-13)(p-1)/24$	$(p-13)/6$
$\alpha(-1) = \beta(-1)$ $\alpha(x) \neq \beta(x)$ $\alpha(a) = \beta(a)$	$(p-1)^2/24$	$(p-1)/6$
$\alpha(-1) = \beta(-1)$ $\alpha(x) = \beta(x)$ $\alpha(a) \neq \beta(a)$	$(p-1)^2/12$	$(p-1)/6$
$\alpha(-1) = \beta(-1)$ $\alpha(x) \neq \beta(x)$ $\alpha(a) \neq \beta(a)$	$(p-1)^2/12$	$(p+11)/6$

Type X_ϕ (dimension $= p-1$)

Restrictions	*Number of Distinct Types*	*Multiplicity of Each Type*
$\phi(-1) = 1$	$(p-1)^2/4$	$(p-1)/6$

$p = 5 \bmod 12$

Type V_α (dimension $= p$)

Restrictions	*Number of Distinct Types*	*Multiplicity of Each Type*
none	$p-1$	$(p+1)/6$

Type $W_{\alpha,\beta}$ (dimension $= p+1$)

Restrictions	*Number of Distinct Types*	*Multiplicity of Each Type*
$\alpha(-1) = \beta(-1)$ $\alpha(x) = \beta(x)$	$(p-1)(p-5)/8$	$(p-5)/6$
$\alpha(-1) = \beta(-1)$ $\alpha(x) \neq \beta(x)$	$(p-1)^2/8$	$(p+7)/6$

Type X_ϕ (dimension $= p-1$)

Restrictions	*Number of Distinct Types*	*Multiplicity of Each Type*
$\phi(-1) = 1$ $\phi(a) = \phi(b)$	$(p-1)(p-5)/12$	$(p+7)/6$
$\phi(-1) = 1$ $\phi(a) \neq \phi(b)$	$(p^2-1)/6$	$(p-5)/6$

$p = 7 \bmod 12$

Type V_α (dimension $= p$)

Restrictions	*Number of Distinct Types*	*Multiplicity of Each Type*
none	$p-1$	$(p-1)/6$

Type $W_{\alpha,\beta}$ (dimension $= p+1$)

Restrictions	*Number of Distinct Types*	*Multiplicity of Each Type*
$\alpha(-1) = \beta(-1)$ $\alpha(a) = \beta(a)$	$(p-1)^2/6$	$(p+5)/6$
$\alpha(-1) = \beta(-1)$ $\alpha(a) \neq \beta(a)$	$(p-1)(p-7)/12$	$(p-7)/6$

Type X_ϕ (dimension $= p-1$)

Restrictions	*Number of Distinct Types*	*Multiplicity of Each Type*
$\phi(x) = 1$	$(p-1)(p-3)/8$	$(p+5)/6$
$\phi(x) = -1$	$(p^2-1)/8$	$(p-7)/6$

$p = 11 \bmod 12$

Type V_α (dimension $= p$)

Restrictions	*Number of Distinct Types*	*Multiplicity of Each Type*
none	$p-1$	$(p+7)/6$

Type $W_{\alpha,\beta}$ (dimension $= p+1$)

Restrictions	*Number of Distinct Types*	*Multiplicity of Each Type*
$\alpha(-1) = \beta(-1)$	$(p-1)(p-3)/4$	$(p+1)/6$

Type X_ϕ (dimension $= p-1$)

Restrictions	*Number of Distinct Types*	*Multiplicity of Each Type*
$\phi(x) = 1$ $\phi(a) = 1$	$(p-1)(p-11)/24$	$(p+13)/6$
$\phi(x) = 1$ $\phi(a) = \omega^{\pm 1}$	$(p^2-1)/24$	$(p+1)/6$
$\phi(x) = -1$ $\phi(a) = 1$	$(p^2-1)/12$	$(p+1)/6$
$\phi(x) = -1$ $\phi(a) = \omega^{\pm 1}$	$(p^2-1)/12$	$(p-11)/6$

APPENDIX C

Coefficients for Combinatorial Eisenstein Classes

In this appendix we present data relating to combinatorial Eisenstein classes. To simplify the data, we have taken the liberty of writing the class using an integral basis for $H^1(\mathscr{Y}(p);\mathbb{C})$. The rational number a_j is the coefficient of the correction cocycle $e_j + e_{-j}$. We have also only displayed the coefficients of the class in the identity component $Y^1(p)$.

$p = 1 \bmod 12$

Level 37:
$a_7 = -1/3$, $a_8 = 1/3$

Level 61:
$a_8 = 0$, $a_{17} = -2/5$, $a_{24} = 1/5$, $a_{22} = -2/5$

Level 73:
$a_{10} = -1/2$, $a_{16} = 1/6$, $a_{31} = -1/3$, $a_{11} = 1/2$, $a_{14} = -1/6$

Level 97:
$a_{10} = 0$, $a_{18} = -5/8$, $a_{26} = -1/2$, $a_{30} = -1/8$, $a_{13} = -5/8$, $a_{19} = 1/4$, $a_{21} = 3/8$

Level 109:
$a_{10} = -2/3$, $a_{15} = -1/9$, $a_{16} = 1/9$, $a_{20} = -5/9$, $a_{25} = 5/9$, $a_{38} = -4/9$, $a_{14} = 0$, $a_{44} = 2/9$

Level 157:
$a_{10} = -9/13$, $a_{16} = 9/13$, $a_{17} = -8/13$, $a_{18} = -1/13$, $a_{19} = 9/13$, $a_{24} = 7/13$, $a_{31} = -5/13$, $a_{32} = 6/13$, $a_{22} = -7/13$, $a_{43} = -7/13$, $a_{67} = 8/13$, $a_{70} = -1/13$

Level 181:
$a_{13} = -11/15$, $a_{24} = -2/3$, $a_{28} = 2/3$, $a_{38} = 1/15$, $a_{39} = 0$, $a_{42} = -1/15$, $a_{58} = -2/15$, $a_{62} = -7/15$, $a_{16} = -2/3$, $a_{50} = 2/15$, $a_{55} = 3/5$, $a_{72} = -2/5$, $a_{17} = 2/3$, $a_{51} = -2/3$

Level 193:
$a_{14} = 0$, $a_{21} = -9/16$, $a_{30} = 5/8$, $a_{38} = -1/4$, $a_{40} = -7/16$, $a_{44} = 11/16$, $a_{60} = 1/16$, $a_{17} = -1/16$, $a_{22} = 5/8$, $a_{27} = -1/8$, $a_{51} = -11/16$, $a_{67} = -3/4$, $a_{86} = 5/16$, $a_{28} = -1/2$, $a_{71} = 0$

$p = 5 \bmod 12$

Level 17:
$a_5 = -1/4$

Level 29:
$a_5 = -3/7$, $a_8 = -2/7$

Level 41:
$a_6 = -1/2$, $a_{12} = -3/10$, $a_{16} = 1/10$

Level 53:
$a_7 = -1/13$, $a_8 = -6/13$, $a_{10} = 5/13$, $a_{11} = 2/13$

Level 89:
$a_9 = -7/11$, $a_{13} = -13/22$, $a_{16} = 1/22$, $a_{20} = 6/11$, $a_{25} = -9/22$, $a_{28} = 1/11$, $a_{36} = 5/22$

Level 101:
$a_{13} = -16/25$, $a_{14} = 3/25$, $a_{15} = -2/25$, $a_{18} = 3/5$, $a_{22} = -13/25$, $a_{32} = -11/25$, $a_{40} = 6/25$, $a_{43} = -16/25$

Level 113:
$a_{12} = -1/14$, $a_{21} = 1/28$, $a_{22} = -3/14$, $a_{31} = -15/28$, $a_{40} = 15/28$, $a_{13} = 1/14$, $a_{17} = -17/28$, $a_{50} = -3/28$, $a_{23} = 1/4$

Level 137:
$a_{10} = -1/34$, $a_{15} = 11/17$, $a_{19} = -2/17$, $a_{30} = -5/34$, $a_{31} = 13/34$, $a_{43} = -8/17$, $a_{50} = -11/17$, $a_{59} = -11/17$, $a_{12} = -21/34$, $a_{20} = -1/2$, $a_{27} = 4/17$

$p = 7 \bmod 12$

Level 19:
$a_4 = -1/3$

Level 31:
$a_7 = -2/5$, $a_{12} = -1/5$

Level 43:
$a_8 = -1/7$, $a_9 = -2/7$, $a_{12} = 3/7$

Level 67:
$a_7 = -6/11$, $a_9 = 5/11$, $a_{10} = 1/11$, $a_{13} = -4/11$, $a_{14} = 4/11$

Level 79:
$a_9 = -8/13$, $a_{11} = 8/13$, $a_{29} = -3/13$, $a_{14} = -7/13$, $a_{18} = -6/13$, $a_{32} = -5/13$

Level 103:
$a_{11} = -10/17$, $a_{12} = -1/17$, $a_{15} = 11/17$, $a_{20} = -3/17$, $a_{21} = -7/17$, $a_{29} = -9/17$, $a_{37} = -10/17$, $a_{24} = 2/17$

Level 127:
$a_{11} = -1/21$, $a_{15} = -2/3$, $a_{25} = -3/7$, $a_{28} = 10/21$, $a_{30} = -4/7$, $a_{34} = 13/21$, $a_{40} = -1/7$, $a_{46} = -5/21$, $a_{12} = 1/21$, $a_{49} = -1/7$

Level 139:
$a_{12} = -16/23$, $a_{15} = 2/23$, $a_{18} = -1/23$, $a_{21} = 15/23$, $a_{25} = -13/23$, $a_{30} = -1/23$, $a_{33} = 3/23$, $a_{41} = 13/23$, $a_{48} = -9/23$, $a_{56} = -10/23$, $a_{63} = 17/23$

$p = 11 \bmod 12$

Level 11:
$a_3 = -1/5$

Level 23:
$a_4 = -1/11$, $a_5 = -3/11$

Level 47:
$a_7 = -12/23$, $a_9 = 4/23$, $a_{10} = -2/23$, $a_{13} = 1/23$

Level 59:
$a_6 = -1/29$, $a_8 = -13/29$, $a_{18} = 4/29$, $a_9 = -2/29$, $a_{25} = -5/29$

Level 71:
$a_8 = -3/5$, $a_{16} = -16/35$, $a_{21} = 2/35$, $a_{22} = 3/35$, $a_{28} = 6/35$, $a_{11} = -4/7$

Level 83:
$a_7 = -1/41$, $a_{17} = -15/41$, $a_{18} = 1/41$, $a_{19} = 2/41$, $a_{30} = 20/41$, $a_{10} = -24/41$, $a_{16} = 17/41$

Level 107:
$a_{10} = -35/53$, $a_{19} = 1/53$, $a_{21} = 14/53$, $a_{22} = 24/53$, $a_{25} = -29/53$, $a_{29} = -4/53$, $a_{31} = -28/53$, $a_{16} = 3/53$, $a_{41} = -31/53$

Level 131:
$a_{11} = -9/13$, $a_{17} = -38/65$, $a_{20} = 3/65$, $a_{24} = 8/13$, $a_{31} = -36/65$, $a_{37} = 4/65$, $a_{39} = -3/5$, $a_{42} = 9/65$, $a_{14} = -1/13$, $a_{52} = -27/65$, $a_{58} = 2/65$

Bibliography

[AMRT75] A. Ash, D. Mumford, M. Rapaportt, and Y. Tai., *Smooth compactifications of locally symmetric varieties*, Interdisciplinary Mathematics, vol. 2, Math. Sci. Press, Brookline, Mass., 1975.

[AR79] A. Ash and L. Rudolph, *The modular symbol and continued fractions in higher dimensions*, Inv. math. **55** (1979), 241–250.

[Ash77] A. Ash, *Deformation retracts with lowest possible dimension of arithmetic quotients of self-adjoint homogeneous cones*, Math. Ann. **225** (1977), 69–76.

[FH91] W. Fulton and J. Harris, *Representation theory: A first course*, Graduate Texts in Mathematics, vol. 129, Springer-Verlag, New York, 1991.

[Hec39] E. Hecke, *Grundlagen einer Theorie der Integralgruppen und der Integralperioden bei den Normalteilern der Modulgruppe*, Math. Ann. **116** (1939), 469–510.

[Lan76] S. Lang, *Introduction to modular forms*, Grundlehren der mathematischen Wissenschaften, vol. 222, Springer-Verlag, 1976.

[Mac90] R. MacPherson, *Modular varieties*, unpublished lecture notes of a course given at MIT, 1990.

[Man72] Y.-I. Manin, *Parabolic points and zeta-functions of modular curves*, Math. USSR Izvestija **6** (1972), no. 1, 19–63.

[McC87] M. McConnell, *Projective configurations and cellulations of locally symmetric spaces associated to $SL(n,\mathbb{R})$*, Ph.D. thesis, Brown University, Providence, R. I., 1987.

[Min87] H. Minkowski, *Zur Theorie der positiven quadratischen Formen*, Crelle **101** (1887), 196–202.

[Sch70] E. Schoneberg, *Elliptic modular functions*, Grundlehren der mathematischen Wissenschaften, vol. 200, Springer-Verlag, New York, 1970.

[Ser73] J.-P. Serre, *A course in arithmetic*, Graduate Texts in Mathematics, vol. 7, Springer-Verlag, New York, 1973.

[Shi71] G. Shimura, *Introduction to the arithmetic theory of automorphic forms*, Princeton University Press, 1971.

[Vor08] G. Voronoï, *Sur quelques propriétés des formes quadratiques positives partaites*, Crelle **133** (1908), 97–178.

4735-12